國立臺灣大學生命科學院分子與細胞生物學研究所

碩士論文

Institute of Molecular and Cellular Biology
College of Life Science
National Taiwan University

Master Thesis

探討減數分裂時期酵母菌 Ssa3 蛋白與粗絲期檢控點之關係

Studies on the relationship between yeast Ssa3 protein and the pachytene checkpoint in meiosis

葉芝廷

Chih-Ting Yeh

指導教授：董桂書 博士

Advisor: Kuei-Shu Tung, Ph.D.

中華民國 101 年 1 月

January, 2012

致謝

兩年半的研究生生涯終於來到尾聲，日子雖忙碌但受益良多。這份論文能順利完成，有諸多要感謝的人。首先感謝我的指導教授 董桂書老師，即使老師非常地忙碌，但仍樂意抽空給予學生指導，謝謝您教會我實驗的技術與思考的邏輯。感謝台大動物所 陳瑞芬老師與台大植科所 王淑美老師百忙之中願擔任學生的口試委員，給予細心的指正與寶貴的意見，使論文更趨完整。另外感謝王淑美老師實驗室提供了許多儀器，使實驗得以順利進行，也很懷念能與王老師聊聊天，抒發心情的日子。

感謝台大生技系 莊榮輝老師實驗室昔日專題生的指導，使我在大學時代能學習到一些實驗的基礎與研究的態度，謝謝怡岑學姊、之儀學姊與庭芳學姊，在我研究所期間也時常捎來鼓勵，祝福三位學姊能順利地完成博士學業。也感謝輔大生科系的所有老師們，多元且認真的教學加深了我對科學的熱誠與興趣。

此外要感謝實驗室的夥伴們，雖然我們人數不多，但一起度過的點點滴滴，相信將深深印在我心中。謝謝建勳學長、偉君學長時常關心我的實驗進度；謝謝一起熬過最多日子的月蓮以及小學妹 Honey，祝福妳們將來一切順利！

也感謝一路走來支持我的所有好朋友們，特別要謝謝從高中及大學時期到現在的好姊妹們–雨璇、佩吟、清怡、AB、Kiki、小郎，無論發生什麼事情總是不斷地為我打氣，能與妳們相遇是很幸福的事。

最後，要感謝我的家人 爸爸、媽媽、弟弟，給了我最好的學習環境，當遇挫折時，總是第一個給我擁抱與安慰，因為有你們做我堅強的後盾，我才能自信地面對每一項挑戰，你們，是我最甜蜜的牽掛；謝謝軒一直以來的支持與包容，甚至陪我熬夜完成實驗，很幸運能遇見你，願自己也能成為你的依靠。謹以此論文獻給最疼愛我的父母與家人，我會繼續努力地朝自己的理想邁進！

中文摘要

老鼠熱休克蛋白質 HSP70-2 (70-kDa Heat shock protein) 在減數分裂過程中扮演重要的角色，在酵母菌 (*Saccharomyces cerevisiae*) 中與老鼠 HSP70-2 最相似的是 Ssa3 (stress-seventy subfamily A) 蛋白質。在減數分裂前期，若染色體重組與聯會複合體 (synaptonemal complex, SC) 組成發生異常 (例如 *zip1* 突變株)，粗絲期檢控點 (pachytene checkpoint) 會讓細胞停滯在粗絲期，阻止核分裂的進行，直到缺失修復完成。先前本實驗室發現 *SSA3* 基因突變能使部分的 *zip1* 突變株略過粗絲期檢控點而繼續進行減數分裂，且 Ssa3 蛋白分布在粗絲期染色體上。本篇論文的主要目標在於進一步確定 Ssa3 蛋白質與粗絲期檢控點之間的關係。*SSA3* 基因突變會使部分 *zip1* 突變株略過粗絲期檢控點，此隱抑 *zip1* 缺失的現象與酵母菌 *PCH2* (pachytene checkpoint) 基因突變相似，不過 *pch2* 會完全地使 *zip1* 突變株略過粗絲期檢控點。此外，*pch2* 亦能使半數的重組缺失細胞 (*dmc1* 突變株) 略過粗絲期檢控點完成核分裂，但 *ssa3* 則無法隱抑 *dmc1* 的缺失，因此我們推測 Ssa3 可能參與在粗絲期檢控點的路徑，但僅針對 *zip1* 缺失所引發的粗絲期檢控點。先前研究顯示 Pch2 也分布於粗絲期染色體上，並參與在粗絲期檢控點的其中一條路徑，於是我們透過免疫螢光染色同時觀察 Ssa3 與 Pch2 在染色體上的位置，結果無論在野生型或 *zip1* 突變株中，兩者在染色體上的位置並無明顯的重疊，顯示 Ssa3 與 Pch2 可能分屬在不同條粗絲期檢控點的路徑。野生型與 *zip1* 突變株中，Ssa3 蛋白會沿著粗絲期染色體分布，在核仁位置有較累積的現象，但在 *zip1* 突變株中有觀察到偏向點狀的 Ssa3 分布。Red1 是染色體 axial element 組成蛋白之一，由 Ssa3 與 Red1 免疫螢光結果得知 Ssa3 可能位於 axial element 與聯會複合體 lateral element 上。因此，本文推測 Ssa3 蛋白可能有助於 axial elements/lateral elements 間的結合，進而穩定染色體或聯會複合體的構造，使粗絲期檢控點能被有效地活化與作用，將 *zip1* 缺失的細胞留滯在粗絲期。但 *zip1 ssa3* 突變株因缺少 Ssa3 使得染色體結構較不穩定，粗絲期檢控點的活化與功能受到影

響，部分突變株因此能略過粗絲期，完成減數分裂產生孢子。

另一方面，*pch2* 突變株在 30℃ 下的產孢率與野生型相同，但高溫 32.5℃ 下卻觀察到 *pch2* 突變株的產孢效能會發生嚴重的延遲與降低，於是進一步探討其原因。*pch2* 突變株的核分裂情形與產孢率會隨著培養溫度越高，而有越嚴重的延遲與降低現象，且細胞可能停滯在粗絲期階段。*NDT80-bc* 片段缺失突變會使細胞完全不受粗絲期檢控點之控制，透過觀察高溫下的 *pch2 NDT80-bc* 突變株，顯示高溫造成 *pch2* 細胞停在粗絲期是粗絲期檢控點的調控所致。此外，不具有 SC 的 *zip1 pch2* 突變株在高溫下能夠完成減數分裂並產生孢子，而具有少量 SC 的 *zip3 pch2* 突變株卻又受到檢控點的調控，大多數細胞會停滯在粗絲期，無法完成減數分裂。由以上結果推論，也許高溫會導致 *pch2* 細胞中的 SC 結構發生異常，而異常的 SC 會發出比缺乏 SC 更嚴重的訊號給檢控點，因此高溫下會觀察到 *pch2* 突變株而非 *zip1 pch2* 突變株受到粗絲期檢控點的調控，無法完成減數分裂與產生孢子。

關鍵詞：減數分裂、粗絲期檢控點、聯會複合體、Ssa3 蛋白、*pch2* 突變株、溫度

ABSTRACT

Mutants that confer defects in meiotic recombination and synapsis (e.g. *zip1*) will trigger the pachytene checkpoint to delay and arrest cells at the pachytene stage of meiotic prophase. Previous studies have found that null mutant of yeast heat-shock protein *SSA3* can partially suppress the checkpoint-mediated arrest of *zip1*; moreover, Ssa3 protein is localized to pachytene chromosomes, suggesting Ssa3 may function in the pachytene checkpoint. Here we show that *SSA3* is specifically required for the pachytene arrest of *zip1*, for *ssa3* fails to suppress pachytene-arrest of *dmc1* mutant, in which the recombination is defective. Pch2, a protein localized to pachytene chromosomes and nucleolus, has been believed that it is involved in the pachytene checkpoint pathway. Using surface-spreading analyses, Ssa3 does not colocalize with Pch2, suggesting that probably Ssa3 does not involved in the Pch2-dependent checkpoint pathway. Ssa3 localizes along the length of pachytene chromosomes, and accumulates in the nucleolus in both wild type and *zip1*; however, we note that Ssa3 is present in dotty form on pachytene chromosomes in some *zip1* mutant. Double staining of Ssa3 and Red1, a prominent component of axial elements/lateral elements of synaptonemal complex (SC), demonstrates that Ssa3 might localize to axial elements/lateral elements of SC. We propose that Ssa3 may provide its chaperon activity for maintaining a proper chromosomal status which is necessary for efficient

activation of the pachytene checkpoint in budding yeast.

On the other hand, we note that sporulation frequency of *pch2* is similar to wild type at 30℃, while it is significantly delayed and reduced at high temperature, 32.5℃, thus we try to investigate the reason. Due to lots of *pch2* mutants are arrested at pachytene at high temperature, we use *pch2 NDT80-bc* mutant to determine whether the pachytene-arrest of *pch2* is mediated by the pachytene checkpoint. *NDT80-bc* is a deletion mutation of *NDT80*, which completely bypasses the checkpoint. *pch2 NDT80-bc* displays a wild type-like level and kinetics of sporulation and nuclear division, indicating that high temperature-modulated arrest of *pch2* is pachytene checkpoint-mediated. Unlike *pch2* mutant, sporulation of *zip1 pch2* would not be affected at 32.5℃; as a result, we speculate may be the presence of SC is important for the activation of the pachytene checkpoint in *pch2* at high temperature. The *zip3 pch2* mutant, which generates partial SCs, is used to compare with *zip1 pch2*, which generates none of SC. Sporulation frequency and nuclear division of *zip3 pch2* is decreased at 32.5℃, suggesting that SCs is required for checkpoint induction in *pch2* at high temperature. For these reasons, we propose that high temperature might make SC aberrant in *pch2*, and the checkpoint signal from aberrant SC is much significant than from absent SC, so *pch2* is arrested by the pachytene checkpoint at elevated temperature.

Keywords: meiosis, pachytene checkpoint, synaptonemal complex (SC), Ssa3, *pch2* mutant, temperature

CONTENTS

LIST OF TABLES

LIST OF FIGURES

CHAPTER 1 INTRODUCTION

1.1 Meiosis Overview

Meiosis is a specialized cell cycle which allows for the exchange of genetic material between parental chromosomes and the production of haploid gametes. During meiosis, one round of DNA replication is followed by two subsequent rounds of chromosome segregations, with homologs segregating during meiosis I, and sister chromatids segregating during meiosis II. To establish the connections between homologs that are essential for their correct segregation at meiosis I, most eukaryotes employ the coordination of chromosome behaviors depend on elaborate processes and structures known as meiotic recombination and the synaptonemal complex (SC). Meiotic recombination is initiated by a Spo11-dependent DNA double-strand breaks (DSBs) (Keeney et al., 1997), and then DSBs can be processed to result in two types of recombinants, crossovers (COs) and non-crossovers (NCOs). At the same time, SC assembly, which is a proteinaceous structure that holds homologs in close association along their entire lengths (Roeder, 1995). COs give rise to formation of chiasmata which provide the physical links between homologs and ensure proper orientation of homologs on the metaphase I plate. Therefore, after the paired and synapsed homologs segregate from each other in meiosis I and sister chromatids segregate in meiosis II, four haploid cells are generated (Rockmill and Roeder, 1990; Roeder, 1997).

Regulation of meiotic progression and chromosome segregation is necessary for producing normal chromosome set in offspring. Errors in the execution of meiotic process can cause aneuploid gametes, resulting in birth defects, infertility and many diseases such as Down syndrome and cancers in humans (Hassold et al., 2007; Sen, 2000); thus, it is important to study how cell-cycle mechanisms ensure the coordination of meiotic events to maintain the precision of this progression.

The gametogenesis in the budding yeast, *Saccharomyces cerevisiae*, is called sporulation, including the process of meiosis and spore formation. It provides an ideal model for study the meiosis, for **a**/α diploid cells can be easily induced to enter a sporulation program in response to nitrogen starvation in the absence of a fermentable carbon source (Mitchell, 1994). After undergoing sporulation, four haploid spores are generated finally.

1.2 Cell-Cycle Checkpoint

1.2.1 The Importance of Cell-Cycle Checkpoint

Cell-cycle checkpoints are surveillance mechanisms in eukaryotic cells, ensuring that chromosomes are intact and that each stage of the cell cycle is completed before the following stage is initiated by arresting or delaying the cycle (Hartwell and Weinert, 1989). There are several checkpoints have been identified during mitosis to monitor

different events such as DNA damage, DNA replication, kinetochore attachment and spindle position (Lew and Burke, 2003). In addition to the checkpoints enforcing in the mitosis, several extra checkpoints exist during meiosis, such as the pachytene checkpoint (Roeder, 1997). Due to the function of checkpoints, cells can prevent chromosome loss or missegregation resulting in aneuploidy and lethality.

1.2.2 The Pachytene Checkpoint

When meiotic recombination and chromosome synapsis are incomplete, the pachytene checkpoint, which has also been referred to as the recombination checkpoint, prevents cells exit from the pachytene stage of meiotic prophase until they have been completed (Roeder and Bailis, 2000). In budding yeast, the pachytene stage is the last stage before cells fully become committed to undergo first meiotic division (Shuster and Byers, 1989; Simchen, 2009), so this stage is a crucial regulatory point during meiosis.

Several mutants with specific defects in meiotic recombination (e.g., *dmc1*, *hop2*, *zip1*) activate the pachytene checkpoint and cause defective cells arrested at the pachytene stage. *DMC1* is a meiosis-specific yeast homolog of bacterial RecA strand exchange enzyme. The *dmc1* mutant is defective in recombination and normal SC formation, and the cells arrest at pachytene with unrepaired DSBs (Bishop et al., 1992; Rockmill et al., 1995). The *hop2* mutant arrests with extensive SC formation between

nonhomologous chromosomes, and DSBs remain unrepaired (Leu et al., 1998; Tsubouchi and Roeder, 2002). Zip1, a major structure component of the central region of the SC, acts as a zipper to bring homologous chromosomes in close apposition. In the absence of Zip1, chromosomes fail to synapse and recombination intermediates accumulate, thereby arresting at pachytene (Sym et al., 1993).

The factors which function as the sensors and involved in the signal transduction of the pachytene checkpoint in yeast include components of the mitotic DNA damage checkpoint, such as Rad17, Rad24, Mec3, Dcd1, and Mec1 (Alani et al., 1990; Lydall et al., 1996; Weinert, 1998), several meiosis-specific chromosomal proteins (Red1, Hop1, and Mek1) (Hollingsworth and Ponte, 1997), and a number of nucleolar proteins (Pch2 and Sir2) (San-Segundo and Roeder, 1999).

The major targets of the checkpoint are cyclin-dependent kinases (CDKs), consisting of a catalytic kinase (CDK) subunit and a regulatory cyclin subunit, subjected to inhibitory regulation in response to checkpoint activation (Hochwagen and Amon, 2006). In budding yeast, two downstream targets of pachytene checkpoint have been identified to control the activity of CDKs: Ndt80 and cyclin-dependent kinase Cdc28. Ndt80, a meiosis-specific transcription factor, induces middle sporulation genes (MSGs) required for meiosis I, including B-type cyclins (Chu and Herskowitz, 1998; Hepworth et al., 1998). Cdc28 is required for both meiotic and vegetative cell cycles (Shuster and

Byers, 1989), and it is proposed Cdc28 is phosphorylated and inactivated by Swe1 when the pachytene checkpoint is activated (Leu and Roeder, 1999). In brief, the pachytene checkpoint controls the meiotic process by decreasing the transcript (and protein) level of cyclins and inactivating Cdc28.

The existence of the pachytene checkpoint is not only in budding yeast but also in other organisms. In *Drosophila*, mutations in spindle-class genes (*okr*, *spn-B* and *spn-C*) cause oocytes arrest in meiotic prophase with unrepaired DSBs (Ghabrial and Schupbach, 1999). In *C. elegans*, mutation of *RAD51* which encodes a homolog of the RecA-like protein prevents pachytene exit in oocytes (Takanami et al., 1998). Moreover, the spermatocytes and oocytes of the Dmc1-deficient mice arrest at pachytene with unsynapsed chromosomes, and recombination is incomplete (Pittman et al., 1998).

1.2.3 Ndt80

Ndt80 (Non-dityrosine) is a meiosis-specific transcription activator with 627 residues, the DNA-binding domain resides in the N-terminal portion (residues 59~330) (Montano et al., 2002) and the activation domain resides in the C-terminal portion (residues 426~627) (Sopko et al., 2002). Ndt80 is a central component of the sporulation transcription cascade due to it induces the expression of more than 150 MSGs, which are necessary for meiotic division (e.g., B-type cyclins) and spore

formation (e.g., *SPS1*), through binding to their middle sporulation elements (MSEs) which is a DNA sequence found upstream of many MSGs (Chu et al., 1998; Chu and Herskowitz, 1998; Hepworth et al., 1998; Lamoureux and Glover, 2006).

The *ndt80* null mutation arrests at the pachytene stage with fully synapsed homologs and duplicated but unseparated spindle pole bodies (SPBs) like cell lacking Clb-Cdc28 activity, suggesting that B-type cyclins activity of Cdc28 are regulated by Ndt80, and Ndt80 is required for pachytene exit and MI entry (Xu et al., 1995). Besides, overproduction of Ndt80 can partially bypass the *zip1* and *dmc1* pachytene arrests, indicating that Ndt80 activity is downregulated by the pachytene checkpoint (Chu and Herskowitz, 1998; Hepworth et al., 1998; Tung et al., 2000).

For the regulatory mechanism of the activity of Ndt80 by the pachytene checkpoint, two models have been proposed. The first model shows that a Sum1-mediated repression may control the transcription of *NDT80*, and there is a competition for binding to some MSEs between Sum1 repressor and Ndt80 activator (Pak and Segall, 2002b; Pierce et al., 2003). Upstream repression sequences 1 (URS1s) and MSEs are present in the promoter region of *NDT80*. First transcription of *NDT80* is dependent on Ime1 and Ume6 transcription factors, which recognize to URS1 sites and cause early genes expression (Chu and Herskowitz, 1998; Mitchell, 1994). After that, a low level of Ndt80 directly binds to its MSE and upregulates its own expression through a positive

autoregulatory loop results in amplifying the amount of Ndt80 (Chu and Herskowitz, 1998; Sopko et al., 2002). In this model, Sum1 is likely to function as a meiotic brake binding to the *NDT80* MSE prohibits Ime1 recognize to *NDT80* URS1 from transcription of *NDT80*; as a result, the expression of *NDT80* and MSGs are inhibited and the cell cycle is arrested (Pak and Segall, 2002a; Pierce et al., 2003).

The second model suggests that the regulation of the activity of Ndt80 could be achieved by posttranslational modification and a cytoplasmic anchor mechanism (Tung et al., 2000; Wang et al., 2011). The level of phosphorylation of Ndt80 is high in wild type but very low in pachytene-arrested mutants, presumably the pachytene checkpoint directly inhibits Ndt80 by preventing it from being phosphorylated and activated (Tung et al., 2000), and the residues T318 and Y216 are possible phosphorylation sites on the Ndt80 protein (Wu, 2001). The data indicate that the activity of Ndt80 is dependent on phosphorylation. Furthermore, the nuclear localization of Ndt80 is regulated by the pachytene checkpoint through a direct protein inhibition mechanism, which blocks the nuclear import of Ndt80 in pachytene-arrested mutants (Wang et al., 2011). The proposition derives from a *ndt80* in-frame deletion mutation, *NDT80-bc* (*NDT80*-bypass checkpoint), in which the amino acid residues from 346 to 402 are deleted, but functions as normal as Ndt80 (Wang et al., 2011). *NDT80-bc* is able to completely bypass the pachytene checkpoint because it can suppress the checkpoint-mediated arrest

of the *zip1*, *dmc1* and *hop2* mutants and relieve the sporulation frequency with a wild-type level. However, the kinetics of nuclear import is different between Ndt80 and Ndt80-bc in the *zip1* mutant. Ndt80 is maintained in cytoplasm around pachytene stage in *zip1*, while most of Ndt80-bc is found in the nucleus, suggesting that the activity of Ndt80 is probably controlled by the pachytene checkpoint through a cytoplasmic anchor mechanism as well (Wang et al., 2011). Together, our previous data support the second model in which posttranslational control on Ndt80 is the main regulation mechanism employed by the pachytene checkpoint.

1.2.4 Pch2

Pch2 (Pachytene checkpoint) is a AAA+-ATPase (ATPases associated with diverse cellular activities) wildly conserved in organisms which construct the SCs in meiosis, and is identified as a pachytene checkpoint factor on the basis of the ability of *pch2* to suppress the meiotic arrest of *zip1* (San-Segundo and Roeder, 1999). However, deletion of *PCH2* does not relieve the arrest of the *hop2* mutant, and only partially bypass the *dmc1* arrest depending on the strain background (Hochwagen et al., 2005; San-Segundo and Roeder, 1999). The nucleolar localization of Pch2 depending on Sir2 and Dot1 appears to be important for its function on the pachytene arrest in *zip1* (San-Segundo and Roeder, 1999; San-Segundo and Roeder, 2000).

Wu and Burgress (2006) has been proposed that Pch2 and Rad17 comprise separate branches of the pachytene checkpoint that ensures proper timing of meiosis I (Wu and Burgess, 2006). The presence of recombination intermediates activates a *RAD17*-dependent DNA damage checkpoint; by contrast, the presence of aberrant SC intermediates activates a *PCH2-ZIP1*-dependent checkpoint (SC-dependent checkpoint), thereby the progression of meiosis I is delayed (Mitra and Roeder, 2007; Wu and Burgess, 2006). Pch2 may function to ensure the proper coupling between SC morphogenesis and meiotic recombination (Mitra and Roeder, 2007). In addition, Pch2 is required for establishing proper meiotic axis organization and promoting wild-type levels of crossover (CO) interference and CO distribution in budding yeast (Börner et al., 2008; Zanders and Alani, 2009).

The Pch2-dependent checkpoint function also monitors chromosomal lesions during meiosis in higher eukaryotes. In *C. elegans*, it is required for the programmed cell death in response to unsynapsed pairing centers (Bhalla and Dernburg, 2005); in *Drosophila*, it is required to delay meiotic progression in CO formation mutants and to monitor the structure of chromosome axes (Joyce and McKim, 2009; Joyce and McKim, 2010); in mouse, it is required for DSB repair, CO interference, CO distribution, and proper organization of meiotic chromosome axes (Li and Schimenti, 2007; Roig et al., 2010; Wojtasz et al., 2009).

1.3 The Roles of Heat-Shock Proteins

Organisms respond to heat and other stresses by inducing rapidly the synthesis of a small number of proteins called the heat-shock proteins (HSPs); the response exists in every organism from prokaryotes to eukaryotes (Lindquist and Craig, 1988). HSPs are involved in the protein biogenesis by aiding protein folding and assembly into complexes and by mediating the translocation of nascent polypeptides into various intracellular compartments (Becker and Craig, 1994; Hartl, 1996). Moreover, certain of HSPs participate in the developmental process: in *Drosophila*, mice and humans have been observed that specific *HSP70* gene family members play distinct roles in the differentiation of the germ cell (Zakeri et al., 1988); some small HSPs such as Hsp26 express during sporulation in yeast (Ho, 2005; Kurtz et al., 1986) and during oogenesis and spermatogenesis in *Drosophila* (Kurtz et al., 1986).

1.3.1 Mouse HSP70-2 Protein

HSP70 genes encode the 70-kDa heat-shock proteins (HSP70s) that function as molecular chaperones, and show a great degree of conservation in all organisms (Georgopoulos and Welch, 1993; Lindquist and Craig, 1988). There are six members of the *HSP70* family in mammals, most of which are expressed constitutively or after induction by heat shock or stresses (Hunt et al., 1993). Two HSP70s are expressed

specifically in mouse spermatogenic cells: HSP70-2 and HSP70t. The HSP70-2 protein is synthesized during the spermatogenesis, and is abundant in pachytene spermatocytes (Allen et al., 1996; Eddy, 1999; Zakeri et al., 1988).

Spermatogenesis is disrupted by the increased temperature, so the testes in most mammals are maintained 5-7℃ below body temperature by their location outside the body (Kandeel and Swerdloff, 1988), implying that HSPs may have functions in spermatogenic cells which differ from those in other cell types. Mouse spermatocytes contain unique HSP70-2 protein expressing at a significant level only during spermatogenesis (Dix et al., 1996a; Rosario et al., 1992; Zakeri et al., 1988). The *HSP70-2* gene mutation causes primary spermatocytes to arrest at pachytene and undergo apoptosis, resulting in infertility in male mice, whereas female mice are fertile (Dix et al., 1996a; Dix et al., 1996b). Electron microscopy and immunostaining of pachytene spermatocytes revealed that HSP70-2 is a component of the lateral elements of the SC (Allen et al., 1996). However, HSP70-2 is not required for SC assembly but for SC desynapsis (Dix et al., 1997).

The mitotic and meiotic cell cycles in eukaryotic cells are controlled by CDKs at two transitions, the G_1/S-phase and the G_2/M-phase transitions. The G_2/M-phase transition required cyclin B-dependent CDC2 protein kinase activity. Zhu and coworkers (1997) used co-immunoprecipitation and *in vitro* reconstitution experiments

found that HSP70-2 is a molecular chaperone required for assembly of a functional CDC2/cyclin B1 complex and for CDC2 to become an active kinase in pachytene spermatocytes, suggesting that interaction between HSP70-2 protein and cyclin-dependent kinase (CDK) is important for the progression of meiotic cell cycle (Zhu et al., 1997).

1.3.2 Yeast Ssa3 Protein

The *S. cerevisiae* genome contains several genes related to HSP70, involving in disassembling aggregates of misfolded proteins, translocating proteins across the mitochondrial membranes and into the endoplasmic reticulum (ER), regulating the expression of other heat-shock proteins (Becker and Craig, 1994; Lindquist and Craig, 1988; Stone and Craig, 1990), and proceeding sporulation (Broach et al., 1992). There are nine cytosolic forms of HSP70, three mitochondrial HSP70s, and two ER HSP70s (Becker and Craig, 1994; Craig et al., 1989; Werner-Washburne et al., 1987). Based on genetic, structural and functional similarities, HSP70s have been divided into five groups: *SSA1-4* (stress seventy subfamily A), *SSB1-2*, *SSC1*, *SSD1*, and *KAR2*. One of them, *SSA3*, is the homolog of mouse HSP70-2, as well as accumulates in sporulating cells (Chen, 2003; Werner-Washburne et al., 1989).

Although *SSA3* is not essential gene, and the gene product is not required for yeast

meiosis since the spore formation and nuclear division are normal in the *ssa3* mutant, (Chen, 2003; Werner-Washburne et al., 1987) absence of Ssa3 can partially suppress the pachytene arrest of *zip1*, which has defects in synapsis and recombination (Chen, 2003). Using surface-spread analyses, the Ssa3 protein localizes to pachytene chromosomes in wild-type and *zip1* mutant cells, suggesting that the Ssa3 protein might involve in maintaining a proper chromosome structure for pachytene checkpoint signaling in yeast (Chen, 2003).

1.3.3 Yeast Ssa2 Protein

Ssa2 is another member of yeast cytosolic HSP70s, sharing 97%, 86%, and 87% amino acid identity with Ssa1, Ssa3, and Ssa4, respectively (Boorstein et al., 1994). Under normal growth conditions, *SSA1* and *SSA2* are expressed at moderate levels, while *SSA3* and *SSA4* are undetectable. After heat shock, increased expression of *SSA1* and strong induction of *SSA3* and *SSA4* can be observed (Werner-Washburne et al., 1987). However, *SSA2* is still constitutively expressed, and changes little by heat or stress (Lindquist and Craig, 1988).

Ssa1 and Ssa2 are considered that function in DNA damage checkpoint regulation as their chaperone activities are required for activating Rad9 and Rad53 and for remodeling Rad9 complexes in budding yeast (Gilbert et al., 2003; van den Bosch and

Lowndes, 2004). Moreover, phosphorylation of both Rad9 and Rad53 are partially defective in the *ssa1 ssa2* double mutants after DNA damage, indicating that Ssa1 and Ssa2 seem to be required during checkpoint-pathway regulation (Gilbert et al., 2003).

1.4 Specific Aims

A checkpoint comprises the four components: a signal (1) that is detected by signal sensors (2), which activate signal-transduction pathways (3) that translate the signal into an output by modifying checkpoint targets (4) (Hochwagen and Amon, 2006). We try to investigate about the upstream (e.g., signal sensor) and the downstream (e.g., target) in the pachytene checkpoint; therefore, there are two main sections in this thesis: the role of Ssa3 in meiosis and the cytoplasmic anchor mechanism of Ndt80.

Although the function of Ssa3 in meiosis is uncertain, we note that some characters between Ssa3 and Pch2 are similar: (1) Deletion of *SSA3* or *PCH2* could bypass the pachytene arrest of *zip1*; (2) Ssa3 and Pch2 are localized to pachytene chromosomes; (3) both are proposed to function in maintaining or monitoring the chromosome structure for the pachytene checkpoint (Börner et al., 2008; Chen, 2003; San-Segundo and Roeder, 1999). For these reasons, we attempt to explore whether Ssa3 and Pch2 act in a common pachytene checkpoint pathway. It is hoped that we could further understand the Ssa3 function during meiosis.

Previous data suggest that the nuclear import of Ndt80 is regulated by the pachytene checkpoint through a cytoplasmic anchor mechanism (Wang et al., 2011). Here we propose that the nuclear import of Ndt80 would be inhibited by a cytoplasmic anchor protein binding to the region that is deleted in Ndt80-bc when the pachytene checkpoint is activated. To identify the potential cytoplasmic anchor protein of Ndt80 is another aim in this study.

CHAPTER 2 MATERIALS AND METHODS

2.1 Yeast Strains, Media and Culture conditions

Yeast strains used in this study are listed in Table 2-1. Yeast were grown in YPAD (1% yeast extract, 2% peptone, 2% D-glucose, 0.004% adenine, and 1.5% agar) or 2X synthetic drop-out (SD) medium (0.15% yeast nitrogen base without amino acids and ammonium sulfate, 0.5% ammonium sulfate, 2% D-glucose, and 1.5% agar) supplemented with 0.2% amino acid stock mixture at 30℃. Sporulation of cells were induced on solid sporulation medium [0.2% yeast extract, 0.1% D-glucose, 2% potassium acetate (KAc), 2% agar, and 0.1% amino acid stock mixture] at the indicated temperature for three days. The frequency of ascus formation was assessed by examination of at least 200 cells by light microscopy. For cytological analyses, cells were grown in YPAD or 2X SD media overnight rolling at 60 rpm till saturated, and refreshed by dilution into YPAD for 10 hours. Cells were harvested, washed, and then resuspended in liquid sporulation medium (2% KAc) for sporulation at the indicated temperature until indicated time points.

2.2 DNA Preparation and Transformation

For DNA manipulation, plasmids were prepared from *E.coli* by a modification of alkaline lysis method as described (Birnboim and Doly, 1979). DNA digestions were

performed by the restriction enzyme purchased from New England Biolabs (NEB) according to the instructions from the manufactures. Digested DNA fragments were segregated through 0.8-2.0% TAE agarose gel and purified by QIAquick® Gel Extraction Kit. Fragments were ligased by the T4 DNA ligase purchased from NBE at 16℃ overnight.

Rapid isolation of plasmid DNA from yeast was followed the modified procedures (Hoffman, 2001; Lorincz, 1984). Yeast cells were harvested from 2ml overnight culture and resuspened in 250μl breaking buffer (100mM NaCl, 10mM Tris-HCl pH8.0, 1mM EDTA, 0.1% SDS) with glass beads (0.45mm diameter). After 2- min vortex at highest speed, transfer the liquid to a new tube. Add phenol/chloroform/isoamyl alcohol (25:24:1 v/v/v) twice and chloroform/isoamyl alcohol (24:1 v/v) once to extract the sample with an equal volume, and add 99.9% ethanol to precipitate the yeast plasmid DNA. The dry pellet of precipitation was dissolved in 25-30μl of sterilized water. Use 1-5μl for *E.coli* transformation.

E.coli transformations were carried out by the calcium chloride method (Sambrook, 2001). Yeast transformations were performed by the lithium acetate procedure (Ito et al., 1983).

2.3 Plasmids Construction

Plasmids and primers used in this study are listed in Table 2-2 and Table 2-3.

pT652 (pSK$^+$-*SSA2*)

A 2.8-kb PCR-generated fragment containing -346~p528 of *SSA2* gene was cloned from yeast genomic DNA using SSA2-U1 and SSA2-D1-XhoI primers. SSA2-U1 primer is from position -346 to -323 upstream of *SSA2*. SSA2-D1-XhoI primer is from p528 to p493 downstream of *SSA2*. The PCR product was cut with *Xba*I and *Xho*I to get a 2.6-kb fragment and then inserted into pBluescript SK (+) vector at the *Xba*I-*Xho*I sites to create pT652.

pT654 (pSK$^+$-*ssa2*::*URA3*)

The 1.4-kb *Hinc*II-*Hinc*II fragment within the *SSA2* ORF (+70~+1429) in pT652 was replaced with a 1.5-kb *Hpa*I-*Pvu*II fragment containing *URA3* from YEp352 to create pT654.

pT659 (pRS424-*SSA2*)

A 2.7-kb *Not*I-*Xho*I fragment of *SSA2* (-240~p512) in pT652 was subcloned into pRS424 at *Not*I-*Xho*I sites for overexpression of *SSA2*.

pT662 (pGBDU-C1-*NDT80Δ404-627*)

The *NDT80Δ404-627* fragment was cloned by PCR using pT424 (YEp351-*NDT80Δ404-627*) as template, NDT80-SalI-1009U (from -11 to +27) and

NDT80-BglII-p59D (from p59 to p23) as primers. The 1.3-kb PCR product was cut with *Sal*I and *Bgl*II and subcloned into *Sal*I-*Bgl*II sites of pT477.

pT665 (YEp351-*NDT80Δ346-627*)

The *NDT80Δ346-627* fragment was cloned by PCR using Tp73 (YEp351-*NDT80*) as template, NDT80-IN2 (from -439 to -414) and NDT80-346D (+1054 to +1018) as primers. The 1.5-kb PCR product was partial digested with *Xho*I and *Hind*III sites to get a 1.2-kb *Xho*I-*Hind*III fragment. On the other hand, a 1.8-kb *Hind*III-*Sca*I fragment getting from 3.2-kb *Hind*III-*Sca*I fragment of pT424. Finally, the 1.2-kb *Xho*I-*Hind*III fragment and the 1.8-kb *Hind*III-*Sca*I fragment inserted into pT424 at *Xho*I and *Sca*I sites for in-frame deletion, which 840bp within *NDT80* ORF was deleted.

pT667 (pGBDU-C1-*NDT80Δ346-627*)

The *NDT80Δ346-627* fragment was cloned by PCR using pT665 as template, NDT80-SalI-1009U (from -11 to +27) and NDT80-BglII-p59D (from p59 to p23) as primers. The 1.1-kb PCR product was cut with *Sal*I and *Bgl*II and subcloned between *Sal*I and *Bgl*II sites of pT477 to generate pT667.

pT669 (pGAD-C3-*SSA2*)

The *SSA2* gene was cloned by PCR using T652 as template, SSA2-U3-SalI (from -9 to +28) and SSA2-D1-XhoI (from p528 to p493) as primers. The 2.5-kb PCR product was partial digested with *Sal*I and cut with *Pst*I and then this 2.4-kb *Sal*I-*Pst*I fragment

inserted into pT410 (pGAD-C3) at *Sal*I and *Pst*I sites.

pT673 (pSK$^+$-*PCH2*)

A 2.8-kb PCR-generated fragment containing -639~p369 of *PCH2* gene was cloned from yeast genomic DNA using PCH2-U1 and PCH2-D1 primers. PCH2-U1 primer is from position -639 to -613 upstream of *PCH2*. PCH2-D1 primer is from p369 to p343 downstream of *PCH2*. The PCR product was cut with *Hind*III and *Pst*I to get a 2.7-kb fragment and then inserted at the *Hind*III and *Pst*I sites of pT566, which is derived from pSK (+) vector with the upstream *Not*I site disrupted, to create pT673.

pT679 (pRS316-*PCH2*)

A 2.8-kb *Hind*III-*Xba*I fragment containing *PCH2* (-588~p358) from pT673 was subcloned into pRS316 at *Hind*III-*Xba*I sites for low-copy expression of *PCH2* and the control of functional test for MYC-tagging.

pT681 (pRS314-*SSA3*)

The 2.9-kb *Sac*I-*Hind*III fragment containing the *SSA3* ORF (-727~p215) from pT125 (SK$^+$-*SSA3*) was inserted into pRS314 at *Sac*I-*Hind*III sites for YCp low-copy expression of *SSA3* and the control of complementation test for HA-tagging.

pT685 (pSK$^+$-*PCH2-Not*I)

Recombinant PCR were used to generate full length of *PCH2* gene (-96~p686) containing a *Not*I site before the stop codon at the 3' terminus and a *Xba*I site (p669).

Two pairs of primers used were listed in Table 2-3. In the first-round PCR, a 1.9-kb fragment was obtained using PCH2-U2 and PCH2-NOT-D2; a 0.7-kb fragment was obtained using PCH2-NOT-U2 and PCH2-XbaI-D1. Both of the reactions used TY178 yeast genomic DNA as template. The products of the first-round PCR were used as templates in the second-round PCR. PCH2-U2 and PCH2-XbaI-D1 were used as primers. Through the second-round PCR, a 2.6-kb fragment containing full-length *PCH2* with a *Not*I site and a *Xba*I site at 3' terminus. The fragment was digested with *Bam*HI (+263) and *Xba*I (p669) to get a 2.2-kb fragment, and then inserted at the *Bam*HI-*Xba*I sites of pT673 to generate pT685.

pT687 (pSK$^+$-*PCH2-3XMYC*)

One DNA fragment encoding three copies of the human c-*myc* (MYC) epitope derived from pTP208 was inserted into *Not*I site in *PCH2* ORF on pT685 (pSK$^+$-*PCH2-Not*I) to create pT687.

pT688 (pRS316-*PCH2-3XMYC*)

A 2.4-kb *Bam*HI-*Xba*I fragment containing *PCH2-3XMYC* from pT687 was inserted into pT679 at *Bam*HI-*Xba*I sites, for YCp low-copy expression of *PCH2-3XMYC* and complementation assay for MYC-tagging.

pT689 (pRS314-*3XHA-SSA3*)

A 3.0-kb *Sac*I-*Hind*III fragment containing *3XHA-SSA3* from pT182

(pRS316-*3XHA-SSA3*) was subcloned into pRS314 at *Sac*I-*Hind*III sites, for YCp low-copy expression of *3XHA-SSA3* and complementation assay for HA-tagging.

pT690 (pRS306-*PCH2-3XMYC*)

A 2.8-kb *Sca*I-*Xba*I fragment containing *PCH2-3XMYC* from pT687 was subcloned into the *Sma*I-*Xba*I sites of the integrating vector, pRS306, to create pT690.

pT691 (pSK$^+$-*ZIP3*)

A 2.6-kb PCR-generated fragment containing -631~p562 of *ZIP3* gene was cloned from yeast genomic DNA using ZIP3-XhoI-U1 and ZIP3-SpeI-D1 primers. ZIP3-XhoI-U1 primer is from position -631 to -592 upstream of *ZIP3*. ZIP3-SpeI-D1 primer is from p562 to p523 downstream of *ZIP3*. The PCR product was cut with *Xho*I and *Spe*I to get a 2.6-kb fragment and then inserted at the *Xho*I-*Spe*I sites of pSK$^+$, to create pT691.

pT696 (pSK$^+$-*zip3::URA3*)

The 0.6-kb *Eco*RV-*Eco*RI fragment within the *ZIP3* ORF (+101~+672) in pT691 was replaced with a 1.6-kb *Hpa*I-*Eco*RI fragment containing *URA3* from YEp352 to create the *ssa2*::*URA3* plasmid pT654.

pT701 (pSK$^+$-*RED1*)

A 3.5-kb *Sal*I-*Xba*I fragment containing *RED1* gene from pT450 was inserted into *Sal*I-*Xba*I sites of pT566, which is derived from pSK (+) vector with the upstream

*Not*I site disrupted, to create pT701.

pT702 (pSK$^+$-*RED1-Not*I)

Recombinant PCR were used to generate a part of *PCH2* gene (+1124~p378) containing a *Not*I site before the stop codon at the 3' terminus. Two pairs of primers used were listed in Table 2-3. In the first-round PCR, a 1.4-kb fragment was obtained using RED1-U3 and RED1-NOT-D1; a 0.4-kb fragment was obtained using RED1-NOT-U1 and RED1-D3. Both of the reactions used TY179 yeast genomic DNA as template. The products of the first-round PCR were used as templates in the second-round PCR. RED1-U3 and RED1-D3 were used as primers. Through the second-round PCR, a 1.7-kb fragment containing partial *RED1* with a *Not*I site at 3' terminus. The fragment was digested with *Bgl*II (+1272) and *Xba*I (p238) to get a 1.5-kb fragment, and then inserted at the *Bgl*II-*Xba*I sites of pT701 to generate pT702.

pT703 (pSK$^+$-*RED1-3XMYC*)

One DNA fragment encoding three copies of the human c-*myc* (MYC) epitope derived from pTP208 was inserted into *Not*I site in *RED1* ORF on pT702 (pSK$^+$-*PCH2-Not*I) to create pT703.

pT705 (pRS314-*RED1-3XMYC*)

A 3.7-kb *Sal*I-*Xba*I fragment containing *RED1-3XMYC* from pT703 (pSK$^+$-*3XHA-SSA3*) was subcloned into pRS314 at *Sal*I-*Xba*I sites, for YCp low-copy

expression of *RED1-3XMYC* with *TRP1* marker.

pT706 (YEp352-*3XHA-SSA3*)

A 3.0-kb *Sac*I-*Hind*III fragment containing *3XHA-SSA3* from pT182 (pRS316-*3XHA-SSA3*) was subcloned into YEp352 at *Sac*I-*Hind*III sites, for overexpression of *3XHA-SSA3* with *URA3* marker.

2.4 Yeast Strains Construction

Disruption of yeast genes was carried out by the one-step gene replacement or two-step gene replacement (pop-in/pop-out strategy) method. Epitope tagging of yeast genes was performed by two-step gene replacement. The detailed process is described as follows and the primers used are listed in Table 2-3.

Construction of yeast mutations

***ssa2::URA3* mutant**

pT654 was used to replace the genomic *SSA2* gene with *ssa2::URA3*, targeting for substitution by cutting with *Xba*I and *Xho*I. The *ssa2* haploid mutants were confirmed by whole cell or genomic DNA 3-primer PCR assay. One primer is SSA2-U1 (from -346 to -323), another is SSA2-D2 (+387 to +362), and the other is URA3-D1 within the *URA3* gene (from +114 to +91 of *URA3* gene). The wild-type *SSA2* gene generate 0.7-kb PCR product through SSA2-U1 and SSA2-D2 primers, and the *ssa2::URA3*

destructed allele generate 0.97-kb PCR product through SSA2-U1 and URA3-D1 primers.

***zip3::URA3* mutant**

pT696 was used to replace the genomic *ZIP3* gene with *zip3::URA3*, targeting for substitution by cutting with *Xho*I and *Spe*I. The *zip3* haploid mutants were confirmed by whole cell 3-primer PCR assay. One primer is ZIP3-U3 (from -30 to -6), another is ZIP3-D2 (+429 to +402), and the other is URA3-D1 within the *URA3* gene (from +114 to +91 of *URA3* gene). The wild-type *ZIP3* gene generate 0.5-kb PCR product through ZIP3-U3 and ZIP3-D2 primers, and the *zip3::URA3* destructed allele generate 0.7-kb PCR product through ZIP3-U3 and URA3-D1 primers.

***URA3*$^+$ strain**

YEp352 (2μm *URA3*) plasmid was used to replace the genomic *ura3-1* gene with *URA3*, targeting for substitution by cutting with *Nsi*I and *Nde*I. The *ura3-1* mutant was a point mutation that G to A transition at residue 701 of the coding sequence, changing residue 234 from glycine to glutamate; as a result, we could reverts *ura3-1* to *URA3* through gene replacement method.

***NDT80-bc* (*NDT80Δ346-627*) mutant**

pT330 (Yeast integrating plasmid containing the *NDT80Δ346-627-HA* allele) was used to replace the chromosomal copy of *NDT80* with *NDT80Δ346-627* by two-step

replacement (pop-in/out strategy). Yeast cells were transformed with pT330 that were cut with *Spe*I to induce recombination between the chromosome and plasmid. Cells were selected on SC-Ura plates for successful transformation (pop-in). Ura^+ transformants were patched on the YPAD plate, on the next day, the YPAD plate was replicated onto 5-fluoro-orotic acid (5-FOA) plate to select cells which had occurred second recombination (pop-out) (Boeke et al., 1984). Successful replacements were checked by PCR using NDT80-971-988-U and NDT80-1710-1654-D primers. The PCR product of *NDT80Δ346-627* is 0.6-kb, and that of *NDT80* is 0.7-kb.

Epitope tagging of Pch2

To construct *PCH2-3XMYC*, pT690 (Yeast integrating plasmid containing the *PCH2-3XMYC* allele) was used to replace the chromosomal copy of *PCH2* with *PCH2-3XMYC* by pop-in/out strategy. Yeast cells were transformed with pT690 that were cut with *Bam*HI to induce recombination between the chromosome and plasmid. Cells were selected on SC-Ura plates for successful transformation (pop-in). After 5-FOA selection, cells which had occurred second recombination (pop-out) were picked and checked by PCR using PH2-U2 and PCH2-D1 as primers. The PCR product of *PCH2-3XMYC* is 0.58-kb, and that of *PCH2* is 0.45-kb.

2.5 Analysis of Kinetics of Meiotic Cells

Time course analysis

Yeast cells were cultured overnight to saturation in 2 ml YPAD or 2X SD medium at 30℃ and re-inoculated 100μl saturated cell culture into 2 ml fresh YPAD or 2X synthetic complete medium at 30℃ next day. After incubating 16-18 hours, the cultures were diluted back 1:2 into YPAD to refresh for 10 hours. 1.5 ml of refreshed cells were collected, washed with sterilized water and resuspended in 10 ml 2% KAc. 180 μl of cells were harvested at 2-hr intervals post-induction from 8 or 10 hour for nuclear division analysis. At the same time, a few cells were examined under the light microscope to assess spore formation, with at least 200 cells counted.

Nuclear division analysis

180 μl of cells collected at each time point were fixed in 20 μl of 37% formaldehyde at room temperature for 30 min with 60 rpm shaking. The fixed cells were washed twice with 200 μl of phosphate-buffered saline (PBS), and resuspended in 200μl of PBS. Poly-lysine coated slides were prepared as following, the stock of 1 mg/ml poly-lysine was thawed and centrifugated at 13,000 rpm for 10 min before use. 25 μl of poly-lysine was added to each well of slides, washed with water after 20 min, and then air dried. 25 μl of cells were dropped onto poly-lysine-coated slides for 15 min

at room temperature. After staining with 20 μl of Vectashield mounting medium(Vector Laboratories, Burlingame, CA) containing 1μg/ml 4',6-diamidino-2-phenylindole (DAPI), slides were covered with cover clips and sealed with nail polish. The slides were stored at -20℃ in black boxes. Quantification of nuclear division was calculated by counting at least 200-DAPI-stained cells under an Olympus AX70 fluorescence microscope (Olympus, Tokyo, Japan) and an Uplan Apo100x objective (Olympus).

2.6 Spore Viability Analyses

Cells induced for sporulation were checked for ascus formation under light microscope, and were taken by toothpick from sporulation plates and mixed with 10 μl of 1/10 diluted glusulase in 1 M sorbitol and left on bench for 15 min. Treated cells were spread on YPAD plates for tetrad dissection.

2.7 Cytology Analyses

Meiotic chromosome spreading and immunostaining

Cells were sporulated in 2% KAc at the indicated temperature till indicated time points. 5 ml of cells were spun down at 2000 rpm for 2 min. The pellets were resuspended in 1 ml of 2% KAc, 0.8 M sorbitol (pH 7.0) containing 10 mM DTT and 50 μg/ml zymolase and incubated at 30℃ on a rolling drum for 20-30 min until 70-80%

of cells have been spheroplasted. Formation of spheroplasts was monitored by using 2% Sarkosyl (N-Lauroylsacosine) under light microscope. The spheroplasts were spun down at 800 rpm for 2 min, and the pellet was washed gently with 1 ml of ice-cold MES with sorbitol solution [0.1 M 2-N-morpholono ethane sulfonic acid (MES) / 1 M sorbitol/ 1 mM EDTA, pH 8.0/ 0.5 mM $MgCl_2$]. After that, the pellet was resuspended in 200 μl of ice-cold MES without sorbitol solution (0.1 M MES/ 1 mM EDTA, pH 8.0/ 0.5 mM $MgCl_2$) and 700 μl of cold 4% paraformaldehyde (pH 7.0), and the mixture was poured immediately onto marked slides. A large cover-slip (24x50 mm) was slapped on the slide, and the slides were incubated at room temperature for 30 min. Then, the coverslips were removed, and the surfaces of the slides were rinsed with 0.4% Photo-Flo (Kodak). The air-dried slides were stored at -20℃ in black boxes or processed immediately for following immunofluorescence.

The slides were washed with 1X PBS in a staining jar on a benchtop shaker for 10 min to wash away the residual paraformaldehyde on the slides. The excess PBS was drained and 0.5 ml of blocking solution [1% BSA in PBS or 1% BSA in PBS plus fetal bovine serum (FBS) at 1 to 1 ratio for anti-HA antibody] was dropped on each slide without coverslips. After 30 min incubation at room temperature, the solution was discarded and 100 μl of 1% BSA in PBS containing primary antibody [mouse monoclonal anti-HA (16B12; Covance) used at 1:100 dilution] was added to each slide.

For double staining of Pch2 and Ssa3, mouse monoclonal anti-MYC (9E10; Santa Cruz) and rabbit polyclonal anti-HA antibody (PRB-101P; Covance) were used at 1:100 dilution. A large cover slip was placed on the slide, and the slide was incubated in a humidified box at 4℃ overnight. On the next day, the coverslips were discarded and the slides were washed for 3 times with 1X PBS in a staining jar on a benchtop shaker, 5 min per wash. The excess PBS was drained and 100 μl of 1% BSA in PBS containing secondary antibody [fluorescein isothiocyanate (FITC) -conjugated donkey anti-mouse and Texas Red-conjugated goat anti-rabbit and antibodies (Jackson ImmunoReseach) used at 1:200 dilution] was added to each slide. After incubating at room temperature in the dark for 3 hours, the slides were washed for 3 times with 1X PBS and mounted with 20 μl of Vectashield mounting medium (Vector Laboratories) containing 1 μg/ml DAPI. Slides were covered with the cover slips and sealed with nail polish. The chromosome spreads were observed under an Olympus AX70 fluorescence microscope (Olympus) and an Uplan Apo100x objective (Olympus).

Image analysis

The images of cells were captured using a PXL cooled charged-coupled device (CCD) camera (Photometrics, Tucson, AZ) and processed with the V for Windows software (Digital Optics, Auckland, New Zealand).

2.8 Yeast two-hybrid Screen

Yeast two-hybrid screen was performed using yeast host strain PJ69-4A and Y2HL libraries (James et al., 1996). PJ69-4A contained three different reporter genes, *HIS3*, *ADE2*, and *lacZ*, each driven by Gal4-inducible promoters *GAL1*, *GAL2*, and *GAL7*, respectively. Y2HL libraries were prey containing *Gal4* activation domain (AD) and the selectable marker *LEU2*, prepared from each of the three libraries, Y2HL-C1, Y2HL-C2, and Y2HL-C3. pGBDU-C1-*NDT80Δ404-627* (pT662) excluding activation domain of *NDT80* ORF was bait containing *Gal4* DNA binding domain (BD) and the selectable marker *URA3*. PJ69-4A (K589) cells were transformed with pT662 in advance to create K589 cells carrying pT662 plasmids. Then, libraries were transformed into K589/pT662 cells, and transformed cells were spread on the synthetic drop-out (SD) -Leu -Ura plates. After incubation at 30℃ for several days, numerous Leu^+ Ura^+ transformants arose. All transformants were replica onto SD-Leu-Ura-Ade plates for first screen. After incubation for another 6-7 days, appearance of Ade^+ colonies meant a positive interaction between bait and prey plasmids. Ade^+ colonies were streaked on SD -Leu-Ura plates; then, 2 single colonies of each transformant were patch on SD-Leu-Ura. The retest of interaction was carried out by replicaing candidates onto SD-Leu-Ura-Ade and SD-Leu-Ura-His containing 3mM 3-amino-1, 2, 4-triazole (3-AT), which functions in prevent *HIS3* reporter gene autoactivation. The candidates were patched on SD-Leu

to select the clones without bait plasmid and subsequently replica onto the SD-Leu containing 5-FOA plates to ensure the clones excluding bait plasmid. Next day, 3 single colonies of each candidate were patched on SD-Leu and then replica onto SD-Leu-Ade for checking if interaction is false positive. After plasmid DNA extraction of yeast and *E.coli* transformation, 12 colonies of bacterial cells of each candidate were inoculated, and plasmids were prepared by alkaline lysis method. Grouping of candidates were performed through digesting with several restriction enzymes. Finally, the plasmid of candidates were sequenced to identify and retransformed into K589/pT662 and K589/pGBDU-C1-*NDT80Δ346-627* (pT667) cells which excluding activation domain and bc region of *NDT80* to reproduce interaction and recognize whether the protein-protein interaction site between Ndt80 and candidate was at bc region of Ndt80.

2.9 Yeast two-hybrid Assay

Yeast two-hybrid assay based on the Gal4 system as described above. The two-hybrid constructions used in this study were generated by PCR and inserted into pGBDU-C1 (T477) or pGAD-C3 (T410). K589 cell was co-transformed with pGBDU-C1, C3-derived plasmids and pGAD-C1, C3-derived plasmids. Transformants were picked from SD-Leu-Ura plate and replica onto SD-Leu-Ura-Ade and SD-Leu-Ura -His containing 3mM 3-AT for protein-protein interaction test.

CHAPTER 3 The Function of Ssa3 in Meiosis

3.1 Ssa3 is uniquely required for checkpoint-mediated arrest of *zip1*

In the BR2495 strain background, *zip1* mutants results in a checkpoint-mediated arrest at the pachytene stage of meiotic prophase and fail to sporulate (Sym et al., 1993; Tung and Roeder, 1998). Deletion of *SSA3* partially abolishes the meiotic arrest of *zip1* with about 31% of a wild-type sporulation frequency (Table 3-1; Chen, 2003); however, *ssa3* mutants fail to bypass other two pachytene-arrest mutants, *hop2* and *dmc1* (Chen, 2003).

Previous study has been shown that mutation of *PCH2* relieves the checkpoint-induced pachytene arrest of the *zip1* with a wild-type sporulation frequency, and about half of *dmc1 pch2* cells have completed at least one division when 96% of *dmc1* mutants which are defective for interhomolog repair remain mononucleate because of *pch2* promotes intersister DSB repair; however, few mature asci are formed (San-Segundo and Roeder, 1999; Zanders et al., 2011). Thus, it is reasonable to speculate whether the *dmc1 ssa3* double mutant could also progress through nuclear divisions. The spore formation and nuclear division of *ssa3* mutation were examined in SK1 *dmc1* cells. After 24 hr in sporulation medium, sporulation frequency and nuclear division were the same in *DMC1/dmc1* (K561) and *DMC1/dmc1 ssa3/ssa3* (K563) cells, whereas both *dmc1/dmc1* (K560) and *dmc1/dmc1 ssa3/ssa3* (K472) cells failed to

sporulate and complete meiotic divisions (Table 3-2), suggesting that pachytene arrest caused by the absence of *DMC1* could not be relieved by *ssa3* mutants. Our results indicate that Ssa3 is likely involved in the pachytene checkpoint but is uniquely required for the checkpoint-mediated arrest of *zip1*.

3.2 Ssa3 and Pch2 probably do not involved in the same pachytene checkpoint pathway

Deletion of *SSA3* allows some *zip1* mutants to enter meiosis I, like deletion of *PCH2* alleviates the pachytene arrest of *zip1* (San-Segundo and Roeder, 1999), which raises the possibility that the Ssa3 and Pch2 proteins act in a common checkpoint pathway responded to *zip1* mutation. In order to explore whether Ssa3 is involved in the *PCH2-ZIP1*-dependent checkpoint pathway, we try to observe the subcellular localization of both Ssa3 and Pch2 proteins.

3.2.1 The N-terminal 3XHA-tagged Ssa3 is functional

To detect the subcellular localization of Ssa3 and Pch2 proteins, two proteins were differentially tagged. The three copies of hemagglutinin (HA) epitope have been fused at N-terminal of Ssa3 protein (Chen, 2003). Complementation assays were used to check the function of HA-tagged Ssa3. In BR2495, the *ssa3* null mutant does not confer obvious defects in growth and sporulation, but the *zip1 ssa3* double mutant relieves a

partial pachytene arrest of *zip1* (Table 3-1). Therefore, we transformed low-copy number plasmids with centromere for expression of *3XHA-SSA3*, and low-copy expression of *SSA3* as a control, into the *zip1 ssa3* double mutant strain to check if 3XHA-Ssa3 protein was functional. As shown in Table 3-3, low-copy expression of 3XHA-Ssa3 in the *zip1 ssa3* double mutant cells could complement *zip1 ssa3*, the sporulation frequency decreased near to the control. The result indicates that 3XHA-Ssa3 protein is functional.

3.2.2 The C-terminal 3XMYC-tagged Pch2 is functional

Ssa3 has been fused with HA tag; therefore, three copies of the c-*myc* (MYC) epitope were fused at the N-terminal or C-terminal of Pch2 protein. To test whether the MYC-tagged Pch2 protein was functional, the complementation assays were performed. The *pch2* null mutant has no apparent effects on mitotic phenotype and sporulation frequency; however, deletion of *PCH2* completely abolishes the meiotic arrest of *zip1*, for the *zip1 pch2* double mutant displays a wild-type sporulation frequency in the BR2495 strain background (San-Segundo and Roeder, 1999). Thus, complementation assay of N-terminal and C-terminal MYC-tagged Pch2 were performed in the *zip1 pch2* double mutant, and low-copy expression of *PCH2* as a control. We found the N-terminal MYC-epitope had interference in the function of Pch2 because the

sporulation frequencies of *zip1 pch2* cells with 3XMYC-Pch2 or 6XMYC-Pch2 were close to the *zip1 pch2* double mutant levels (Table 3-4), while the C-terminal 3XMYC-tagged Pch2 was functional since low copy expression of Pch2-3XMYC complemented about 32.2% of *zip1 pch2* cells as did low copy expression of Pch2 (Table 3-4). As a result, we used *PCH2-3XMYC* and *3XHA-SSA3* to detect their subcellular localizations.

3.2.3 Ssa3 and Pch2 do not co-localize to the pachytene chromosomes

To examine whether Ssa3 and Pch2 colocalized to the pachytene chromosome in wild type and the *zip1* mutant, diploid strains homozygous for spread meiotic nuclei and double stained with rabbit polyclonal anti-HA antibodies (PRB-101P; Covance) and mouse monoclonal anti-MYC antibodies (9E10; Santa Cruz). No staining was detected in wild-type and *zip1* control strains lacking the MYC and HA epitopes (Figure 3-1 A-E; Figure 3-2 A-E). In wild-type pachytene nuclei, Pch2 was found in the nucleolus and also detected in foci of chromosomes, which was seen in earlier cytological studies (Figure 3-1 I, N, and S; (San-Segundo and Roeder, 1999), and Ssa3 spread throughout pachytene chromosomes with an even pattern (Figure 3-1 G, L, and Q). In fact, it was difficult to determine whether Pch2 and Ssa3 colocalized to wild-type pachytene chromosomes. However, our images suggest that two proteins might not significantly

colocalize in wild type (Figure 3-1 J, O, and T).

In *zip1* pachytene nuclei, Pch2 mainly localized to nucleolus with a lower amount than which in wild type, and few of Pch2 foci still can be detected on chromosomes (Figure 3-2 I, N and S), which did not be showed in previous report (San-Segundo and Roeder, 1999). Ssa3 also localized to pachytene chromosomes in *zip1*, but we noted that the distribution of Ssa3 staining was not as even as in wild type, for Ssa3 proteins are detected in dotty form on pachytene chromosomes (Figure 3-2 G, L, and Q). The chromosomal localization of Ssa3 and Pch2 reveals that two proteins probably do not exhibit colocalization in the *zip1* mutant as well (Figure 3-2 J, O, and T). Together, these data suggest that Ssa3 and Pch2 may be involved in two distinct *zip1*-induced pachytene checkpoint pathways.

3.3 Ssa3 localizes to axial element/lateral element of synaptonemal complex

In the experiment which Ssa3 and Pch2 double staining, we note the distribution of Ssa3 may be a little different between wild-type and *zip1* mutant cells. As a result, the chromosomal localization of Ssa3 were further confirmed in wild type and *zip1* mutant by enhancing HA-Ssa3 signal, that is, the high-copy number plasmid carrying *3XHA-SSA3* (pT202) was used for overproducing 3XHA-Ssa3, and high-copy number plasmid carrying *SSA3* (pT199) as a no-tagged control. Overexpression of *SSA3* does

not result in the effect on sporulation (Chen, 2003). The high-copy number plasmids were transformed into wild type (BR2495) and *zip1* mutant (MY152). Meiotic chromosomes were surface-spread and stained with mouse monoclonal anti-HA antibodies (16B12; Covance).

Distributions of Ssa3 are mildly different between in wild-type and *zip1* overproduing HA-Ssa3 strains. In wild-type pachytene nuclei, we observed two types of pattern of Ssa3 localization. The First type was overproduced Ssa3 was condensed, and continuously localized as lines along chromosomes (Figure 3-3 D-I). The second type was overproduced Ssa3 was present in a loose and linear form along chromosomes (Figure 3-3 J-L). In addition to chromosomal arms, some of Ssa3 were accumulated in a region where like the unsynapsed region which was one character of the nucleolus (Figure 3-3 F and I). Localization of a part of Ssa3 to the nucleolus was confirmed by double staining with Ssa3 and the nucleolar protein Pch2 (Figure 3-3 Q-T). Ssa3 does not accumulate in the nucleolus in some of wild-type spreads would be the result of different intracellular concentrations of Ssa3 protein or there is a dynamic change of Ssa3 loading between chromosomes and nucleolus. In *zip1*, we also observed two types of the localization pattern of Ssa3. The first type was overproduced Ssa3 localized along the pachytene chromosomes and accumulated in the nucleolus in *zip1*, but it was not as condensed as in wild type (Figure 3-4 D-I and Q-T). The second type was overproduced

Ssa3 was present in a dotty form on pachytene chromosomes and undetectable in the nucleolus (Figure 3-4 J-L). One explanation for these opposing effects in two types of Ssa3 staining pattern in both wild type and *zip1* mutant is that different intracellular concentrations of Ssa3 protein, caused by variation in plasmid copy number, have different effects on Ssa3 protein loading. Based on cytological data, we suggest that probably Ssa3 loading on the pachytene chromosomes in the *zip1* mutant is slightly different from in wild type.

To determine whether the difference of Ssa3 pattern between wild type and *zip1* mutant would result from absence of Zip1, or it was a general appearance in pachytene-arrested cells, the chromosomal localization of Ssa3 was examined in the *ndt80* mutant cells. The *ndt80* null mutation arrests at the pachytene stage, with homologs connected by SCs and spindle pole bodies duplicated but unseparated (Xu et al., 1995). In *ndt80*, Ssa3 was loaded continuously along pachytene-arrested chromosomes as did in wild type (Figure 3-5), indicating that the dotty form of Ssa3 loading could be caused by absence of Zip1, rather than being a result of pachytene arrest. Zip1 protein is the central element of SC, we thus suggest that Ssa3 probably localize to SC and is involved in chromosome morphology.

To further investigate the exact localization of Ssa3 in *zip1* chromosomes, MYC-tagged Red1 fusion protein was constructed and served as a marker for axial

element/lateral element of SC. Red1, a component of meiosis-specific axial elements and lateral elements of mature SCs, associates with meiotic chromosomes before pachytene with smaller dot-like foci, and extends over the lengths of unsynapsed axial elements with the continuities at pachytene in the *zip1* mutant (Smith and Roeder, 1997). Double staining of HA-Ssa3 and Red1-MYC showed that Ssa3 colocalizes to Red1 in *zip1* pachytene-arrested chromosomes (Figure 3-6 I and N). The results suggest that Ssa3 protein probably localizes to axial element/lateral element of SC.

On the other hand, we also tried to detect endogenous HA-Ssa3 signal on both wild-type and *zip1* pachytene chromosomes; however, Ssa3 signal was weak, and tends to dotty form rather than to linear form either in wild-type or *zip1* mutant strain.

3.4 Analysis of *SSA3* at high temperature

3.4.1 Suppression of *zip1* by *ssa3* is temperature dependent

Ssa3 is a member of HSP70 family, inducing by heat shock or stresses prompt an investigation of whether temperature is an important variable for *ssa3* suppress *zip1*. Sporulation and nuclear division of *ssa3* were examined in parallel at high temperature, 32.5℃, and at the standard temperature for yeast studies, 30℃. The *ssa3* single mutant sporulated with a wild-type level at 32.5℃; however, only 2% and 8% of *zip1 ssa3* cells have generated asci and completed meiotic divisions at 32.5℃ (Table 3-5), indicating

that *ssa3* suppress *zip1* arrest is temperature dependent.

Sporulation frequencies of *pch2* and *zip1 pch2* mutants were examined at high temperature as well. Compared with at 30℃, *pch2* mutant was defective in asci formation and nuclear division at 32.5℃ (Table 3-5; see Chapter 4), while the sporulation of *zip1 pch2* double mutant did not be affected at 32.5℃ (Table 3-5).

3.4.2 The chromosomal localization of Ssa3 at high temperature is similar to that at low temperature

Localization studies show that chromosomal localization of Ssa3 during pachytene stage is different between wild type and *zip1* at normal temperature. Whether the localization of Ssa3 would be changed when cells are incubated at higher temperature? We observed the localization of Ssa3 protein in both wild type and *zip1* overexpressing *3XHA-SSA3* at 32.5℃ and 30℃. As shown in Figure 3-7, Ssa3 proteins also localized along wild-type pachytene chromosomes, and were concentrated in the nucleolus at 32.5℃, like at 30℃ (Figure 3-7). In *zip1*, the distribution of Ssa3 was present in dotty form at 32.5℃ as well as at 30℃ (Figure 3-8). The data show that the localization of Ssa3 is constant even the incubation temperature is elevated, so probably the localization of Ssa3 is excluded from the possible reasons of deletion of *SSA3* can not suppress arrest of *zip1* at high temperature.

CHAPTER 4 Analysis of *pch2* Mutant at High Temperature

4.1 The *pch2* mutant is defective in spore formation and nuclear division at high temperature

In the experiment examining sporulation frequency and meiotic division of the *zip1 ssa3* double mutant at high temperature, we noted a dramatic decrease of about 37.8% in sporulation frequency in *pch2* at 32.5℃ (Table 3-5). In addition to sporulation frequency, a decrease of nuclear division was also exhibited in the *pch2* mutant at high temperature. As shown in Table 3-5, about 73% of *pch2* mutants have completed at least one division at 30℃, but only 36.5% at 32.5℃, indicating that the reduced sporulation frequency in *pch2* mutants at high temperature is due to the decrease in the progression through nuclear divisions, but not in the process of spore formation.

Although MI/spore formation in *pch2* mutant is delay at high temperature has been showed (Börner et al., 2008), we still performed time course analyses to monitor the kinetics of meiosis in the wild-type, *pch2*, *zip1*, and *zip1 pch2* mutant cells at different temperatures. Cells were inoculated into sporulation medium to induce meiosis, and then harvested at a 2-hr interval to assess spore formation and nuclear divisions. The *pch2* mutants exhibited nearly wild-type kinetics and frequencies of nuclear division and spore formation at 30℃ with a two-hour delay (Figure 4-1) consistent with previous study (Hochwagen et al., 2005). At 32.5℃, the *pch2* mutant exhibited significantly delayed and reduced levels of nuclear division and spore formation (Figure

4-2), and the phenomenon was more significant at 33.5℃ (Figure 4-3). On the other hand, unlike the *pch2* mutant, the *zip1 pch2* double mutant displayed a wild-type level of kinetics of nuclear division and spore formation without delay at 30℃ (Figure 4-1); however, they were also delayed and reduced at 32.5℃ and 33.5℃ but were less pronounced than in the *pch2* mutant (Figures 4-2 and 4-3). These results indicate that the level of sporulation in *pch2* could be affected obviously by incubation condition (e.g., high temperature) though limiting *pch2* cells for pachytene exit and MI entry.

4.2 Wild type-like patterns of asci type, spore viability and tetrad distribution in the *pch2* mutant at high temperature

Following observation of high temperature-modulated interference in *pch2*, we next examined the asci type and spore viability in *pch2* mutant at 32.5℃ and 30℃. Asci produced from wild type, *pch2* and *zip1 pch2* cells were classified as tetrad/triad, dyad or monad. As shown in Table 4-1, the percentage of tetrad/triad, dyad, and monad production were similar in wild-type, *pch2,* and *zip1 pch2* mutant cells at both temperatures. The spore viability of *pch2* mutant exhibited a nearly WT level at 32.5℃ (82.1% versus 86.7%) (Table 4-2), indicating that the asci with normal spore viability were produced in the *pch2* mutant at high temperature. Spore viabilities of the *zip1 pch2* mutant were alike at both temperatures with about only 50% of spores are viable (Table 4-2) due to crossover is affected by *zip1* (San-Segundo and Roeder, 1999).

Besides, the tetrad distributions were also compared between wild type, *pch2*, and *zip1 pch2* cells. In wild type at 32.5℃, 70.5% of tetrads underwent normal meiotic chromosome segregation as suggested by levels of four spore-viable tetrads, compared to 80.7% in wild type sporulated at 30℃ in parallel (Figure 4-4, blue bars). At 30℃, a wild type-like pattern of tetrad distribution was observed in *pch2* consistent with earlier reports in the SK1 strain background (Figure 4-4A, red bar; Joshi et al., 2009; Zanders and Alani, 2009); however, at 32.5℃, the *pch2* mutant produced 52.3% four spore-viable tetrads, compared to frequency of 79.6% at 30℃ (Figure 4-4, red bars). The *zip1* mutant is defective for crossover interference and results in homolog nondisjunction, so tetrads with two-viable or zero-viable spores are present (Sym and Roeder, 1994). Thus, at both 30℃ and 32.5℃, the *zip1 pch2* mutant gave rise to about 20-25% of two spore-viable and zero spore-viable tetrads (Figure 4-4, green bars). Taken together, high temperature could result in the defective sporulation in *pch2* with normal asci, but somehow the spore viability and chromosome segregation are likely to be affected by high temperature either in *pch2* or in wild type.

4.3 The high temperature-modulated pachytene arrest in *pch2* mutant is stage-dependent reversible

To test whether the defective sporulation causing by high temperature in *pch2* mutants could be reversible when the cells were down-shifted to normal temperature,

the reversible thermal treatments were performed at the time points around the timing of MI entry (Figures 4-2 A and C; 24 hour) or the completion of divisions (Figures 4-2 A and C; 32 hour), and the nuclear division and spore formation were examined at the late time points after inducing sporulation (44 hour and 48 hour). The sporulation in *pch2* was able to be recovered nearly to the 30℃ level when a temperature down-shift from 32.5℃ to 30℃ was treated around the timing of MI (at 24 hour time point), for there are about 78.9% of pachytene-arrested *pch2* cells progressed through two meiotic divisions and 63.6% of *pch2* cells sporulated (Figure 4-5, open circles). Nevertheless, it was nonreversible when a down-shift from 32.5℃ to 30℃ was occurred around the timing of cells almost completed two meiotic divisions (at 32 hour time point) (Figure 4-5, open triangles). The results indicate that elevated temperature-modulated pachytene arrest in *pch2* mutant could be reversible only when the incubation temperature is lowered to 30℃ at the timing before MI entry, suggesting that the reversible pachytene arrest in the *pch2* mutant is stage-dependent.

4.4 The pachytene checkpoint is likely to be involved in the high temperature-modulated arrest in *pch2* mutant

Temperature is an effector of early stages of meiotic recombination (Börner et al., 2004), and absence of Pch2 dramatically delays in crossover/noncrossover formation and pachytene exit at high temperature (Börner et al., 2008). To further determine if the

pachytene arrest of *pch2* at high temperature was mediated though the pachytene checkpoint, K1094 strain was used, whose *NDT80* was replaced by *NDT80-bc* in *pch2* mutant. *NDT80-bc* mutation is able to completely bypass the pachytene checkpoint (Wang et al., 2011). At 30℃, *pch2 NDT80-bc* cells displayed a wild-type level of sporulation frequency and nuclear division (Table 4-3); furthermore, *pch2* cells themselves exhibited a two-hour delay in meiotic progression, and it was able to be suppressed by *NDT80-bc* (Figure 4-6). At 32.5℃, the reduced sporulation frequency and nuclear division exhibited in the *pch2* mutant did not occur in the *pch2 NDT80-bc* cells (Table 4-3), and the kinetics of meiosis in the *pch2 NDT80-bc* was similar to wild type at 32.5℃ (Figure 4-7), indicating that the high temperature-modulated arrest in *pch2* mutant is probably pachytene checkpoint dependent.

The *NDT80-bc* mutant provides a full bypass of the pachytene checkpoint in the several pachytene-arrested mutants, producing spores with low spore viability, suggesting that the defects in chromosomes persist in the double mutants (Wang et al., 2011). As a result, we reasonably speculate that the spore viability of the *pch2 NDT80-bc* mutant at high temperature would be much lower than that in the *pch2* single mutant. However, spore viability of *pch2 NDT80-bc* was about 84.7% and 93.8% of *pch2* at 30℃ and 32.5℃, respectively (Table 4-2). In addition, *pch2 NDT80-bc* produced 62.5% four spore-viable tetrads compared to frequency of ~80% of wild type

and *pch2* at 30℃ (Figure 4-4 A, purple bars); at 32.5℃, *pch2 NDT80-bc* produced 51.1% four spore-viable tetrads similar to 52.3% in *pch2* (Figure 4-4 B, purple bars). These results reveal that most of pachytene-arrested cells of *pch2* conferred by high temperature are nearly normal in spore viability, suggesting that probably the chromosomal damage conferred by high temperature in *pch2* is mild even the pachytene checkpoint is induced to arrest most of *pch2* cells, and a two-hour delay of MI in *pch2* at normal temperature is required for ensuring that accurate of meiotic progression.

At normal temperature, the *pch2* mutant exhibits a wild-type level of sporulation, and *pch2* can completely abolish the *zip1* pachytene arrest; however, at high temperature, most of the *pch2* mutants arrest at pachytene, whereas the *zip1 pch2* double mutant still displays a near-WT sporulation frequency. Zip1, which encodes the central element of the SC (Sym et al., 1993), is a member of ZMM proteins (Zip1-4, Mer3, and Msh4/5) reported that function in SC formation, recombination, and meiotic progression (Börner et al., 2004). Whether the presence of SC is required for the induction of the pachytene checkpoint in *pch2* mutant at high temperature? To test this hypothesis, we analyzed spore formation and meiotic division in the *zip3 pch2* double mutant. In absence of Zip3, meiotic crossover and MI entry are reduced and delayed like the *zip1* mutant; however, *zip3* mutant exhibits partial SC formation, while *zip1* mutant exhibits none (Agarwal and Roeder, 2000). Our prediction is that the *zip3 pch2*

mutant exhibits partial SC and thus can not completely activate SC-dependent pachytene checkpoint at high temperature, resulting in double mutants could not undergo MI division, and final product level should be lower than the *zip1 pch2* mutant. The results are consistent with our prediction; only 26.5% and 35.5% of the *zip3 pch2* mutants generated asci and completed nuclear divisions at 32.5℃, compared to 70% and 77.5% of cells sporulated at 30℃, respectively (Table 4-4). On the other hand, *zip3* mutant exhibited the severe decrease in sporulation frequency and nuclear division at high temperature (Table 4-4), also showed in earlier report (Börner et al., 2004). Our data suggest that a SC-dependent pachytene checkpoint inducing at high temperature is present in the *pch2* mutant.

4.5 The chromosomal localization of Pch2 at high and low temperatures are alike

Previous reports on Pch2 have suggested that nucleolar Pch2 is as the mediator of MI arrest in *zip1* mutant (San-Segundo and Roeder, 1999), and the chromosomal Pch2 promotes progression of crossover and noncrossover recombination during wild-type meiosis (Börner et al., 2008), implying that the localization of Pch2 is important for its function. To investigate whether the function of Pch2 may be different at high temperature from low temperature, we attempted to observe the chromosomal localization of Pch2 in wild type and the *zip1* mutant in parallel at 32.5℃ and 30℃. As

shown in Figure 4-8, Pch2 also localized to nucleolar region and chromosomal arm at 32.5℃ (Figure 4-8 D-F), and the amount of Pch2 loading like which at 30℃ (Figure 4-8 G-I). In the *zip1* mutant, most Pch2 proteins localized to the nucleolus and some chromosomal foci were detected at 32.5℃ (Figure 4-9 D-F) as did at 30℃ (Figure 4-9 G-I). The data show that the chromosomal localization of Pch2 does not change when the incubation temperature is elevated.

CHAPTER 5 The Cytoplasmic Anchor Protein of Ndt80

In our hypothesis, the nuclear import of Ndt80 is regulated by the pachytene checkpoint through a physical interaction between Ndt80 and an unknown cytoplasmic anchor protein. We employ three strategies to identify the potential anchor protein of Ndt80: *Saccharomyces* Genome Database search, yeast two-hybrid screen, and immunoprecipitation. In this thesis, we focus on database search and yeast two-hybrid screen.

5.1 Analysis of *SSA2*

A search in the *Saccharomyces* Genome Database (http://avis.princeton.edu/pixie/viewgraph.php?graphID=19) showed that Ssa2 protein may physically interact with Ndt80. This analysis data was obtained by the genome-wide screen for protein-complexes in budding yeast, using tandem-affinity purification and mass spectrometry (TAP-MS). Through systematic tagging of ORFs, the majority of protein-complexes were purified several times and were quantified the propensity of proteins to form partnerships, after that, the protein-protein interactions were identified (Gavin et al., 2006; Krogan et al., 2006).

5.1.1 Sporulation frequency and nuclear division are mildly increased in the *zip1 ssa2* double mutant

To investigate whether the yeast Ssa2 protein was the potential anchor protein of Ndt80, null mutant of *SSA2* was generated and analyzed its effect on sporulation. Disruption of *SSA2* was performed in W303 strains, cells were sporulated at 30℃ for three days. Sporulation frequency in *SSA2/ssa2* (heterozygous) and *ssa2/ssa2* (homozygous) mutants are little higher than in wild type. As shown in Table 5-1, the sporulation frequency of the heterozygous *ssa2* mutant was 146.8% of wild-type; the homozygous *ssa2* mutant was 138.4% of wild-type.

Absence of Zip1, a structure component of the central region of the SC, cells arrest at the pachytene stage with unsynapsed chromosomes and fail to sporulate (Sym et al., 1993). If Ssa2 was the anchor protein of Ndt80, we expected that the *zip1 ssa2* double mutant may sporulate with a wild-type level since the nuclear import of Ndt80 can not be inhibited by the pachytene checkpoint though Ssa2. The *zip1* mutant displays a low level (5.8%) of spore formation in the W303 strain background (Table 5-2). In contrast, 13.8% and 14.0% of cells sporulated in the *zip1/zip1 SSA2/ssa2* and *zip1/zip1 ssa2/ssa2* mutants (Table 5-2). Besides, we examined the sporulation of *zip1 ssa2* in another strain background, BR2495, the sporulation frequency of either *zip1/zip1 SSA2/ssa2* or *zip1/zip1 ssa2/ssa2* was similar to *zip1* single mutant, unlike that in W303 (Table 5-2). The results suggest that *ssa2* somehow raises the sporulation in wild type and results in

a partial bypass of *zip1* meiotic arrest, however, dependent on the strain background.

In addition to examine the sporulation frequency, we also observed nuclear division of the *ssa2* mutant. Cells were inoculated into sporulation medium at 30℃ to induce meiosis, and were harvested at 36 hours and 48 hours. Meiotic nuclear divisions were examined by DAPI staining. After 36 hours in sporulation medium, 12.9% of *zip1/zip1 SSA2/ssa2* cells and 10.8% of *zip1/zip1 ssa2/ssa2* cells undergone meiotic division. After 48 hours in sporulation medium, 62.9% wild-type cells have completed nuclear divisions and 95% of *zip1* cells remain mononucleate, while about 24.5% of *zip1/zip1 SSA2/ssa2* and 24.0% of *zip1/zip1 ssa2/ssa2* mutants have undergone meiotic nuclear divisions (Table 5-3). In both time points, we observed that the frequencies of spore formation and nuclear division in the *zip1/zip1 SSA2/ssa2* and *zip1/zip1 ssa2/ssa2* mutants were higher than that in *zip1* mutant in the W303 strain background (Table 5-3), indicating that Ssa2 might be required for pachytene checkpoint machinery.

There is a point mutation of *URA3* gene in W303 strain, *ura3-1*, which guanine (G) to adenine (A) transition at residue 701 of the coding sequence, changing amino acid residue 234 from glycine (Gly, G) to glutamate (Glu, E) (Yan Li, Glenn Manthey, and Adam Bailis, unpublished results). Disruption of *SSA2* was performed by replacement of *SSA2* gene with *URA3* gene used as an auxotrophic marker. In order to ensure the increased sporulation frequency and nuclear division in the *zip1 ssa2* double mutant

were the results of *SSA2* deletion rather than the interference of *URA3* gene, we created a strain in the W303 strain background, *URA3*$^{+}$, whose *ura3-1* alleles were replaced by *URA3*, and compared with *ssa2::URA3* mutant in sporulation frequency and nuclear division after 48 hours in sporulation medium. The results showed that the frequencies of spore formation and nuclear division in the *URA3*$^{+}$ cells were near to wild-type levels and in the *zip1 URA3*$^{+}$ cells were also similar to the *zip1* mutant (Table 5-4). On the other hand, we found that the sporulation frequency was 10.0% and nuclear division was 9.5% in the *zip1 ssa2* double mutant, but they were only 6.5% and 5.0% in the *zip1 URA3*$^{+}$ cells (Table 5-4), suggesting that the effect on meiosis in the *zip1 ssa2* double mutant as a consequence of the lack of Ssa2.

5.1.2 Overproduction of Ssa2 in the Ndt80-overexpressed cells does not decrease sporulation frequency

Ndt80 overproduction (OP) could bypass the pachytene checkpoint without suppressing the *zip1* defects, and allow defective cells to sporulate; the sporulation frequency increased from 0 to 18% (Tung et al., 2000), for some Ndt80 might escape the control of checkpoint protein and induce the expression of MSG (Model in (Wang et al., 2011); Figure 5-1D). Therefore, we next asked whether overexpression of *SSA2* would affect the pachytene checkpoint in the *zip1* mutant overexpressing *NDT80* strain. A hypothetic model as shown in Figure 5-1E, if Ssa2 plays a role in anchoring Ndt80

when the pachytene checkpoint is triggered, it is reasonable to hypothesize that overproduce Ssa2 might completely anchor Ndt80 which escape from the pachytene checkpoint in *zip1 NDT80-OP* cells, then lower the sporulation frequency (Figure 5-1 E).

Two high-copy number plasmids pTP73 (YEp351-*NDT80*) and pT659 (pRS424-*SSA2*) were co-transformed into wild-type and *zip1* cells in BR2495 for Ndt80 and Ssa2 overproduction. Sporulation frequency of wild-type cells expressing *NDT80* and *SSA2* is indistinguishable from cells carrying two empty control plasmids (Table 5-5). Ndt80-OP modulated sporulation frequency in *zip1* from 0 to 10.7% was consistent with previous data, and the *zip1* cells expressing *NDT80* and *SSA2* sporulated with a *zip1 NDT80-OP* cell level (Table 5-5), suggesting that overproduction of Ssa2 could not confer ability of targeting escape of Ndt80 by the pachytene checkpoint. The data indicate that Ssa2 may not interfere with the nuclear import of Ndt80 and not be a unique control factor of Ndt80.

5.1.3 An unapparent physical interaction between Ssa2 and Ndt80

Although our results reveal that Ssa2 is not a cytoplasmic anchor protein of Ndt80, we try to use yeast two-hybrid analysis to confirm the physical interaction between Ndt80 and Ssa2, proposed by yeast database. Due to Ndt80 is a transcription activator,

we have to eliminate the possibility of self-activation of Ndt80. As a result, *NDT80* without its activation domain, amino acid residues from 424-627, was constructed for further experiments use, and the loss of self-activation function of *NDT80Δ424-627* has been ensured (Figure 5-2). For this study, *NDT80*Δ424-627 (*NDT80 w/o AD*) in-frame deletion fragment was cloned into a plasmid containing the Gal4 binding domain (BD), and full length of *SSA2* gene was cloned into a plasmid containing the Gal4 activation domain (AD). In addition, we constructed a BD-derived plasmid that *NDT80* without both activation domain and bc region (amino acid residue 346-627) (Wang et al., 2011), abbreviating to *NDT80 w/o bc & AD*, which was used as a negative control to confirm the interactive site between Ndt80 and Ssa2 is localized to bc region.

Yeast two-hybrid analysis showed that Ndt80 did not significantly interact with Ssa2, for when in the presence of BD-Ndt80 w/o AD and AD-Ssa2, cells do not grow on the selective plates, SD-Leu -Ura -Ade and SD-Leu -Ura -His containing 3mM 3-AT (Figure 5-3). Vector plasmids of the activation domain (pGAD) and the binding domain (PGBDU) were used as negative controls and showed no self-activation effect (Figure 5-3). Ssa2 may have no interaction with Ndt80, or the interactive site between Ssa2 and Ndt80 is localized to activation domain of Ndt80, suggesting that Ssa2 is not the potential checkpoint-activated cytoplasmic anchor protein of Ndt80.

5.2 Yeast Two-Hybrid Screen

To identify the potential anchor protein of Ndt80, we performed yeast two-hybrid screen using the Y2H genomic library that a large pool of yeast proteins fused with Gal4 activation domain (AD-Library) as prey (James et al., 1996). Ndt80 removing its activation domain as bait, thereby eliminating the doubt about the self-activation interference of Ndt80 (Figure 5-2). Ndt80 w/o AD was cloned into a pGBDU-C1 vector containing the Gal4 DNA binding domain to create BD-Ndt80 w/o AD fusion protein.

In order to improve the yeast transformation efficiency of AD-Library, PJ69-4A (K589) cells were transformed with pGBDU-C1-Ndt80 w/o AD previously, and then AD-Library plasmids were transformed into PJ69-4A containing pGBDU-C1-Ndt80 w/o AD and spread on SD-Leu and Ura plates. The colonies could be visible about 3 days; transformed cells were subsequently replicated onto SD minus Leu, Ura and Ade plates for the first screening. *ADE2* gene was used as the reporter gene to select positive colonies which meant their *ADE2* gene were activated, and supported the growth of the single cells to form the colonies. The positive $Ade2^{+}$ colonies to arise on SD minus Leu, Ura, Ade media were picked and streaked on SD minus Leu, Ura media. Then, two single colonies from each positive colony were replicated onto SD minus Leu, Ura, Ade media and SD minus Leu, Ura, His media (containing 3mM 3-AT) for the second screening. *HIS3* gene is another reporter gene used to confirm the positive effect

observing in the first screening and to eliminate the false positives.

About $1.1X10^5$ independent tranformants have been screened, and twenty-one colonies were isolated as candidates. However, the interaction between bait and candidates are non-reproducible during retransformation test. So far, we do not find candidate of potential cytoplasmic anchor protein of Ndt80.

CHAPTER 6 DISCUSSION

6.1 Ssa3 is likely part of the synaptonemal complex

HSP70-2, a homolog of budding yeast *SSA3* in mice, is expressed and synthesized mainly during early meiotic prophase of spermatogenesis, suggesting that the protein has a role in meiosis (Allen et al., 1988). The HSP70-2 protein begins to associate with axial elements and accumulate in nucleolus at early prophase (leptotene-zygotene), increases in amount along the synaptonemal complexes (SCs) and decreases in nucleolus during mid-prophase (pachytene), and persists until SCs disassemble in late prophase (diplotene) spermatocytes (Allen et al., 1996). As a result, HSP70-2 has been implicated in a part of the SC, and it participates in SC function during meiosis in mice spermatocytes (Allen et al., 1996). In our immunostaining data, we found that the Ssa3 protein localizes along pachytene chromosome and accumulates in nucleolus in some wild type and *zip1* mutants. Like HSP70-2 in mice spermatocytes, we speculate that yeast Ssa3 is associated with axial element/lateral element of SC in meiotic cells. Besides, whether the Ssa3 signal in SC development and nucleolus display a dynamic change, which like HSP70-2 in mouse, is at present unknown.

Evidence that the Ssa3 protein could be a component of axial elements/lateral elements of SCs comes from the surface-spread and immunostaining experiments in which Ssa3 and Red1 colocalize to pachytene chromosomes in the *zip1* mutant. Red1 is

a major component of SC lateral elements and the axial elements which serves as precursors to lateral element (Smith and Roeder, 1997). Thus, we next can determine whether Ssa3 has physical interaction with Red1, other components of axial element such as Hop1, or assistant protein of axial element by gene mutation, yeast two-hybrid analysis or co-immunoprecipitation.

6.2 The role of meiotic chromosomal proteins in the pachytene checkpoint

In budding yeast, the meiosis-specific chromosomal proteins Red1, Hop1 and Mek1 are required for recombination, proper segregation of homologs, and the pachytene checkpoint. Red1 is a prominent structural component of meiotic axial elements and lateral elements of SCs (Smith and Roeder, 1997). Red1 interacts with itself and Hop1, which colocalizes with Red1 only in early meiotic prophase, and its assembly onto chromosomes depends on Red1 (de los Santos and Hollingsworth, 1999; Hollingsworth and Ponte, 1997; Smith and Roeder, 1997; Woltering et al., 2000). Mek1 is a protein kinase which functions together with Red1 and Hop1 to promote interhomolog recombination by suppressing DSB repair between sister chromatids (Bailis and Roeder, 1998; Hollingsworth and Ponte, 1997; Niu et al., 2007; Wan et al., 2004). Absence of Red1, Mek1 or Hop1 inactivates the pachytene checkpoint and allows mutants (such as *zip1*) undergoing checkpoint-mediated arrest exhibit meiotic

nuclear division and sporulation with a wild-type level (Woltering et al., 2000; Xu et al., 1997). Overproduction of either Red1 or Mek1, but not Hop1, suppresses checkpoint-mediated arrest at pachytene in *zip1*; however, co-overproduction of Red1 with Mek1 or co-overproduction of Hop1 with either Red1 or Mek1restores checkpoint function, indicating the correct stoichiometry of Red1, Mek1, and Hop1 is required for the pachytene checkpoint function (Bailis et al., 2000).

Kleckner and colleagues (1997) proposed that a properly developed interhomolog recombination complex emits a signal to inhibit SC disassembly, spindle pore body separation, and then delay meiotic progression until recombination is complete (Xu et al., 1997). Some studies suggest that modification of Red1 could be an inhibitory signal of the checkpoint. Red1 is a phosphoprotein that has been reported to be phosphorylated by Mek1 in earlier papers (Bailis and Roeder, 1998; Bailis and Roeder, 2000; de los Santos and Hollingsworth, 1999), but in later paper, they demonstrated that Red1 is phosphorylated by other unknown kinase (Wan et al., 2004). Phosphorylated Red1 prevents exit from pachytene, and the completion of meiotic recombination triggers the Glc7-mediated dephosphorylation of Red1 (Bailis and Roeder, 1998; Bailis and Roeder, 2000). Furthermore, recently studies reported that Red1 becomes small ubiquitin-like modifier (SUMO)-modified to promote the interaction of it and the central element protein Zip1, thereby securing SC assembly; moreover, Red1 could bind to 9-1-1

checkpoint complex (Ddc1/Mec3/Rad17) has been thought that Red1 is important for meiotic checkpoint activation (Eichinger and Jentsch, 2010; Lin et al., 2010). These researches reveal that meiotic chromosomal proteins such as axial elements and lateral elements of SC could confer the proper chromosomal structure for the pachytene checkpoint execution.

6.3 A model for the possible relationship between Ssa3 and the pachytene checkpoint

Hsp70-2$^{-/-}$ male mice are infertile, whereas *Hsp70-2*$^{-/-}$ female mice are fertile. Since spermatogenesis is disrupted with accumulation of late pachytene spermatocyte, in which SC structure is abnormal. Thus, HSP70-2 protein is thought to provide a link between SC structure and the G_2-M phase transition in prophase of meiosis I (Dix et al., 1996a; Zhu et al., 1997). This transition is mainly regulated through the pachytene checkpoint in yeast. Our present studies show that Ssa3 localizes to SCs, and deletion of *SSA3* partially relieves checkpoint-mediated arrest of *zip1*, with about quarter of the double mutant sporulate. Based on these data, we propose a model in which Ssa3 chaperone activity might be required for proteins of meiotic axial element or lateral element of SC to properly assemble into correct functional complex, thereby the pachytene checkpoint is efficiently activated to monitor the meiotic progression (Figure 6-1 A, B and C). Absence of Ssa3 protein in the *zip1* mutant, the chromosomal structure

may be too unstable or improper to efficiently activate the pachytene checkpoint, thus unsynapsed mutants could bypass pachytene checkpoint and undergo meiotic nuclear division (Figure 6-1 D). We can further confirm the chromosomal status of wild-type, *ssa3*, *zip1*, and *zip1 ssa3* cells by electron microscopy or chromosome sections.

6.4 Whether Ssa3 is required for checkpoint-mediated arrest of other *zmm* mutations?

Yeast mutants lacking meiotic proteins Zip1, Zip2, Zip3, Zip4, Mer3, Msh4 and Msh5 [ZMM proteins, also known as the synapsis initiation complex (SIC)] exhibit defects in SC formation, recombination, and meiotic progression (Börner et al., 2004). ZMM proteins are necessary for the ordered assembly of Zip1 into the SC. Zip1, a structural protein of the central region of the SC (Sym et al., 1993), starts to polymerize at sites of synapsis initiates, where other ZMM proteins are already present. Zip2, Zip3, and Zip4 mediate protein-protein interactions (Agarwal and Roeder, 2000; Chua and Roeder, 1998); Mer3, Msh4, and Msh5 promote recombination (Hollingsworth et al., 1995; Nakagawa and Ogawa, 1999; Novak et al., 2001).

Colocalization of ZMM proteins along meiotic chromosomes and similarities of *zmm* mutant phenotypes suggest functional collaboration between these proteins. Our data show that Ssa3 is specifically involved in the checkpoint-mediated arrest of *zip1*; therefore, we speculate that maybe Ssa3 protein is required for not only the meiotic

arrest of *zip1* but also for other *zmm* mutants. To address this possibility, we can examine the sporulation frequencies of double mutations which non-*zip1 zmm* mutants combine respectively with *ssa3* in the future.

6.5 Dependence of the *pch2* phenotype on incubation temperature

Pch2 is required for establishing proper organization of Hop1 and Zip1 in meiotic chromosomes, wild-type kinetics of meiotic progression, crossover (CO) interference, SC morphogenesis, and promoting interhomolog repair (Börner et al., 2008; Joshi et al., 2009; Zanders and Alani, 2009; Zanders et al., 2011). Meiosis-specific axis component Hop1 and the major SC central element Zip1 occur with differential abundance along pachytene chromosomes in wild type, whereas absence of Pch2 results in Hop1 and Zip1 both occur abundantly along the entire lengths of pachytene chromosome axes (Börner et al., 2008), so the SC length is increased (Joshi et al., 2009). Absence of Pch2 also dramatically delays progression along both CO and noncrossover (NCO) recombination pathways, thus pachytene exit and meiosis I are delayed (Börner et al., 2008). However, the levels of spore formation and nuclear division are only mildly affected by *pch2* mutation at 30℃ (Hochwagen et al., 2005; San-Segundo and Roeder, 1999; Wu and Burgess, 2006). In this study, we show that sporulation is significant delayed and reduced in *pch2* cells at elevated temperature (32.5℃, and the phenomena

are more pronounced at 33.5℃); the finding has been seen in another strain background, SK1 (Börner et al., 2008). Most *pch2* cells are arrested at the pachytene stage of meiotic prophase (Figures 4-2 and 4-3), suggesting that incubation temperature may have a role in affecting chromosomal metabolism or enhancing the defects conferred by *pch2*.

Temperature has been considered as an effector of meiotic progression. In yeast, the DSBs to single-end invasion strand exchange intermediates (SEIs) transition occurs earlier at high temperature (Börner et al., 2004). In mice, *HSP70-2* $^{-/-}$ male mice fail to form normal SCs and the spermatocytes are arrested at pachytene, but in *HSP70-2* $^{-/-}$ female mice oocytes are normal (Dix et al., 1996a). One reason of the difference between meiosis in the two sexes of mouse is meiosis occurs at different temperatures, at lower temperature in male, where meiosis occurs in the body periphery, while at higher temperature in female, where meiosis occurs internally. Furthermore, Börner and coworkers (2004) suggest that temperature could change the state of the DNA and the chromatin, due to the chromosomal events are likely driven by mechanical forces generated by chromatin expansion, higher temperature may promote occurrence of chromosomal events by increasing the chromatin expansion, so the forces are generated (Börner et al., 2004). To our studies, this suggestion may explain the *pch2* mutant phenotypes are significant at elevated temperature because of high temperature exerts its effects by changing the chromosomal status in *pch2* cells.

6.6 *pch2* undergoes SC-dependent checkpoint-induced cell cycle arrest at elevated temperature

Pachytene-arrest of *pch2* at high temperature is probably checkpoint-mediated. *NDT80-bc*, an in-frame deletion mutation which can completely bypass the pachytene checkpoint (Wang et al., 2011), relieves the reduced sporulation and exhibit a WT-like pattern of kinetics of meiosis in *pch2* at 32.5℃ (Table 4-2 and Figure 4-7), suggesting that the pachytene arrest present in *pch2* mutant at high temperature is the result of control of the pachytene checkpoint. However, unlike *pch2*, the *zip1 pch2* double mutant displays nearly wild-type levels of sporulation frequency and nuclear division at 32.5℃, indicating that the existence of SC would induce the pachytene checkpoint in *pch2* at elevated temperature. Mutation of *ZIP3* could form partial SC. Sporulation frequency of *zip3 pch2* is between *pch2* and *zip1 pch2* at 32.5℃ (Table 4-4), thus we propose that may be a SC-dependent checkpoint is induced in *pch2* when mutant is incubated at elevated temperature.

The idea is come from the pachytene arrest of a nonnull *ZIP1* mutation is severer than a null *ZIP1* mutation (Mitra and Roeder, 2007). This nonnull mutation, called *zip1-4LA*, results from replacing four leucine (L) residues in the central coiled-coil region to alanines (A). The *zip1-4LA* mutant might make the aberrant structure of the SC, and then may be trigger the synapsis checkpoint that monitors SC morphology (Mitra and Roeder, 2007). Perhaps the mutation region of *zip1-4LA* is required for

interacting with another protein, or possibly a component of SC. In *zip1* mutant, which fails to form SC, this protein might be absent from SC; in *zip1-4LA* mutant, this protein might be present in an aberrant SC. The presence of this protein might function as a signal of severer aberrant SC monitored by the checkpoint; as a result, the different severity of cell cycle arrest between *zip1* and *zip1-4LA* mutation could be explained (Mitra and Roeder, 2007). In our studies, perhaps high temperature could make SC structure unstable or defective in *pch2* mutant, and the checkpoint-induced signal may be stronger in the mutant whose SC is aberrant (e.g. *pch2*) than in the mutant which fails to form SC (e.g. *zip1 pch2*); therefore, *pch2* mutant rather than *zip1 pch2* mutant is arrested at pachytene by the checkpoint at elevated temperature.

6.7 Reversible pachytene arrest is present in yeast at high temperature

It was found that pachytene-arrested *pch2* cells at 32.5℃ could be reverted to meiotic process by lowering the temperature to 30℃ (Figure 4-5). Previous studies have reported that cells incubated in sporulation medium at a temperature inhibitory to sporulation became arrested at pachytene (Byers and Goetsch, 1982). The meiotic cells incubated at 36.5℃ was arrested at pachytene, and they could be released by two routes. First, cells transferred to rich medium can return to the mitotic cell cycle (vegetative growth). The second route of release was toward the completion of meiosis and

sporulation by leaving the cells in sporulation medium and lowering the incubation temperature to 20℃ (Byers and Goetsch, 1982; Simchen, 2009). In our experiment, it could resume to meiosis and sporulation when the pachytene-arrested *pch2* cell was shifted from 32.5℃ to 30℃ at 24 hr after incubating in sporulation medium, which meant the culture was arrested at 32.5℃ for about 12 hr, whereas the reversion was not present in the same strain shifting from 32.5℃ to 30℃ at 32 hr after inducing sporulation, which culture was arrested at 32.5℃ for about 20 hr. Byers and Goetsch (1982) describe that the efficiency of the reversion to vegetative growth is dependent on the timing that culture is held at the arrest. For 8-12 hr maintain at 36.5℃, nearly 100% of cells undergo budding within 3 hr after transferring to rich medium; however, for 16 hr maintain at 36.5℃, the reversion is more slowly and reduced (Byers and Goetsch, 1982). May be the factors required for meiotic process are normal in the *pch2* cells which are arrested at pachytene for shorter time, yet they are abnormal in *pch2* which are held at pachytene arrest for longer time; hence, only short-time arrested *pch2* cells at elevated temperature could complete meiosis and sporulation when the incubation temperature is lowered.

REFERENCES

Agarwal, S., and G.S. Roeder. 2000. Zip3 provides a link between recombination enzymes and synaptonemal complex proteins. *Cell*. 102:245-255.

Alani, E., R. Padmore, and N. Kleckner. 1990. Analysis of wild-type and rad50 mutants of yeast suggests an intimate relationship between meiotic chromosome synapsis and recombination. *Cell*. 61:419-436.

Allen, J.W., D.J. Dix, B.W. Collins, B.A. Merrick, C. He, J.K. Selkirk, P. Poorman-Allen, M.E. Dresser, and E.M. Eddy. 1996. HSP70-2 is part of the synaptonemal complex in mouse and hamster spermatocytes. *Chromosoma*. 104:414-421.

Allen, R.L., D.A. O'Brien, C.C. Jones, D.L. Rockett, and E.M. Eddy. 1988. Expression of heat shock proteins by isolated mouse spermatogenic cells. *Mol. Cell Biol*. 8:3260-3266.

Börner, G.V., A. Barot, and N. Kleckner. 2008. Yeast Pch2 promotes domainal axis organization, timely recombination progression, and arrest of defective recombinosomes during meiosis. *Proc. Natl. Acad. Sci. U S A*. 105:3327-3332.

Börner, G.V., N. Kleckner, and N. Hunter. 2004. Crossover/noncrossover differentiation, synaptonemal complex formation, and regulatory surveillance at the leptotene/zygotene transition of meiosis. *Cell*. 117:29-45.

Bailis, J.M., and G.S. Roeder. 1998. Synaptonemal complex morphogenesis and sister-chromatid cohesion require Mek1-dependent phosphorylation of a meiotic chromosomal protein. *Genes Dev*. 12:3551-3563.

Bailis, J.M., and G.S. Roeder. 2000. Pachytene exit controlled by reversal of Mek1-dependent phosphorylation. *Cell*. 101:211-221.

Bailis, J.M., A.V. Smith, and G.S. Roeder. 2000. Bypass of a meiotic checkpoint by overproduction of meiotic chromosomal proteins. *Mol. Cell Biol*. 20:4838-4848.

Becker, J., and E.A. Craig. 1994. Heat-shock proteins as molecular chaperones. *Eur. J. Biochem*. 219:11-23.

Bhalla, N., and A.F. Dernburg. 2005. A conserved checkpoint monitors meiotic chromosome synapsis in Caenorhabditis elegans. *Science*. 310:1683-1686.

Birnboim, H.C., and J. Doly. 1979. A rapid alkaline extraction procedure for screening recombinant plasmid DNA. *Nucleic Acids Res*. 7:1513-1523.

Bishop, D.K., D. Park, L. Xu, and N. Kleckner. 1992. DMC1: a meiosis-specific yeast homolog of E. coli recA required for recombination, synaptonemal complex formation, and cell cycle progression. *Cell*. 69:439-456.

Boeke, J.D., F. LaCroute, and G.R. Fink. 1984. A positive selection for mutants lacking orotidine-5'-phosphate decarboxylase activity in yeast: 5-fluoro-orotic acid resistance. *Mol. Gen. Genet*. 197:345-346.

Boorstein, W.R., T. Ziegelhoffer, and E.A. Craig. 1994. Molecular evolution of the HSP70 multigene family. *J. Mol. Evol*. 38:1-17.

Broach, J.R., J.R. Pringle, and E.W. Jones. 1992. The Molecular and cellular biology of the yeast Saccharomyces. Cole Spring Harbor Laboratory Press, Cold Spring Harbor, NY.

Byers, B., and L. Goetsch. 1982. Reversible pachytene arrest of Saccharomyces cerevisiae at elevated temperature. *Mol. Gen. Genet*. 187:47-53.

Chen, I.C. 2003. The function of yeast Ssa3 protein in meiosis. M. S. Thesis. National Taiwan University, Taipei.

Chu, S., J. DeRisi, M. Eisen, J. Mulholland, D. Botstein, P.O. Brown, and I. Herskowitz. 1998. The transcriptional program of sporulation in budding yeast. *Science*. 282:699-705.

Chu, S., and I. Herskowitz. 1998. Gametogenesis in yeast is regulated by a transcriptional cascade dependent on Ndt80. *Mol. Cell*. 1:685-696.

Chua, P.R., and G.S. Roeder. 1998. Zip2, a meiosis-specific protein required for the initiation of chromosome synapsis. *Cell*. 93:349-359.

Craig, E.A., J. Kramer, J. Shilling, M. Werner-Washburne, S. Holmes, J. Kosic-Smithers, and C.M. Nicolet. 1989. SSC1, an essential member of the yeast HSP70 multigene family, encodes a mitochondrial protein. *Mol. Cell Biol*. 9:3000-3008.

de los Santos, T., and N.M. Hollingsworth. 1999. Red1p, a MEK1-dependent phosphoprotein that physically interacts with Hop1p during meiosis in yeast. *J. Biol. Chem*. 274:1783-1790.

Dix, D.J., J.W. Allen, B.W. Collins, C. Mori, N. Nakamura, P. Poorman-Allen, E.H. Goulding, and E.M. Eddy. 1996a. Targeted gene disruption of Hsp70-2 results in failed meiosis, germ cell apoptosis, and male infertility. *Proc. Natl. Acad. Sci. U S A*. 93:3264-3268.

Dix, D.J., J.W. Allen, B.W. Collins, P. Poorman-Allen, C. Mori, D.R. Blizard, P.R. Brown, E.H. Goulding, B.D. Strong, and E.M. Eddy. 1997. HSP70-2 is required for desynapsis of synaptonemal complexes during meiotic prophase in juvenile and adult mouse spermatocytes. *Development*. 124:4595-4603.

Dix, D.J., M. Rosario-Herrle, H. Gotoh, C. Mori, E.H. Goulding, C.V. Barrett, and E.M. Eddy. 1996b. Developmentally regulated expression of Hsp70-2 and a Hsp70-2/lacZ transgene during spermatogenesis. *Dev. Biol*. 174:310-321.

Eddy, E.M. 1999. Role of heat shock protein HSP70-2 in spermatogenesis. *Rev. Reprod*. 4:23-30.

Eichinger, C.S., and S. Jentsch. 2010. Synaptonemal complex formation and meiotic checkpoint signaling are linked to the lateral element protein Red1. *Proc. Natl. Acad. Sci. U S A*. 107:11370-11375.

Gavin, A.C., P. Aloy, P. Grandi, R. Krause, M. Boesche, M. Marzioch, C. Rau, L.J. Jensen, S. Bastuck, B. Dumpelfeld, A. Edelmann, M.A. Heurtier, V. Hoffman, C. Hoefert, K. Klein, M. Hudak, A.M. Michon, M. Schelder, M. Schirle, M. Remor, T. Rudi, S. Hooper, A. Bauer, T. Bouwmeester, G. Casari, G. Drewes, G. Neubauer, J.M. Rick, B. Kuster, P. Bork, R.B. Russell, and G. Superti-Furga. 2006. Proteome survey reveals modularity of the yeast cell machinery. *Nature*. 440:631-636.

Georgopoulos, C., and W.J. Welch. 1993. Role of the major heat shock proteins as molecular chaperones. *Annu. Rev. Cell Biol*. 9:601-634.

Ghabrial, A., and T. Schupbach. 1999. Activation of a meiotic checkpoint regulates translation of Gurken during Drosophila oogenesis. *Nat. Cell Biol*. 1:354-357.

Gilbert, C.S., M. van den Bosch, C.M. Green, J.E. Vialard, M. Grenon, H. Erdjument-Bromage, P. Tempst, and N.F. Lowndes. 2003. The budding yeast Rad9 checkpoint complex: chaperone proteins are required for its function. *EMBO Rep*. 4:953-958.

Hartl, F.U. 1996. Molecular chaperones in cellular protein folding. *Nature*. 381:571-579.

Hartwell, L.H., and T.A. Weinert. 1989. Checkpoints: controls that ensure the order of cell cycle events. *Science*. 246:629-634.

Hassold, T., H. Hall, and P. Hunt. 2007. The origin of human aneuploidy: where we have been, where we are going. *Hum. Mol. Genet*. 16 Spec No. 2:R203-208.

Hepworth, S.R., H. Friesen, and J. Segall. 1998. NDT80 and the meiotic recombination checkpoint regulate expression of middle sporulation-specific genes in Saccharomyces cerevisiae. *Mol. Cell Biol*. 18:5750-5761.

Ho, T.M. 2005. The role of yeast Hsp26 in sporulation. M. S. Thesis. National Taiwan University, Taipei.

Hochwagen, A., and A. Amon. 2006. Checking your breaks: surveillance mechanisms of meiotic recombination. *Curr. Biol*. 16:R217-228.

Hochwagen, A., W.H. Tham, G.A. Brar, and A. Amon. 2005. The FK506 binding protein Fpr3 counteracts protein phosphatase 1 to maintain meiotic recombination checkpoint activity. *Cell*. 122:861-873.

Hoffman, C.S. 2001. Preparation of Yeast DNA. *Current Protocols in Molecular Biology*:13.11.11-13.11.14.

Hollingsworth, N.M., and L. Ponte. 1997. Genetic interactions between HOP1, RED1 and MEK1 suggest that MEK1 regulates assembly of axial element components during meiosis in the yeast Saccharomyces cerevisiae. *Genetics*. 147:33-42.

Hollingsworth, N.M., L. Ponte, and C. Halsey. 1995. MSH5, a novel MutS homolog, facilitates meiotic reciprocal recombination between homologs in Saccharomyces cerevisiae but not mismatch repair. *Genes Dev*. 9:1728-1739.

Hunt, C.R., D.L. Gasser, D.D. Chaplin, J.C. Pierce, and C.A. Kozak. 1993. Chromosomal localization of five murine HSP70 gene family members: Hsp70-1, Hsp70-2, Hsp70-3, Hsc70t, and Grp78. *Genomics*. 16:193-198.

Ito, H., Y. Fukuda, K. Murata, and A. Kimura. 1983. Transformation of intact yeast cells treated with alkali cations. *J. Bacteriol*. 153:163-168.

James, P., J. Halladay, and E.A. Craig. 1996. Genomic libraries and a host strain designed for highly efficient two-hybrid selection in yeast. *Genetics*. 144:1425-1436.

Joshi, N., A. Barot, C. Jamison, and G.V. Börner. 2009. Pch2 links chromosome axis remodeling at future crossover sites and crossover distribution during yeast meiosis. *PLoS Genet*. 5:e1000557.

Joyce, E.F., and K.S. McKim. 2009. Drosophila PCH2 is required for a pachytene checkpoint that monitors double-strand-break-independent events leading to meiotic crossover formation. *Genetics*. 181:39-51.

Joyce, E.F., and K.S. McKim. 2010. Chromosome axis defects induce a checkpoint-mediated delay and interchromosomal effect on crossing over during Drosophila meiosis. *PLoS Genet*. 6: e1001059.

Kandeel, F.R., and R.S. Swerdloff. 1988. Role of temperature in regulation of spermatogenesis and the use of heating as a method for contraception. *Fertil Steril*. 49:1-23.

Keeney, S., C.N. Giroux, and N. Kleckner. 1997. Meiosis-specific DNA double-strand breaks are catalyzed by Spo11, a member of a widely conserved protein family. *Cell*. 88:375-384.

Krogan, N.J., G. Cagney, H. Yu, G. Zhong, X. Guo, A. Ignatchenko, J. Li, S. Pu, N. Datta, A.P. Tikuisis, T. Punna, J.M. Peregrin-Alvarez, M. Shales, X. Zhang, M. Davey, M.D. Robinson, A. Paccanaro, J.E. Bray, A. Sheung, B. Beattie, D.P. Richards, V. Canadien, A. Lalev, F. Mena, P. Wong, A. Starostine, M.M. Canete, J. Vlasblom, S. Wu, C. Orsi, S.R. Collins, S. Chandran, R. Haw, J.J. Rilstone, K. Gandi, N.J. Thompson, G. Musso, P. St Onge, S. Ghanny, M.H. Lam, G. Butland, A.M. Altaf-Ul, S. Kanaya, A. Shilatifard, E. O'Shea, J.S. Weissman, C.J. Ingles, T.R. Hughes, J. Parkinson, M. Gerstein, S.J. Wodak, A. Emili, and J.F. Greenblatt. 2006. Global landscape of protein complexes in the yeast Saccharomyces cerevisiae. *Nature*. 440:637-643.

Kurtz, S., J. Rossi, L. Petko, and S. Lindquist. 1986. An ancient developmental induction: heat-shock proteins induced in sporulation and oogenesis. *Science*. 231:1154-1157.

Lamoureux, J.S., and J.N. Glover. 2006. Principles of protein-DNA recognition revealed in the structural analysis of Ndt80-MSE DNA complexes. *Structure*. 14:555-565.

Leu, J.Y., P.R. Chua, and G.S. Roeder. 1998. The meiosis-specific Hop2 protein of S. cerevisiae ensures synapsis between homologous chromosomes. *Cell*. 94:375-386.

Leu, J.Y., and G.S. Roeder. 1999. The pachytene checkpoint in S. cerevisiae depends on Swe1-mediated phosphorylation of the cyclin-dependent kinase Cdc28. *Mol. Cell*. 4:805-814.

Lew, D.J., and D.J. Burke. 2003. The spindle assembly and spindle position checkpoints. *Annu. Rev. Genet*. 37:251-282.

Li, X.C., and J.C. Schimenti. 2007. Mouse pachytene checkpoint 2 (trip13) is required for completing meiotic recombination but not synapsis. *PLoS Genet*. 3:e130.

Lin, F.M., Y.J. Lai, H.J. Shen, Y.H. Cheng, and T.F. Wang. 2010. Yeast axial-element protein, Red1, binds SUMO chains to promote meiotic interhomologue recombination and chromosome synapsis. *EMBO J*. 29:586-596.

Lindquist, S., and E.A. Craig. 1988. The heat-shock proteins. *Annu. Rev. Genet*. 22:631-677.

Lorincz, A. 1984. Quick preparation of plasmid DNA from yeast. *Focus*. 6:11.

Lydall, D., Y. Nikolsky, D.K. Bishop, and T. Weinert. 1996. A meiotic recombination checkpoint controlled by mitotic checkpoint genes. *Nature*. 383:840-843.

Mitchell, A.P. 1994. Control of meiotic gene expression in Saccharomyces cerevisiae. *Microbiol. Rev*. 58:56-70.

Mitra, N., and G.S. Roeder. 2007. A novel nonnull ZIP1 allele triggers meiotic arrest with synapsed chromosomes in Saccharomyces cerevisiae. *Genetics*. 176:773-787.

Montano, S.P., M. Pierce, M.L. Cote, A.K. Vershon, and M.M. Georgiadis. 2002. Crystallographic studies of a novel DNA-binding domain from the yeast transcriptional activator Ndt80. *Acta. Crystallogr D. Biol. Crystallogr*. 58:2127-2130.

Nakagawa, T., and H. Ogawa. 1999. The Saccharomyces cerevisiae MER3 gene, encoding a novel helicase-like protein, is required for crossover control in meiosis. *EMBO J*. 18:5714-5723.

Niu, H., X. Li, E. Job, C. Park, D. Moazed, S.P. Gygi, and N.M. Hollingsworth. 2007. Mek1 kinase is regulated to suppress double-strand break repair between sister chromatids during budding yeast meiosis. *Mol. Cell Biol*. 27:5456-5467.

Novak, J.E., P.B. Ross-Macdonald, and G.S. Roeder. 2001. The budding yeast Msh4 protein functions in chromosome synapsis and the regulation of crossover distribution. *Genetics*. 158:1013-1025.

Pak, J., and J. Segall. 2002a. Regulation of the premiddle and middle phases of expression of the NDT80 gene during sporulation of Saccharomyces cerevisiae. *Mol. Cell Biol*. 22:6417-6429.

Pak, J., and J. Segall. 2002b. Role of Ndt80, Sum1, and Swe1 as targets of the meiotic recombination checkpoint that control exit from pachytene and spore formation in Saccharomyces cerevisiae. *Mol. Cell Biol*. 22:6430-6440.

Pierce, M., K.R. Benjamin, S.P. Montano, M.M. Georgiadis, E. Winter, and A.K. Vershon. 2003. Sum1 and Ndt80 proteins compete for binding to middle sporulation element sequences that control meiotic gene expression. *Mol. Cell Biol*. 23:4814-4825.

Pittman, D.L., J. Cobb, K.J. Schimenti, L.A. Wilson, D.M. Cooper, E. Brignull, M.A. Handel, and J.C. Schimenti. 1998. Meiotic prophase arrest with failure of chromosome synapsis in mice deficient for Dmc1, a germline-specific RecA homolog. *Mol. Cell*. 1:697-705.

Rockmill, B., and G.S. Roeder. 1990. Meiosis in asynaptic yeast. *Genetics*. 126:563-574.

Rockmill, B., M. Sym, H. Scherthan, and G.S. Roeder. 1995. Roles for two RecA homologs in promoting meiotic chromosome synapsis. *Genes Dev*. 9:2684-2695.

Roeder, G.S. 1995. Sex and the single cell: meiosis in yeast. *Proc. Natl. Acad. Sci. U S A*. 92:10450-10456.

Roeder, G.S. 1997. Meiotic chromosomes: it takes two to tango. *Genes Dev*. 11:2600-2621.

Roeder, G.S., and J.M. Bailis. 2000. The pachytene checkpoint. *Trends Genet*. 16:395-403.

Roig, I., J.A. Dowdle, A. Toth, D.G. de Rooij, M. Jasin, and S. Keeney. 2010. Mouse TRIP13/PCH2 is required for recombination and normal higher-order chromosome structure during meiosis. *PLoS Genet*. 6: e1001062.

Rosario, M.O., S.L. Perkins, D.A. O'Brien, R.L. Allen, and E.M. Eddy. 1992. Identification of the gene for the developmentally expressed 70 kDa heat-shock protein (P70) of mouse spermatogenic cells. *Dev. Biol*. 150:1-11.

Sambrook, J., and Russell, D.W. 2001. Molecular cloning. *Cold Spring Harbor Laboratory*. 3.

San-Segundo, P.A., and G.S. Roeder. 1999. Pch2 links chromatin silencing to meiotic checkpoint control. *Cell*. 97:313-324.

San-Segundo, P.A., and G.S. Roeder. 2000. Role for the silencing protein Dot1 in meiotic checkpoint control. *Mol. Biol Cell*. 11:3601-3615.

Sen, S. 2000. Aneuploidy and cancer. *Curr. Opin. Oncol*. 12:82-88.

Shuster, E.O., and B. Byers. 1989. Pachytene arrest and other meiotic effects of the start mutations in Saccharomyces cerevisiae. *Genetics*. 123:29-43.

Simchen, G. 2009. Commitment to meiosis: what determines the mode of division in budding yeast? *Bioessays*. 31:169-177.

Smith, A.V., and G.S. Roeder. 1997. The yeast Red1 protein localizes to the cores of

meiotic chromosomes. *J. Cell Biol*. 136:957-967.

Sopko, R., S. Raithatha, and D. Stuart. 2002. Phosphorylation and maximal activity of Saccharomyces cerevisiae meiosis-specific transcription factor Ndt80 is dependent on Ime2. *Mol. Cell Biol*. 22:7024-7040.

Stone, D.E., and E.A. Craig. 1990. Self-regulation of 70-kilodalton heat shock proteins in Saccharomyces cerevisiae. *Mol. Cell Biol*. 10:1622-1632.

Sym, M., J.A. Engebrecht, and G.S. Roeder. 1993. ZIP1 is a synaptonemal complex protein required for meiotic chromosome synapsis. *Cell*. 72:365-378.

Sym, M., and G.S. Roeder. 1994. Crossover interference is abolished in the absence of a synaptonemal complex protein. *Cell*. 79:283-292.

Takanami, T., S. Sato, T. Ishihara, I. Katsura, H. Takahashi, and A. Higashitani. 1998. Characterization of a Caenorhabditis elegans recA-like gene Ce-rdh-1 involved in meiotic recombination. *DNA Res*. 5:373-377.

Tsubouchi, H., and G.S. Roeder. 2002. The Mndl protein forms a complex with Hop2 to promote homologous chromosome pairing and meiotic double-strand break. *Mol. Cell Biol*. 22:3078-3088.

Tung, K.S., E.J. Hong, and G.S. Roeder. 2000. The pachytene checkpoint prevents accumulation and phosphorylation of the meiosis-specific transcription factor Ndt80. *Proc. Natl. Acad. Sci. U S A*. 97:12187-12192.

Tung, K.S., and G.S. Roeder. 1998. Meiotic chromosome morphology and behavior in zip1 mutants of Saccharomyces cerevisiae. *Genetics*. 149:817-832.

van den Bosch, M., and N.F. Lowndes. 2004. Remodelling the Rad9 checkpoint complex: preparing Rad53 for action. *Cell Cycle*. 3:119-122.

Wan, L., T. de los Santos, C. Zhang, K. Shokat, and N.M. Hollingsworth. 2004. Mek1 kinase activity functions downstream of RED1 in the regulation of meiotic double strand break repair in budding yeast. *Mol. Biol. Cell*. 15:11-23.

Wang, Y., C.Y. Chang, J.F. Wu, and K.S. Tung. 2011. Nuclear localization of the meiosis-specific transcription factor Ndt80 is regulated by the pachytene checkpoint. *Mol. Biol. Cell*. 22:1878-1886.

Weinert, T. 1998. DNA damage and checkpoint pathways: molecular anatomy and interactions with repair. *Cell*. 94:555-558.

Werner-Washburne, M., J. Becker, J. Kosic-Smithers, and E.A. Craig. 1989. Yeast Hsp70 RNA levels vary in response to the physiological status of the cell. *J. Bacteriol*. 171:2680-2688.

Werner-Washburne, M., D.E. Stone, and E.A. Craig. 1987. Complex interactions among members of an essential subfamily of hsp70 genes in Saccharomyces cerevisiae. *Mol. Cell Biol*. 7:2568-2577.

Wojtasz, L., K. Daniel, I. Roig, E. Bolcun-Filas, H. Xu, V. Boonsanay, C.R. Eckmann, H.J. Cooke, M. Jasin, S. Keeney, M.J. McKay, and A. Toth. 2009. Mouse

HORMAD1 and HORMAD2, two conserved meiotic chromosomal proteins, are depleted from synapsed chromosome axes with the help of TRIP13 AAA-ATPase. *PLoS Genet*. 5:e1000702.

Woltering, D., B. Baumgartner, S. Bagchi, B. Larkin, J. Loidl, T. de los Santos, and N.M. Hollingsworth. 2000. Meiotic segregation, synapsis, and recombination checkpoint functions require physical interaction between the chromosomal proteins Red1p and Hop1p. *Mol. Cell Biol*. 20:6646-6658.

Wu, H.Y., and S.M. Burgess. 2006. Two distinct surveillance mechanisms monitor meiotic chromosome metabolism in budding yeast. *Curr. Biol*. 16:2473-2479.

Wu, J.F. 2001. Relationship between Ndt80 phosphorylation and its function. M. S. Thesis. National Taiwan University, Taipei.

Xu, L., M. Ajimura, R. Padmore, C. Klein, and N. Kleckner. 1995. NDT80, a meiosis-specific gene required for exit from pachytene in Saccharomyces cerevisiae. *Mol. Cell Biol*. 15:6572-6581.

Xu, L., B.M. Weiner, and N. Kleckner. 1997. Meiotic cells monitor the status of the interhomolog recombination complex. *Genes Dev*. 11:106-118.

Zakeri, Z.F., D.J. Wolgemuth, and C.R. Hunt. 1988. Identification and sequence analysis of a new member of the mouse HSP70 gene family and characterization of its unique cellular and developmental pattern of expression in the male germ line. *Mol. Cell Biol*. 8:2925-2932.

Zanders, S., and E. Alani. 2009. The pch2Delta mutation in baker's yeast alters meiotic crossover levels and confers a defect in crossover interference. *PLoS Genet*. 5:e1000571.

Zanders, S., M. Sonntag Brown, C. Chen, and E. Alani. 2011. Pch2 Modulates Chromatid Partner Choice During Meiotic Double-Strand Break Repair in Saccharomyces cerevisiae. *Genetics*.3:511-521

Zhu, D., D.J. Dix, and E.M. Eddy. 1997. HSP70-2 is required for CDC2 kinase activity in meiosis I of mouse spermatocytes. *Development*. 124:3007-3014.

Table 2-1. Yeast strains

Strain	Genotype
W303 strain background:	
TY178	*MAT***a** *ade2-1 trp1-1 his3-11,15 ura3-1 leu2-3,112 can1-100*
TY179	*MATα ade2-1 trp1-1 his3-11,15 ura3-1 leu2-3,112 can1-100*
W303	TY178 x TY179
	*MAT***a** *ade2-1 trp1-1 his3-11,15 ura3-1 leu2-3,112 can1-100*
	MATα ade2-1 trp1-1 his3-11,15 ura3-1 leu2-3,112 can1-100
TY171	TY178 but *zip1::LEU2*
TY172	TY179 but *zip1::LEU2*
TY173	TY171 x TY172
	W303 but homozygous *zip1::LEU2*
K972	TY178 but *ssa2::URA3*
K973	TY179 but *ssa2::URA3*
K975	K972 x TY179
	W303 but heterozygous *ssa2::URA3*
K977	K972 x K973
	W303 but homozygous *ssa2::URA3*
K978	TY171 but *ssa2::URA3*
K981	TY172 but *ssa2::URA3*
K982	K978 x TY172
	W303 but homozygous *zip1::LEU2,* heterozygous *ssa2::URA3*
K984	K978 x K981
	W303 but homozygous *zip1::LEU2, ssa2::URA3*
K992	TY178 but $URA3^+$
K995	TY179 but $URA3^+$
K996	K992 x K995
	W303 but $URA3^+$
K998	K992 but *zip1::LEU2*
K1000	K995 but *zip1::LEU2*
K1001	K998 x K1000
	W303 but homozygous $URA3^+$ *, zip1::LEU2*

BR2495 strain background:

S1560	*MAT***a** *leu2-27 his4-280 arg4-8 thr1-1 ade2-1 ura3-1 trp1-1 cyh10*
S1561	*MATα leu2-3,112 his4-260 thr1-4 ade2-1 ura3-1 trp1-289*
BR2495	S1560 x S1561
	*MAT***a** *leu2-27 his4-280 arg4-8 thr1-1 ade2-1 ura3-1 trp1-1 cyh10*
	MATα leu2-3,112 his4-260 ARG4 thr1-4 ade2-1 ura3-1 trp1-289 CYH10
MY150	S1561 but *zip1::URA3*
MY151	S1560 but *zip1::URA3*
MY152	MY150 x MY151
	BR2495 but homozygous *zip1::URA3*
MY61	S1561 but *zip1::LEU2*
MY62	S1560 but *zip1::LEU2*
MY63	MY61 x MY62
	BR2495 but homozygous *zip1::LEU2*
TY57	BR2495 but homozygous *ndt80::URA3*
K430	BR2495 but homozygous *ssa3::LEU2*
K431	BR2495 but homozygous *zip1::URA3, ssa3::LEU2*
K497	BR2495 but homozygous *zip1::LEU2, NDT80/NDT80-bc*
K554	S1560 but *pch2::TRP1*
K555	S1561 but *pch2::TRP1*
K556	K554 x K555
	BR2495 but homozygous *pch2::TRP1*
K559	BR2495 but homozygous *zip1::LEU2, pch2::TRP1*
K820	BR2495 but *NDT80-6XHA/NDT80-bc-6XMYC*
K822	BR2495 but *zip1::LEU2, NDT80-6XHA/NDT80-bc-6XMYC*
K985	MY61 but *ssa2::URA3*
K988	MY62 but *ssa2::URA3*
K989	K985 x MY62
	BR2495 but homozygous *zip1::LEU2,* heterozygous *ssa2::URA3*
K991	K985 x K988
	BR2495 but homozygous *zip1::LEU2, ssa2::URA3*
K420	S1560 but *3XHA-SSA3*
K422	S1561 but *3XHA-SSA3*
K424	MY61 but *3XHA-SSA3*
K426	MY62 but *3XHA-SSA3*
K428	K420 x K422
	BR2495 but *3XHA-SSA3*

K429	K424 x K426
	BR2495 but homozygous *zip1::LEU2, 3XHA-SSA3*
K1037	K822 but homozygous *ssa2::URA3*
K1069	K424 but *PCH2-3XMYC*
K1070	K426 but *PCH2-3XMYC*
K1071	K1069 x K1070
	BR2495 but homozygous *zip1::LEU2, 3XHA-SSA3, PCH2-3XMYC*
K1075	K420 but *PCH2-3XMYC*
K1076	K422 but *PCH2-3XMYC*
K1077	K1075 x K1076
	BR2495 but homozygous *3XHA-SSA3, PCH2-3XMYC*
K1092	K554 but *NDT80-bc*
K1093	K555 but *NDT80-bc*
K1094	BR2495 but homozygous *pch2::TRP1, NDT80-bc*
K1098	S1560 but *zip3::URA3*
K1099	S1561 but *zip3::URA3*
K1100	BR2495 but homozygous *zip3::URA3*
K1107	K554 but *zip3::URA3*
K1108	K555 but *zip3::URA3*
K1109	BR2495 but homozygous *pch2::TRP1, zip3::URA3*
K589	PJ69-4A
	*MAT***a** *trp1-901 leu2-3,112 ura3-52 his3-200 gal4Δ gal80Δ*
	LYS2::GAL1-HIS3 GAL2-ADE2 met2::GAL7-lacZ

SK1 strain background:

K529 (BS188)	*MAT***a** *ho-LYS2 lys2 ura3 leu2-hisG dmc1::ARG4 his4-LEU2*
K530 (BS190)	*MATα ho-LYS2 lys2 ura3 leu2-hisG dmc1::ARG4 his4-LEU2*
K531 (BS193)	*MATα ho-LYS2 lys2 ura3 leu2-hisG DMC1 his4-LEU2*
K560	K529 x K530
	SK1 but homozygous *dmc1::ARG4*
K561	K529 x K531
	SK1 but heterozygous *dmc1::ARG4*
K563	SK1 but heterozygous *dmc1::ARG4*, homozygous *ssa3::URA3*
K472	SK1 but homozygous *dmc1::ARG4, ssa3::URA3*

Table 2-2. Plasmids

Plasmid	Characteristics	
pRS306	pBluescript, *URA3*	Integrating plasmid
pRS314	pBluescript, *TRP1*, *CEN*, *ARS*	Low-copy number plasmid
pRS316	pBluescript, *URA3*, *CEN*, *ARS*	Low-copy number plasmid
pRS424	2μm *TRP1*	High-copy number plasmid
YEp351	2μm *LEU2*	High-copy number plasmid
YEp352	2μm *URA3*	High-copy number plasmid
TP73	YEp352-*NDT80 URA3*	
TP208	Carry 3XMYC encoding sequence	
T138	SK(+)-*ssa3::URA3*	
T199	YEp351-*SSA3 LEU2*	
T202	YEp351-*3XHA-SSA3 LEU2*	
T330	pRS306-*NDT80Δ346-627-HA URA3*	
T410	2μm pGAD-C3 *LEU2*	AD vector
T424	YEp351-*NDT80Δ404-627 LEU2*	*NDT80Δ404-627* deletion
T477	2μm pGBDU-C1 *URA3*	BD vector
T487	pGAD-C1-*HSP26 LEU2*	AD vector (positive control)
T509	pGBDU-C3-*TEM1 URA3*	BD vector (positive control)
T652	SK(+)-*SSA2*	
T654	SK(+)-*ssa2::URA3*	
T659	pRS424-*SSA2 TRP1*	High-copy number plasmid
T662	pGBDU-C1- *NDT80Δ404-627 URA3*	BD vector
T665	YEp351- *NDT80Δ346-627 LEU2*	*NDT80Δ346-627* deletion
T667	pGBDU-C1- *NDT80Δ346-627 URA3*	BD vector
T669	pGAD-C3-*SSA2 LEU2*	AD vector
T673	SK(+)-*PCH2*	
T679	pRS316-*PCH2 URA3*	Low-copy number plasmid
T681	pRS314-*SSA3 TRP1*	Low-copy number plasmid
T685	SK(+)-*PCH2-Not*I	
T687	SK(+)-*PCH2-3X MYC*	
T688	pRS316-*PCH2-3X MYC URA3*	Low-copy number plasmid
T689	pRS314-*3X HA-SSA3 TRP1*	Low-copy number plasmid
T690	pRS306-*PCH2-3X MYC URA3*	Integrating plasmid
T691	SK(+)-*ZIP3*	
T696	SK(+)-*zip3::URA3*	
T701	SK(+)-*RED1*	

T702	SK(+)-*RED1-Not*I	
T703	SK(+)-*RED1-3XMYC*	
T705	pRS314-*RED1-3XMYC TRP1*	Low-copy number plasmid
T706	YEp352-*3XHA-SSA3 URA3*	

Table 2-3. Primer sequences

Name	Sequences (5'-3')
SSA2-U1	GGTGAATTGACTGCATGGCACTGC
SSA2-U2	GCCGCAATTGGGCTGGGTTTTCTCC
SSA2-U3-SalI	ATTTATACAATGTCGACAGCTGTCGGTATTGATTTAG
SSA2-D1-XhoI	GTCCCATGGTACTCGAGCAGATTGAGACCAGCCATC
SSA2-D2	CGGCAGTTTCCTTCATCTTACCCAAG
SSA3-U2	GGGGAGTTGCAGTTTGCGTTCTTA
SSA3-D2	TGGAAAAATGAGCAACACACGAGT
PCH2-U1	AGGATCTTGGAGGGAAGAAAAGGCATG
PCH2-U2	GGGCGGCAAATCTACGAAATGCGAGGC
PCH2-D1	TTCCATAGATGTCTCCGCATCAGTAGC
PCH2-XbaI-D1	GCCATTTCCTCCTCTAGACCTGCATCCTTAGACATCTC
PCH2-NotI-U2	GCAGCGCGGAAGGGCGGCCGCTGACGGAGGAGCTTTTTCC TTTTTTTCG
PCH2-NotI-D2	GCTCCTCCGTCAGCGGCCGCCCTTCCGCGCTGCGCTCAGCT TCCG
PH2-U2	CTTCCGGACATTTCCTGTAGACGACG
NDT80-IN2	CACAACAATGAATCTATCGCCCTGTG
NDT80-346D	GTGCTGTTTTGTGAAGCTTTGACACTCGACGGTGTTC
NDT80-SalI-1009-U	AAGCGCTTAAAATGGTCGACATGGAAAACACAGATCCAG
NDT80-BglII-p59-D	GTACCCGGGGATCCACAGATCTCGCATATTTTTTTAACG
NDT80-971-988-U	GAGGAAGATCACCTTCTAACTATGCGTC
NDT80-1710-1654-D	TGTCCTTGGCACATCCTCTTCCGTAGC
ZIP3-XhoI-U1	GAATTCAGCAAATCTCGAGTTTATGACGTGCAAGTCTTCC
ZIP3-U3	GTTGACGCTTTGTGCGGCGGCCAAC
ZIP3-SpeI-D1	GTGCCAACAGATGACTAGTACGACAGCTAAGAGAAGTAGC
ZIP3-D2	GATAGTATTGACACTGTTTCGAAAGCCC
RED1-U3	CGGAAGGGCAGCTGAGCAGAAAG
RED1-D3	CCACCACGAGAACCGGTACGGC
RED1-NOT-U1	GATAACAACAAGAGAGGCGGCCGCTAAATAGTATACATAT ACGCAATTC
RED1-NOT-D1	GTATACTATTTAGCGGCCGCCTCTCTTGTTGTTATCAAATTT TCTTGTCC
URA3-D1	GAACATCCAATGAAGCACACAAGT
LEU2-U2	CGGCCTTAACGACGTACCGGATC

Table 3-1. Sporulation frequency of *zip1 ssa3* double mutant

Stains	Genotype	Sporulation frequency (%)
BR2495	*SSA3/SSA3*	72.9 ± 3.4
K430	*ssa3/ssa3*	69.6 ± 3.7
MY152	*zip1/zip1*	0.1 ± 0.1
K431	*zip1/zip1, ssa3/ssa3*	22.7 ± 1.1

BR2495 wild-type, *ssa3, zip1* and *zip1 ssa3* strains were induced meiosis on the sporulation plate at 30℃ for three days. Sporulation frequencies represent the averages of four independent cultures, with at least 200 cells counted for each culture.

Table 3-2. Sporulation frequency and nuclear division of *dmc1 ssa3* double mutant

Stains	Genotype	Sporulation frequency (%)	Nuclear division (%)
K561	*DMC1/dmc1*	97.5 ± 0.7	92.5 ± 2.1
K563	*DMC1/dmc1, ssa3/ssa3*	97.3 ± 0.4	95.0 ± 2.8
K560	*dmc1/dmc1*	0	3.0 ± 1.4
K472	*dmc1/dmc1, ssa3/ssa3*	0.3 ± 0.4	5.5 ± 0.7

SK1 *DMC1/dmc1, DMC1/dmc1 ssa3/ssa3, dmc1* and *dmc1 ssa3* strains were cultured in 2% KAc to induce meiosis at 30℃ and were examined with phase-contrast microscope to assess spore formation for 24 hours; meanwhile, cells were collected, fixed, and stained with DAPI. Meiotic nuclear divisions were determined by DAPI staining. At least 200 cells were counted.

Table 3-3. Complementation assay of the HA-tagged Ssa3

Stain	Plasmid	Sporulation frequency (%)
BR2495 (wild type)	pRS314	72.3 ± 2.2
BR2495 *zip1* (MY63)	pRS314	0.5 ± 0.4
BR2495 *zip1 ssa3* (K431)	pRS314	19.2 ± 1.4
	pRS314-*SSA3*	5.9 ± 1.6
	pRS314-*3XHA-SSA3*	8.6 ± 1.3

pRS314, pRS314-*SSA3* (pT681) and pRS314-*3XHA-SSA3* (pT689) were transformed into BR2495 *zip1 ssa3* double mutant (K431) for low-copy expression of *SSA3* and *3XHA-SSA3* for complementation assay. Transformed cells were induced meiosis on the sporulation plate at 30℃ for three days. Sporulation frequencies represent the averages of four independent cultures, with at least 200 cells counted for each culture.

Table 3-4. Complementation assay of the MYC-tagged Pch2

Stain	Plasmid	Sporulation frequency (%)
BR2495 (wild type)	pRS316	67.1 ± 2.4
BR2495 *zip1* (MY63)	pRS316	0.3 ± 0.5
BR2495 *zip1 pch2* (K559)	pRS316	70.2 ± 2.8
	pRS316-*PCH2*	22.0 ± 2.6
	pRS316-*3XMYC-PCH2*	62.9 ± 6.0
	pRS316-*6XMYC-PCH2*	63.8 ± 2.1
	pRS316-*PCH2-3XMYC*	22.6 ± 2.3

pRS316, pRS316-*PCH2* (pT679), pRS316-*3XMYC-PCH2* (pT675), pRS316-*6XMYC-PCH2* (pT676) and pRS316-*PCH2-3XMYC* (pT688) were transformed into BR2495 *zip1 pch2* double mutant (K559) for low-copy expression of *PCH2*, *3XMYC-PCH2*, *6XMYC-PCH2* and *PCH2-3XMYC* for complementation assay. Transformed cells were induced meiosis on the sporulation plate at 30℃ for three days. Sporulation frequencies represent the averages of four independent cultures, with at least 200 cells counted for each culture.

Table 3-5. Sporulation frequency and nuclear division of *ssa3* mutant and *pch2* mutant cells at different temperatures

Stains	Genotype	Sporulation frequency (%)		Nuclear division (%)	
		32.5℃	30℃	32.5℃	30℃
BR2495	Wild-type	72.3 ± 1.1	70.5 ± 0.8	74.0 ± 1.4	73.0 ± 1.4
K430	*ssa3/ssa3*	72.5 ± 1.4	70.0 ± 1.4	73.6 ± 1.4	69.5 ± 0.7
K556	*pch2/pch2*	27.3 ± 1.8	70.8 ± 1.8	36.5 ± 2.8	73.3 ± 1.1
MY152	*zip1/zip1*	0	0.3 ± 0.4	4.0 ± 1.1	4.3 ± 2.5
K431	*zip1/zip1, ssa3/ssa3*	2.0 ± 1.4	26.5 ± 3.5	8.8 ± 1.1	36.0 ± 1.4
K559	*zip1/zip1, pch2/pch2*	67.3 ± 1.8	68.8 ± 2.1	73.8 ± 1.8	72.3 ± 1.8

Cells were cultured in 2% KAc to induce meiosis at 30℃ and were examined with phase-contrast microscope to assess spore formation for 42 hours. Meiotic nuclear divisions were determined by DAPI staining. At least 200 cells were counted.

Table 4-1. Sporulation frequencies and types of asci produced in wild-type, *pch2*, *zip1 pch2* cells at 32.5℃ and 30℃

Sporulation at 32.5℃

Stains	Genotype	Sporulation frequency (%)	% of Total asci (%)		
			Tetrad/ Triad	Dyad	Monad
BR2495	Wild-type	71.5 ± 3.4	83.6 ± 5.1	16.3 ± 4.4	0.2 ± 0.3
K556	*pch2/pch2*	25.1 ± 1.8	77.1 ± 3.0	21.9 ± 3.6	1.0 ± 0.5
MY63	*zip1/zip1*	0	—	—	—
K559	*zip1/zip1, pch2/pch2*	62.9 ± 4.1	76.9 ± 3.4	22.9 ± 4.9	0.2 ± 0.3

Sporulation at 30℃

Stains	Genotype	Sporulation frequency (%)	% of Total asci (%)		
			Tetrad/ Triad	Dyad	Monad
BR2495	Wild-type	68.3 ± 4.3	83.5 ± 5.1	15.6 ± 3.5	0.9 ± 0.5
K556	*pch2/pch2*	70.9 ± 2.1	77.4 ± 5.2	22.2 ± 2.7	0.4 ± 0.5
MY63	*zip1/zip1*	0	—	—	—
K559	*zip1/zip1, pch2/pch2*	72.3 ± 1.0	83.9 ± 1.9	15.9 ± 1.5	0.2 ± 0.3

BR2495 (wild-type), K556 (*pch2*), MY63 (*zip1*) and K559 (*zip1 pch2*) strains were cultured on the sporulation plate to induce meiosis at 32.5℃ and 30℃ for three days. Cells were examined with the phase contrast microscope to assess spore formation, and asci were classified as containing four/three (tetrad/triad), two (dyad), or one spore (monad). The value was an average of four independent cultures, with at least 200 cells were scored for each culture.

Table 4-2. The spore viability of the *pch2* mutant cells at different temperatures

Stains	Genotype	Sporulation frequency (%)		Spore viability (%)	
		32.5℃	30℃	32.5℃	30℃
BR2495	Wild-type	71.1	68.3	86.7	94.9
K556	*pch2/pch2*	25.0	70.9	82.1	92.6
MY63	*zip1/zip1*	0	0	—	—
K559	*zip1/zip1, pch2/pch2*	66.4	72.4	52.2	57.9
K1094	*pch2/pch2,NDT80-bc/ NDT80-bc*	67.8	66.5	77.0	78.4

BR2495 wild-type, *pch2* (K556), *zip1* (MY63), *zip1 pch2* (K559), and *pch2 NDT80-bc* (K1094) mutants were cultured on the sporulation plate to induce meiosis at 32.5℃and 30℃. Asci of three days on sporulation plate were used for tetrad dissection. Spore viability was determined by dissecting at least 88 tetrads in each strain.

Table 4-3. Sporulation frequency and nuclear division of the *pch2 NDT80-bc* mutant cells at different temperatures

Stains	Genotype	Sporulation frequency (%)		Nuclear division (%)	
		32.5℃	30℃	32.5℃	30℃
BR2495	Wild-type	62.7 ± 3.8	62.8 ± 1.9	67.3 ± 3.8	65.2 ± 2.8
K556	*pch2/pch2*	24.6 ± 1.2	63.3 ± 2.5	32.7 ± 2.5	65.5 ± 3.0
K1094	*pch2/pch2,NDT80-bc/ NDT80-bc*	59.8 ± 2.1	63.3 ± 4.0	67.2 ± 4.3	66.2 ± 1.4

Cells were cultured on the sporulation plate to induce meiosis at 32.5℃ and 30℃ for three days. Sporulation frequencies and meiotic nuclear divisions represent the averages of three independent cultures. At least 200 cells were counted for each culture.

Table 4-4. Sporulation frequency and nuclear division of the *zip3 pch2* double mutant cells at different temperatures

Stains	Genotype	Sporulation frequency (%)		Nuclear division (%)	
		32.5℃	30℃	32.5℃	30℃
BR2495	Wild-type	72.5 ± 4.7	70.3 ± 5.3	82.8 ± 3.3	78.8 ± 3.3
MY63	*zip1/zip1*	0	0.5 ± 0.6	0	0.8 ± 1.0
K1100	*zip3/zip3*	20.3 ± 2.4	47.0 ± 6.1	31.8 ± 2.4	57.3 ± 2.5
K556	*pch2/pch2*	11.3 ± 1.0	67.5 ± 3.1	26.3 ± 1.9	78.0 ± 1.4
K559	*zip1/zip1, pch2/pch2*	67.8 ± 3.3	65.3 ± 4.8	80.3 ± 2.6	75.5 ± 3.5
K1109	*zip3/zip3, pch2/pch2*	26.5 ± 1.0	70.0 ± 4.2	35.5 ± 3.7	77.5 ± 1.9

Cells were cultured on the sporulation plate to induce meiosis at 32.5℃ and 30℃ for three days. Sporulation frequencies and meiotic nuclear divisions represent the averages of four independent cultures. At least 100 cells were counted for each culture.

Table 5-1. Sporulation frequency of wild-type and *ssa2* mutant cells

Stains	Genotype	Sporulation frequency (%)	% of wild type
W303	Wild-type	42.5 ± 4.4	
K975	*SSA2/ssa2*	62.4 ± 8.3	146.8
K977	*ssa2/ssa2*	58.8 ± 6.5	138.4

Sporulation frequency of wild-type and *ssa2* mutant cells were determined by counting at least 200 cells after inducing meiosis at 30℃ for 3 days on sporulation plate.

Table 5-2. Sporulation frequency of wild-type and *zip1 ssa2* double mutant cells

Stains	Genotype	Sporulation frequency (%)	% of *zip1*
W303	Wild-type	43.8 ± 1.8	—
TY173	*zip1/zip1*	5.8 ± 0.4	
K982	*zip1/zip1, SSA2/ssa2*	13.8 ± 5.9	237.9
K984	*zip1/zip1, ssa2/ssa2*	14.0 ± 0.7	241.4
BR2495	Wild-type	68.5 ± 6.1	—
MY63	*zip1/zip1*	0.5 ± 0.4	
K989	*zip1/zip1, SSA2/ssa2*	0.4 ± 0.3	
K991	*zip1/zip1, ssa2/ssa2*	0.5 ± 0.2	

Sporulation frequency of wild-type, *zip1* mutant and *zip1 ssa2* double mutant cells in two strains, W303 and BR2495, were determined by counting at least 200 cells after inducing meiosis at 30℃ for three days on sporulation plate.

Table 5-3. Sporulation frequency and nuclear division of *ssa2* mutant cells

Sporulate for 36 hr

Stains	Genotype	Sporulation frequency (%)	Nuclear division (%)
W303	Wild-type	59.1 ± 1.6	52.0 ± 2.3
TY173	*zip1/zip1*	0	3.0 ± 1.5
K982	*zip1/zip1, SSA2/ssa2*	1.0 ± 0.7	12.9 ± 2.6
K984	*zip1/zip1, ssa2/ssa2*	3.1 ± 0.7	10.8 ± 3.7

Sporulate for 48 hr

Stains	Genotype	Sporulation frequency (%)	Nuclear division (%)
W303	Wild-type	62.7 ± 3.9	64.5 ± 3.5
TY173	*zip1/zip1*	1.0 ± 5.5	5.0 ± 3.5
K982	*zip1/zip1, SSA2/ssa2*	5.2 ± 0.9	24.5 ± 2.9
K984	*zip1/zip1, ssa2/ssa2*	8.8 ± 2.1	24.0 ± 4.2

W303 wild-type, *zip1* and *zip1 ssa2* strains were cultured in 2% KAc to induce meiosis at 30℃ and were examined with phase-contrast microscope to assess spore formation for 36 and 48 hours; meanwhile, cells were collected, fixed, and stained with DAPI. Meiotic nuclear divisions were determined by DAPI staining. At least 200 cells were counted.

Table 5-4. Sporulation frequency and nuclear division of *ssa2::URA3* mutant and *URA3*$^+$ strain

Stains	Genotype	Sporulation frequency (%)	Nuclear division (%)
W303	Wild-type	64.0 ± 0.8	71.5 ± 6.4
TY173	*zip1/zip1*	5.5 ± 1.1	8.5 ± 2.9
K982	*zip1/zip1, SSA2/ssa2*	5.0 ± 0.4	7.5 ± 1.4
K984	*zip1/zip1, ssa2/ssa2*	10.0 ± 0.4	9.5 ± 0.7
K996	*URA3*$^+$*/URA3*$^+$	56.0 ± 1.7	64.5 ± 0.1
K1001	*zip1/zip1, URA3*$^+$*/URA3*$^+$	6.5 ± 0.7	5.0 ± 0.7

Meiosis was initiated by pregrowth in YPAD medium followed by transfer into 2% KAc and incubate at 30℃ for 48 hours. At least 200 cells were counted.

Table 5-5. Sporulation frequency of cells overproducing Ndt80 and Ssa2

Stains	Sporulation frequency (%)
Wild type + vectors	75.5 ± 4.5
Wild type + Ndt80-OP	72.0 ± 6.1
Wild type + Ssa2-OP	72.8 ± 5.0
Wild type + Ndt80-OP + Ssa2-OP	69.2 ± 2.0
zip1 + vectors	0
zip1 + Ndt80-OP	10.7 ± 1.8
zip1 + Ssa2-OP	0.1 ± 0.3
zip1 + Ndt80-OP + Ssa2-OP	11.2 ± 2.8

YEp352-*NDT80* (TP73) and pRS424-*SSA2* (pT659) were transformed into the BR2495 wild-type cells and *zip1* mutant (MY152) for higch-copy expression of *NDT80* and *SSA2* for overproducing. Both YEp352 and pRS424 were vectors. Cells were cultured on the sporulation plate to induce meiosis at 30℃ for three days. At least 200 cells were scored to assess the sporulation frequency. OP, overproduction.

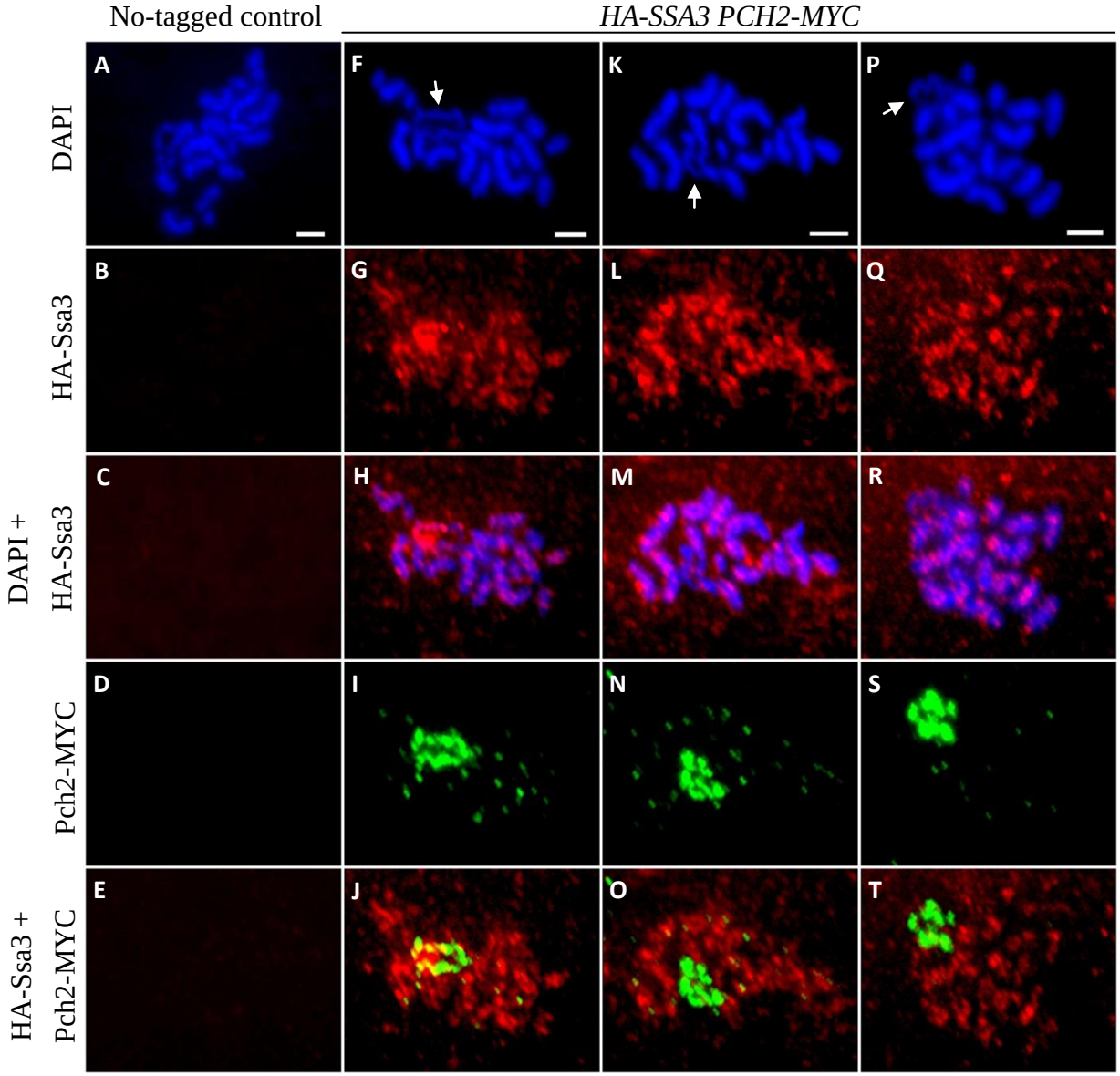

Figure 3-1. Subcellular localization of Ssa3 and Pch2 in wild-type cells. Spread nuclei from wild-type carrying *HA-SSA3* allele and *PCH2-MYC* allele (K1077; F-T) were stained with DAPI (blue; F, K and P), anti-HA (red; G, L and Q), and anti-MYC (green; I, N and S) antibodies. Spreads were prepared at 15-16 hr (around pachytene stage) after transfer to sporulation medium. BR2495 (A-E) were used as no-tagged control. Staining of DAPI and HA-Ssa3, and HA-Ssa3 and Pch2-MYC are merged, respectively (C-R; E-T). The arrow in each panel points to the nucleolus. Bar, 2μm.

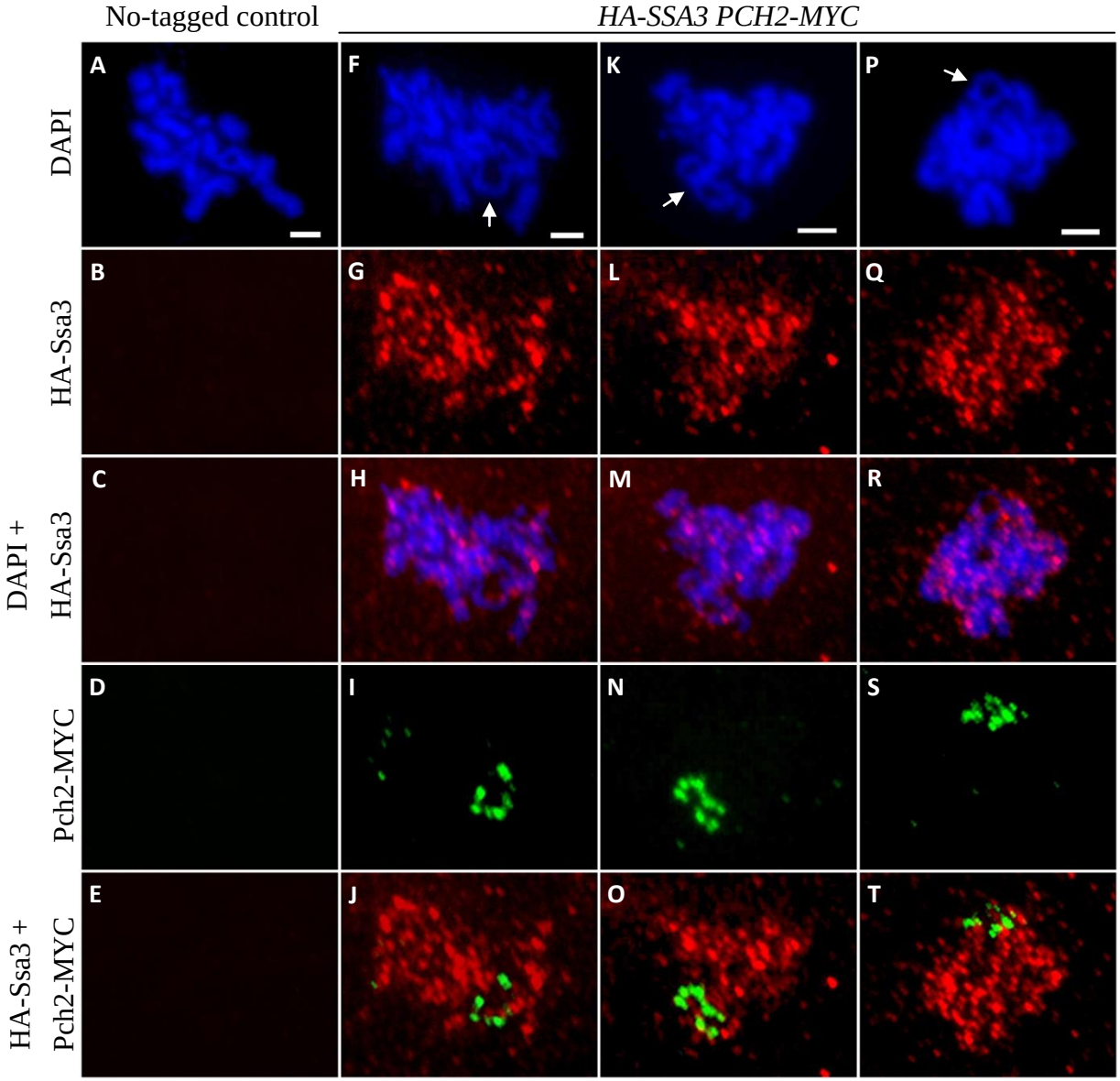

Figure 3-2. Subcellular localization of Ssa3 and Pch2 in the *zip1* mutant cells. Spread nuclei from wild-type carrying *HA-SSA3* allele and *PCH2-MYC* allele (K1071; F-T) were stained with DAPI (blue; F, K and P), anti-HA (red; G, L and Q), and anti-MYC (green; I, N and S) antibodies. Spreads were prepared at 15-16 hr (around pachytene stage) after transfer to sporulation medium. MY63 (A-E) were used as no-tagged control. Staining of DAPI and HA-Ssa3, and HA-Ssa3 and Pch2-MYC are merged, respectively (C-R; E-T). The arrow in each panel points to the nucleolus. Bar, 2μm.

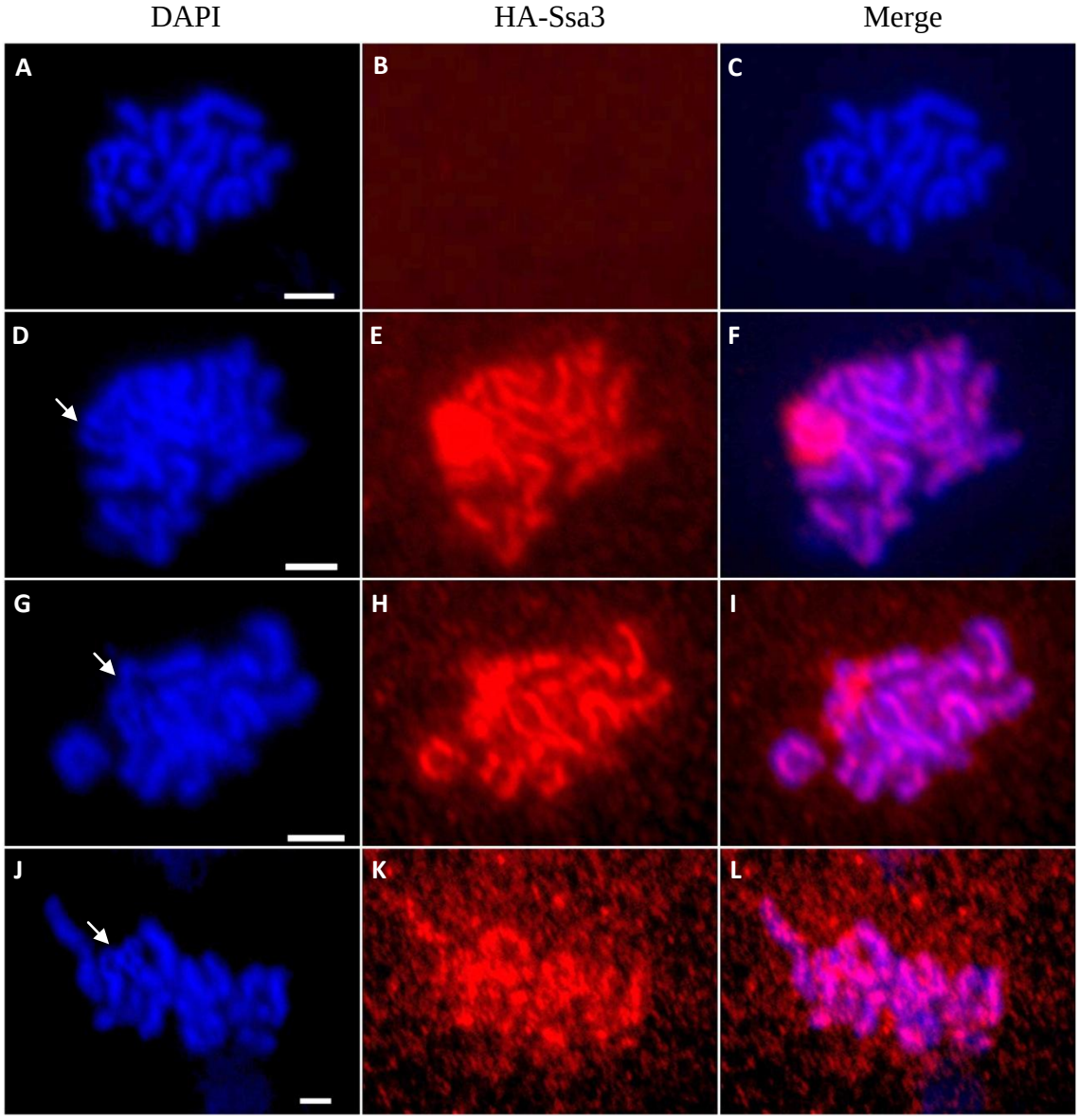
DAPI
HA-Ssa3
Merge
A
B
C
D
E
F
G
H
I
J
K
L

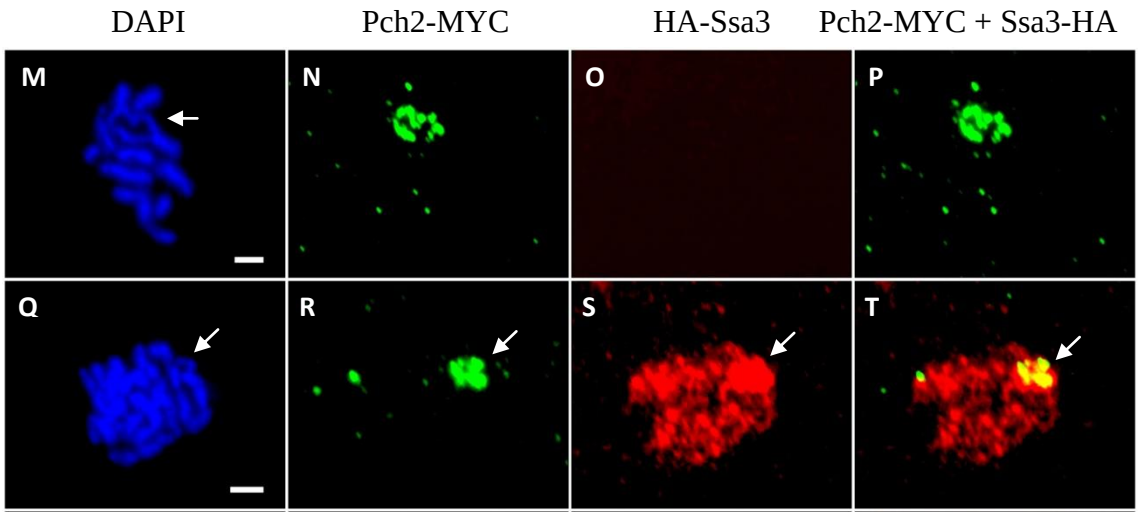
DAPI
Pch2-MYC
HA-Ssa3
Pch2-MYC + Ssa3-HA
M
N
O
P
Q
R
S
T

Figure 3-3. Localization of Ssa3 protein in wild type. Spread pachytene nuclei from wild-type overexpressing *SSA3* (BR2495 + pT199; A-C) and overexpressing *HA-SSA3* (BR2495 + pT202; D-L) were stained with DAPI (blue) and anti-HA (red) antibodies. Spread pachytene nuclei from wild-type carrying *PCH2-MYC* allele and overexpressing *SSA3* (K1086 + pT199; M-P) or overexpressing *HA-SSA3* (K1086 + pT202; Q-T) were stained with DAPI (blue), anti-MYC (green) and anti-HA (red) antibodies. The arrow in each panel points to the nucleolus. Bar, 2μm.

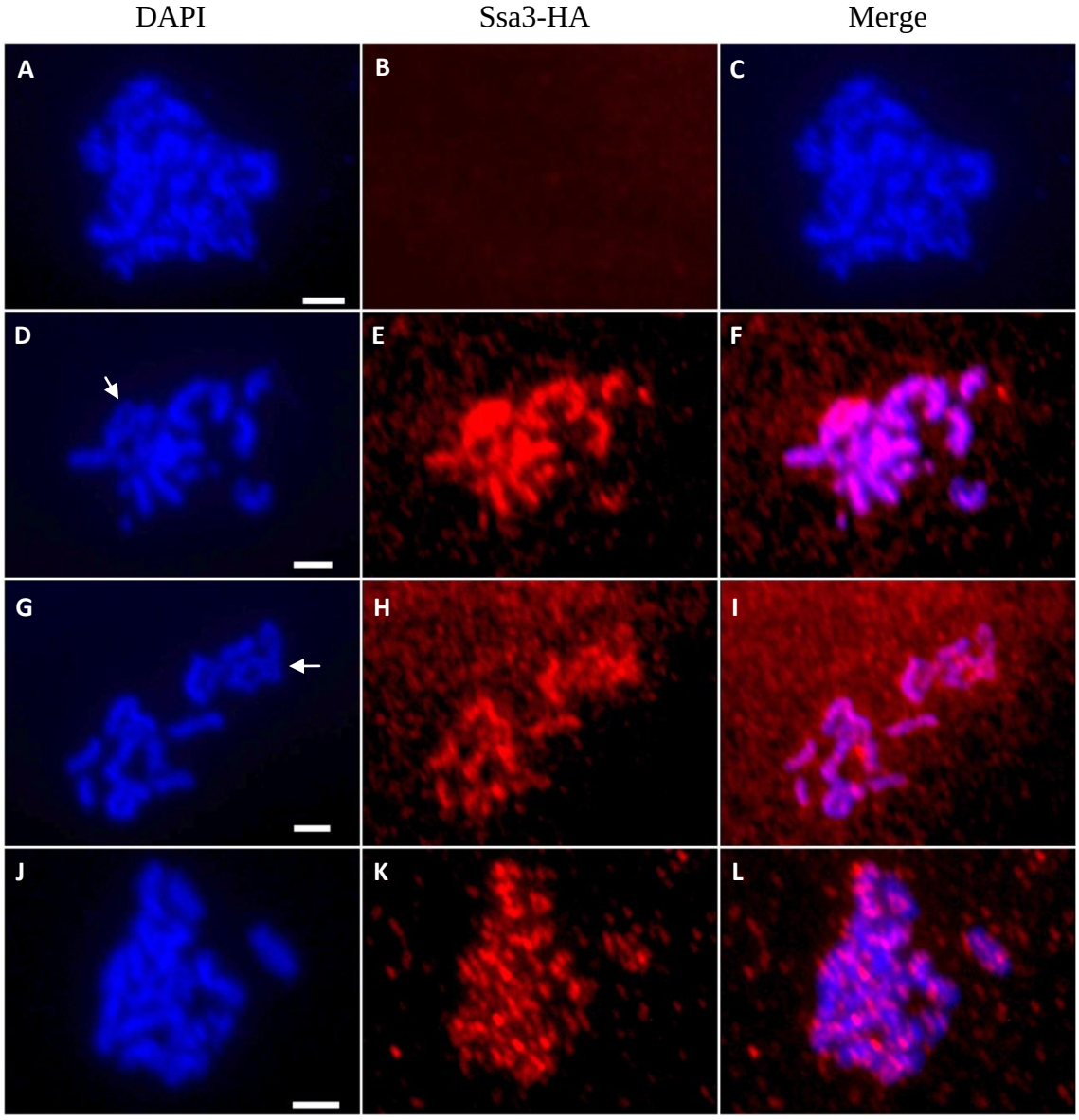
DAPI
Ssa3-HA
Merge
A
B
C
D
E
F
G
H
I
J
K
L

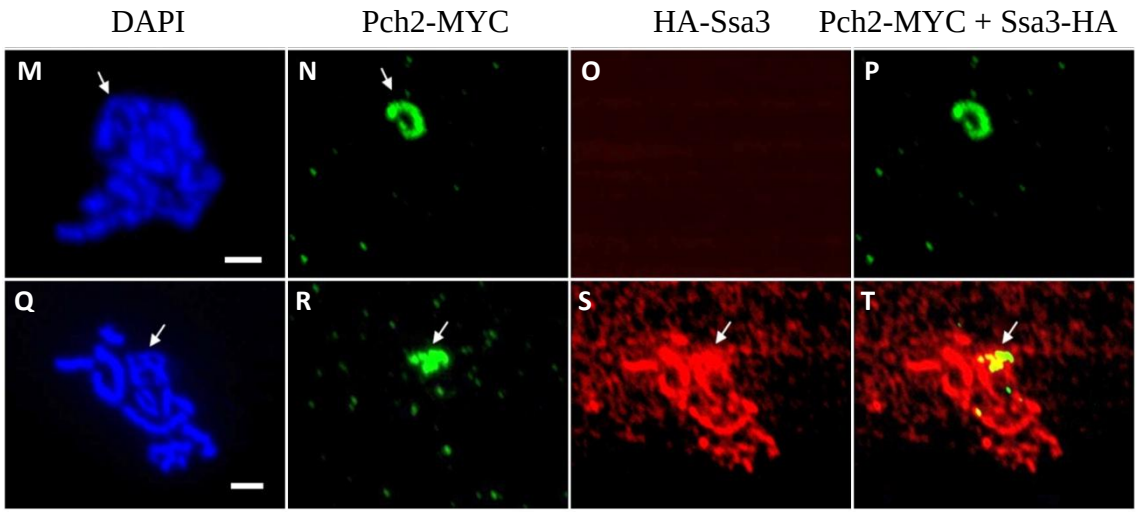
DAPI
Pch2-MYC
HA-Ssa3
Pch2-MYC + Ssa3-HA
M
N
O
P
Q
R
S
T

Figure 3-4. Localization of Ssa3 protein in the *zip1* mutant. Spread pachytene nuclei from the *zip1* mutant overexpressing *SSA3* (MY152 + pT199; A-C) and overexpressing *SSA3-HA* (MY152 + pT202; D-I) were stained with DAPI (blue) and anti-HA (red) antibodies. Spread pachytene nuclei from *zip1* carrying *PCH2-MYC* allele and *2μ* vector (K1090 + YEp352; M-P) or overexpressing *HA-SSA3* (K1090 + pT706; Q-T) were stained with DAPI (blue), anti-MYC (green) and anti-HA (red) antibodies. The arrow in each panel points to the nucleolus.Bar, 2μm.

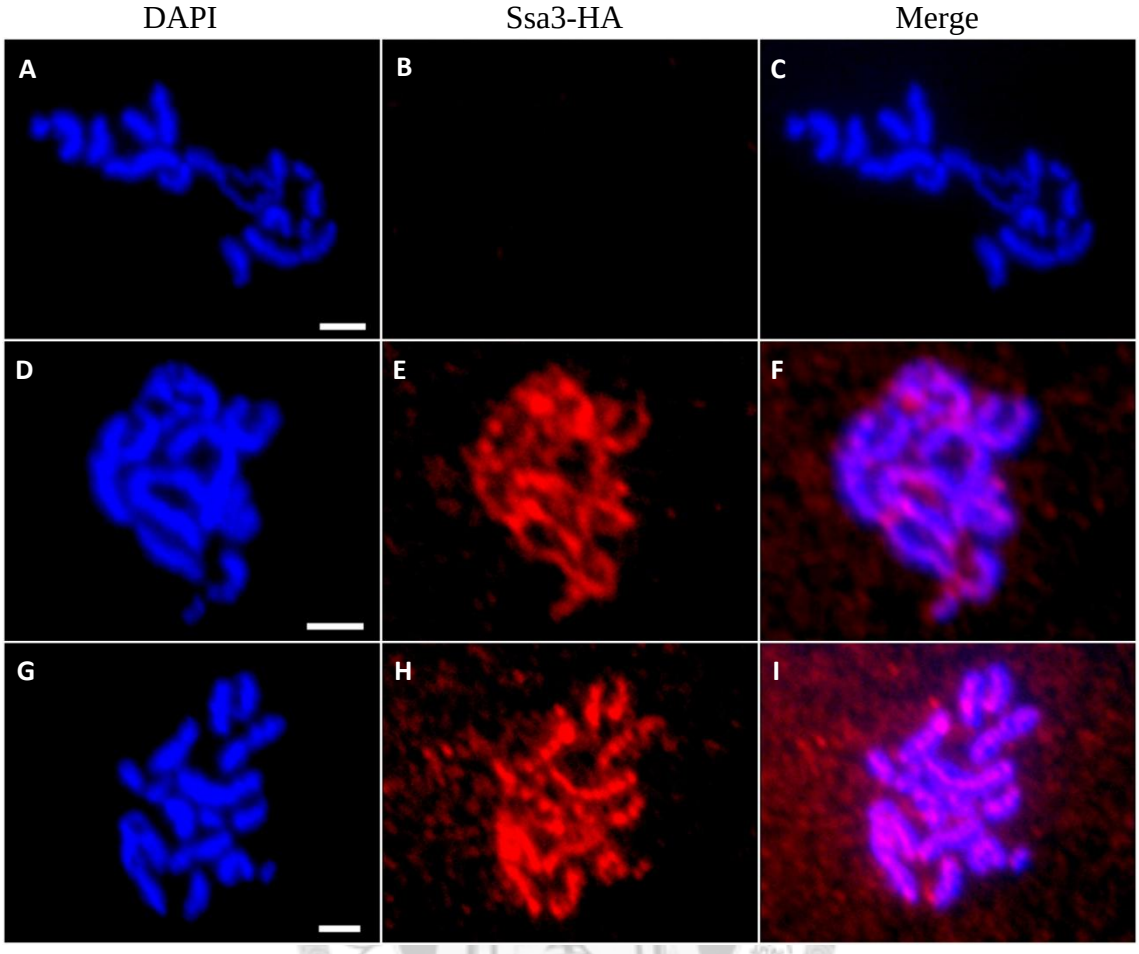

Figure 3-5. Localization of Ssa3 protein in the *ndt80* mutant. Spread pachytene nuclei from the *ndt80* mutant overexpressing *SSA3* (TY57 + pT199; A-C) and overexpressing *SSA3-HA* (TY57 + pT202; D-I) were stained with DAPI (blue) and anti-HA (red) antibodies. Bar, 2μm.

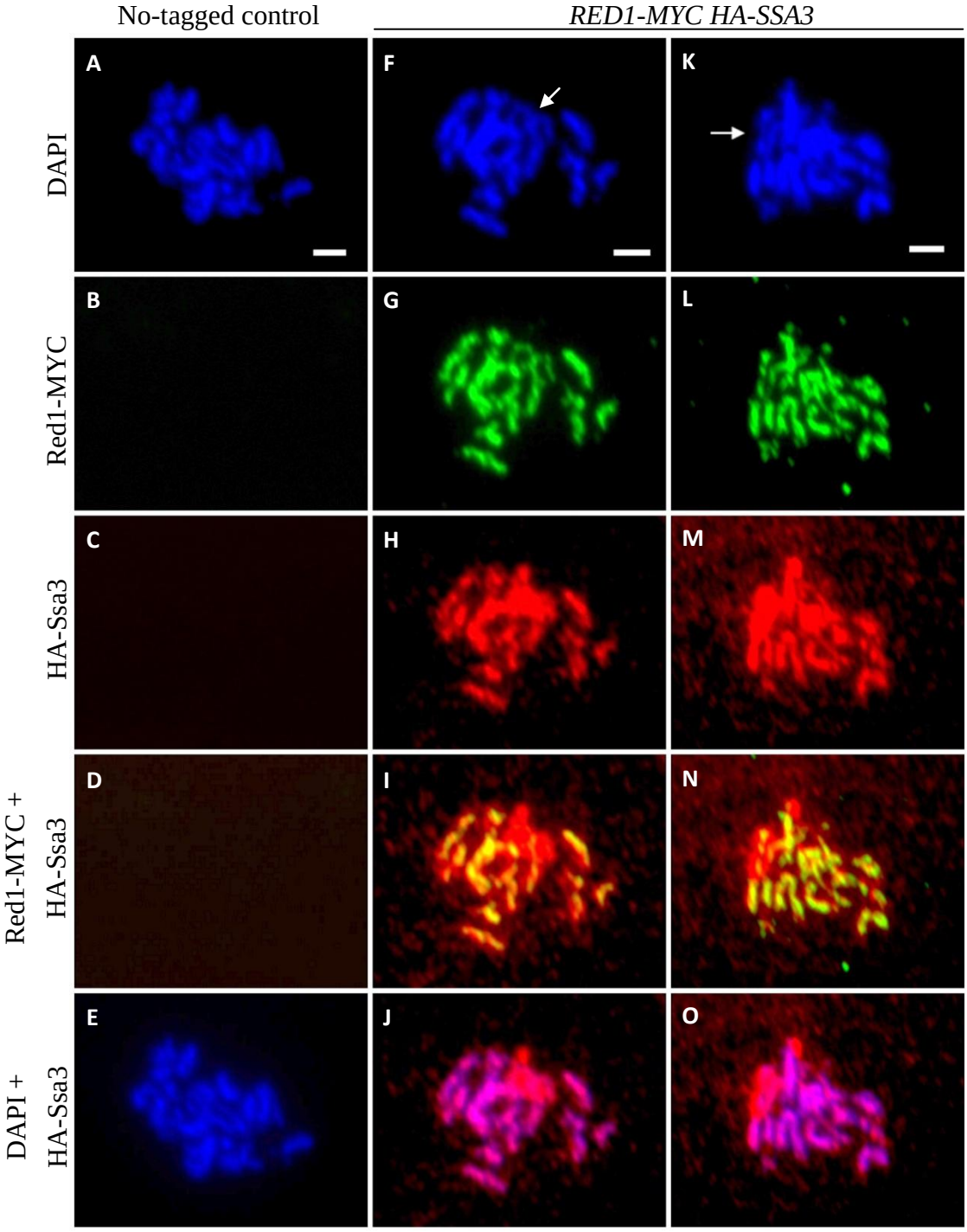

Figure 3-6. Localization of Red1 and Ssa3 in the *zip1* mutant. Spread pachytene nuclei from *zip1* carrying high-copy number plasmid overexpressing *SSA3* and low-copy number vector (MY152 + pT199 and pRS314; A-E) as no-tagged control. Spreads from *zip1* carrying high-copy number plasmid overexpressing *HA-SSA3* and low-copy number plasmid expressing *RED1-MYC* (MY152 + pT202 and pT705; F-O) were stained with DAPI (blue), anti-MYC (green) and anti-HA (red) antibodies. The arrow in each panel points to the nucleolus. Bar, 2μm.

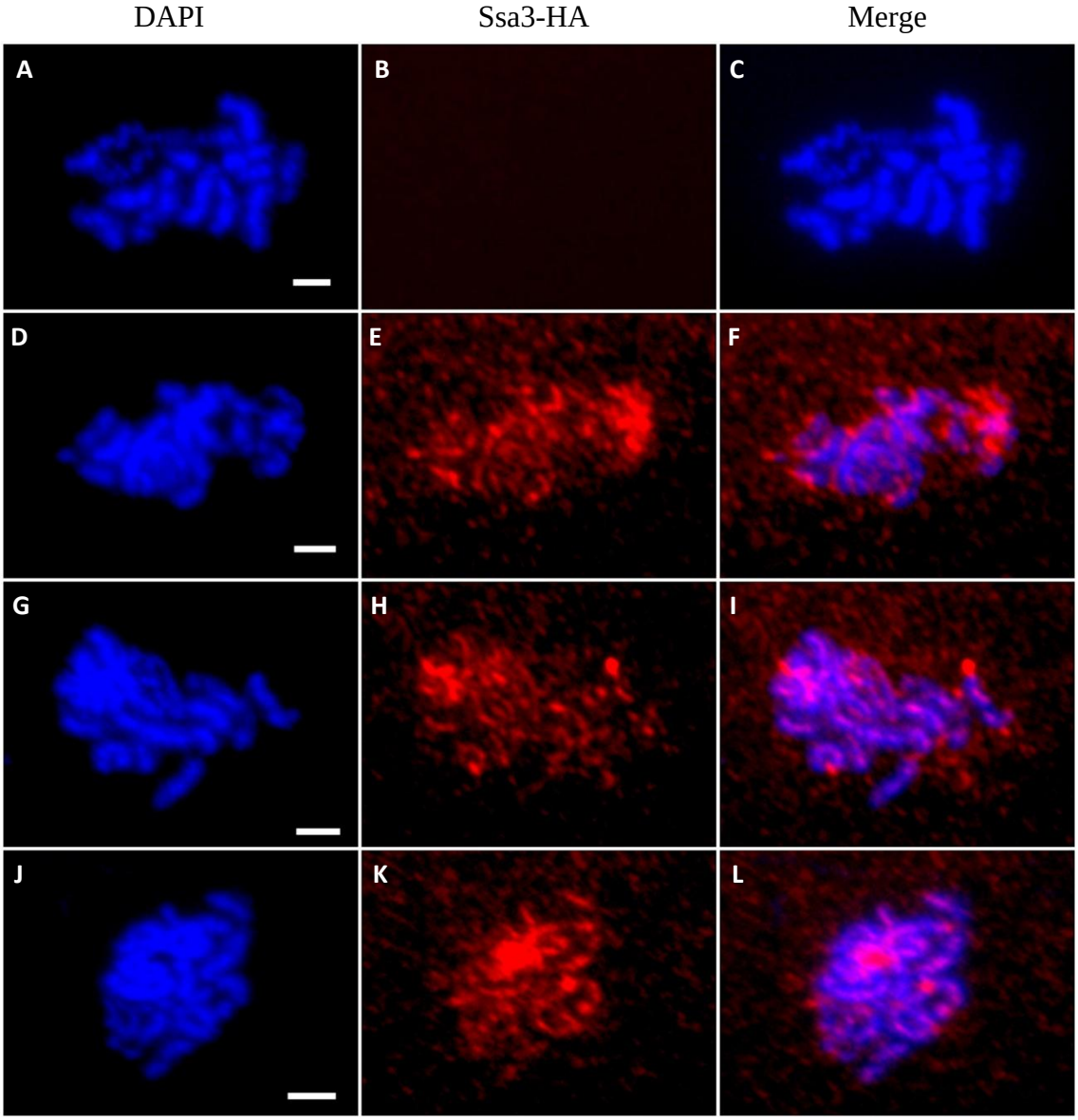

Figure 3-7. Localization of Ssa3 in wild type at high temperature. Spread pachytene nuclei from wild-type overexpressing *SSA3* (BR2495 + pT199; A-C) and overexpressing *SSA3-HA* (BR2495 + pT202; D-L) were stained with DAPI (blue) and anti-HA (red). Meiosis was induced in parallel at 32.5℃ (A-I) and 30℃ (J-L). Bar, 2μm.

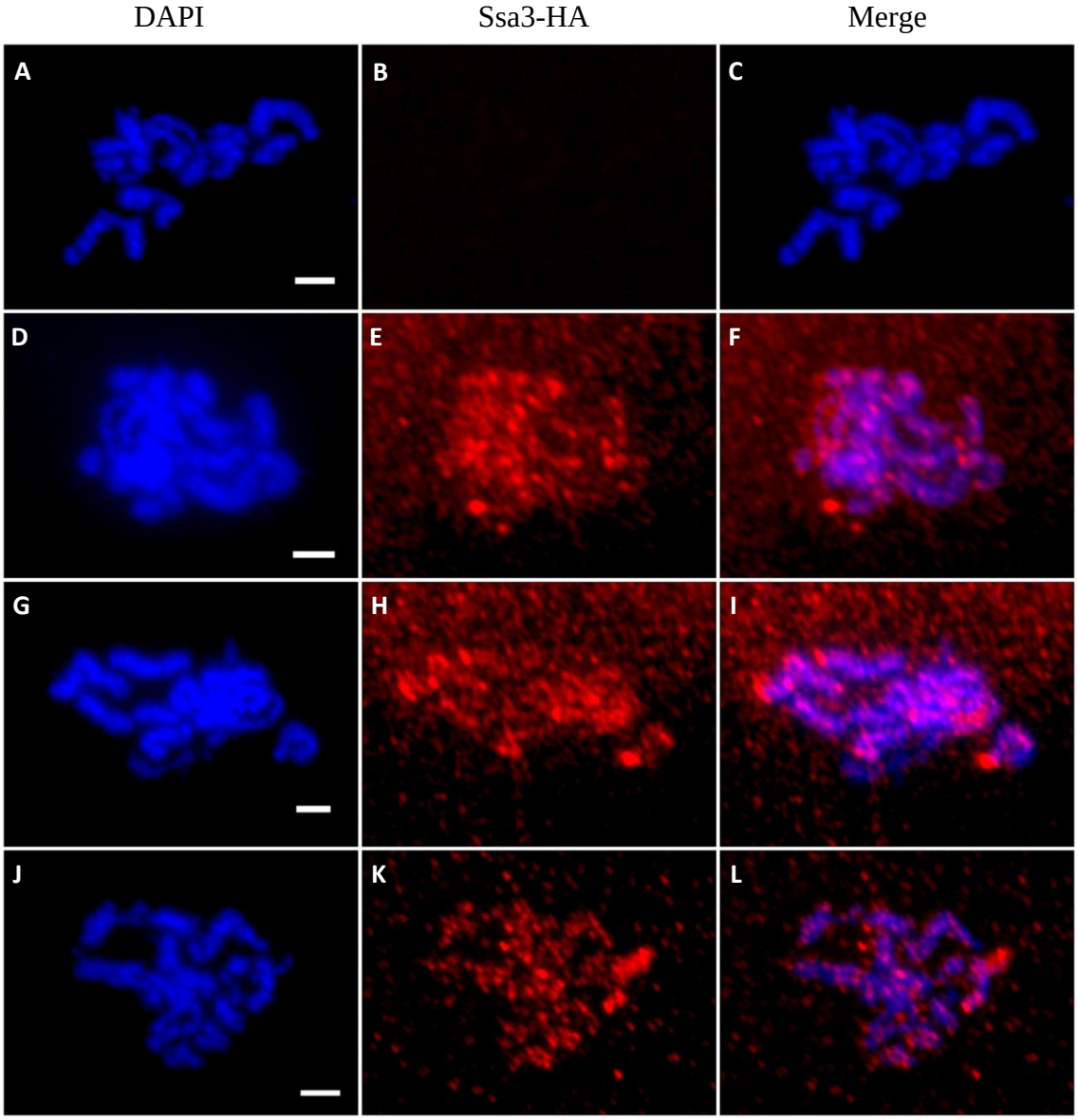

Figure 3-8. Localization of Ssa3 in *zip1* mutant cells at high temperature. Spread pachytene nuclei from the *zip1* mutants overexpressing *SSA3* (MY152 + pT199; A-C) and overexpressing *SSA3-HA* (MY152 + pT202; D-L) were stained with DAPI (blue) and anti-HA (red). Meiosis was induced in parallel at 32.5℃ (A-I) and 30℃ (J-L). Bar, 2μm.

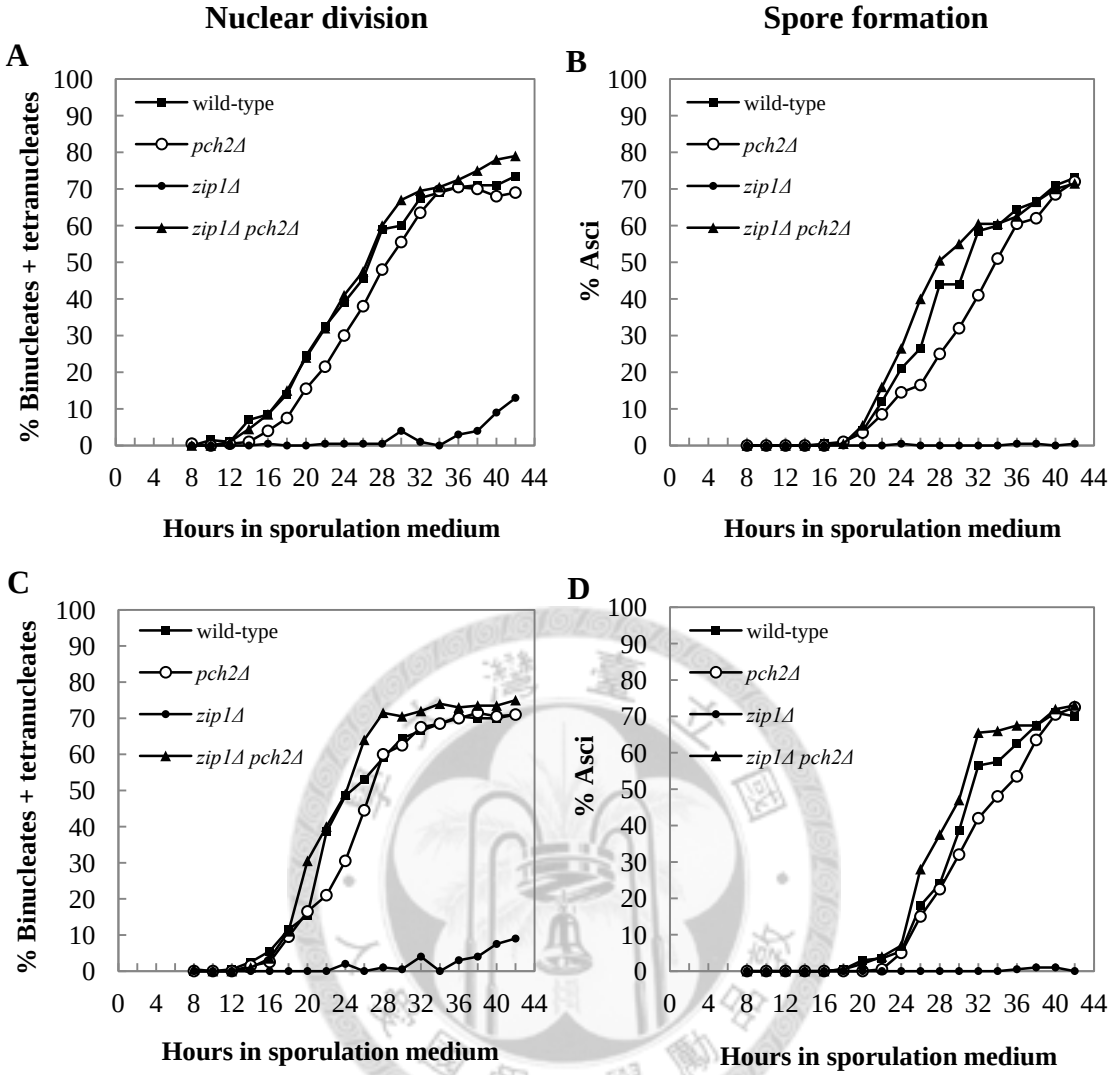

Figure 4-1. Kinetics of meiosis in wild type, *zip1*, *pch2*, *zip1 pch2* mutants at 30℃. Nuclear division (A, C) and spore formation (B, D) in BR2495 wild-type, *zip1* (MY63), *pch2* (K556) and *zip1 pch2* (K559) mutant cells were examined throughout meiosis. Cells were cultured in 2% KAc to induce meiosis at 30℃ and were examined with phase contrast microscope to assess spore formation at a 2-hr interval from 8-42 hr after transfer to sporulation medium. At the same time, cells were collected, fixed, and stained with DAPI. At least 200 cells per time point were counted and these experiments were repeated two times, with qualitatively similar results.

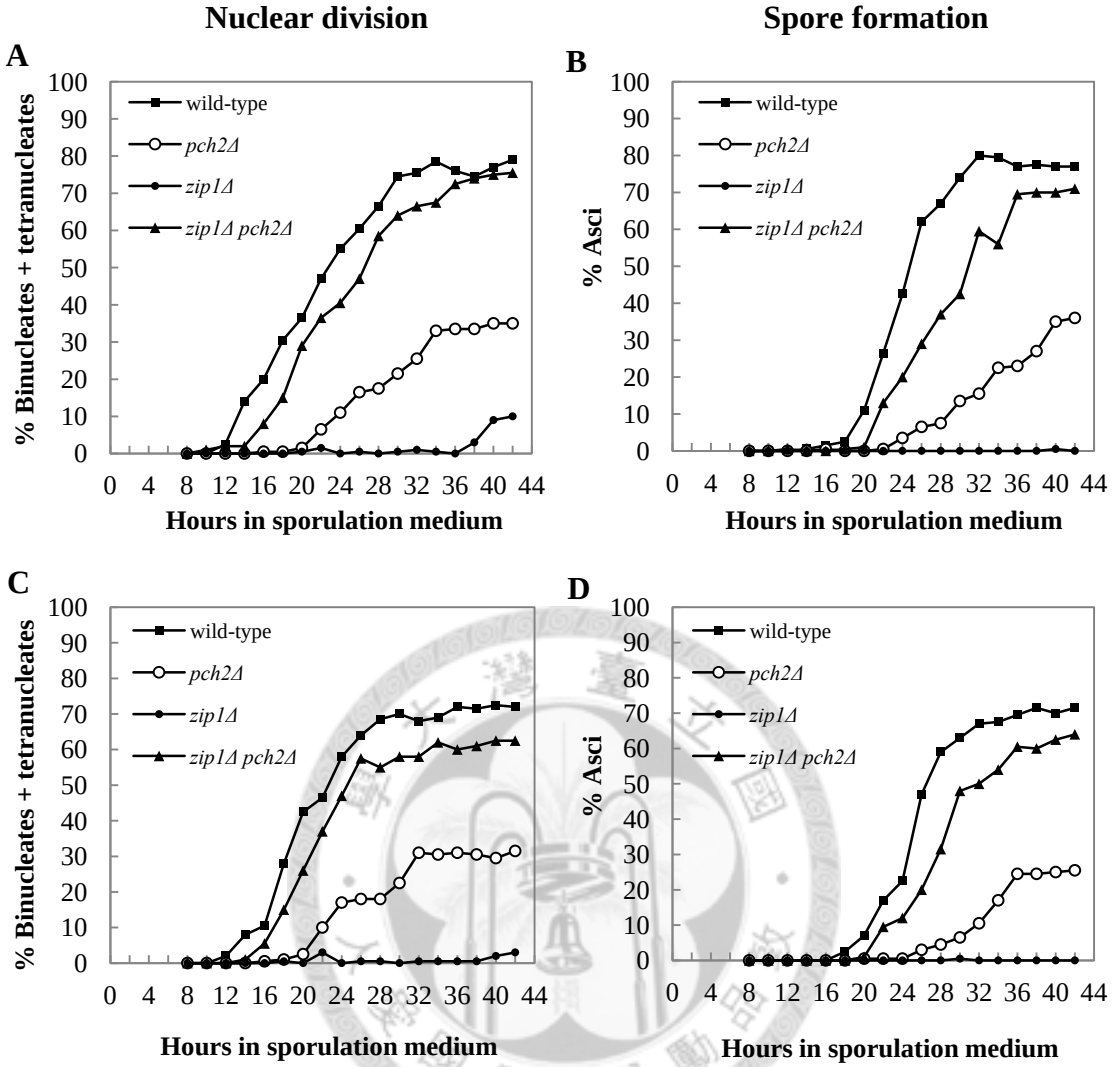

Figure 4-2. Kinetics of meiosis in wild type, *zip1*, *pch2*, *zip1 pch2* mutants at 32.5℃.
Nuclear division (A, C) and spore formation (B, D) in BR2495 wild-type, *zip1* (MY63), *pch2* (K556) and *zip1 pch2* (K559) mutant cells were examined throughout meiosis. Cells were cultured in 2% KAc to induce meiosis at 32.5℃and were examined with phase contrast microscope to assess spore formation at a 2-hr interval from 8-42 hr after transfer to sporulation medium. At the same time, cells were collected, fixed, and stained with DAPI. At least 200 cells per time point were counted and these experiments were repeated two times, with qualitatively similar results.

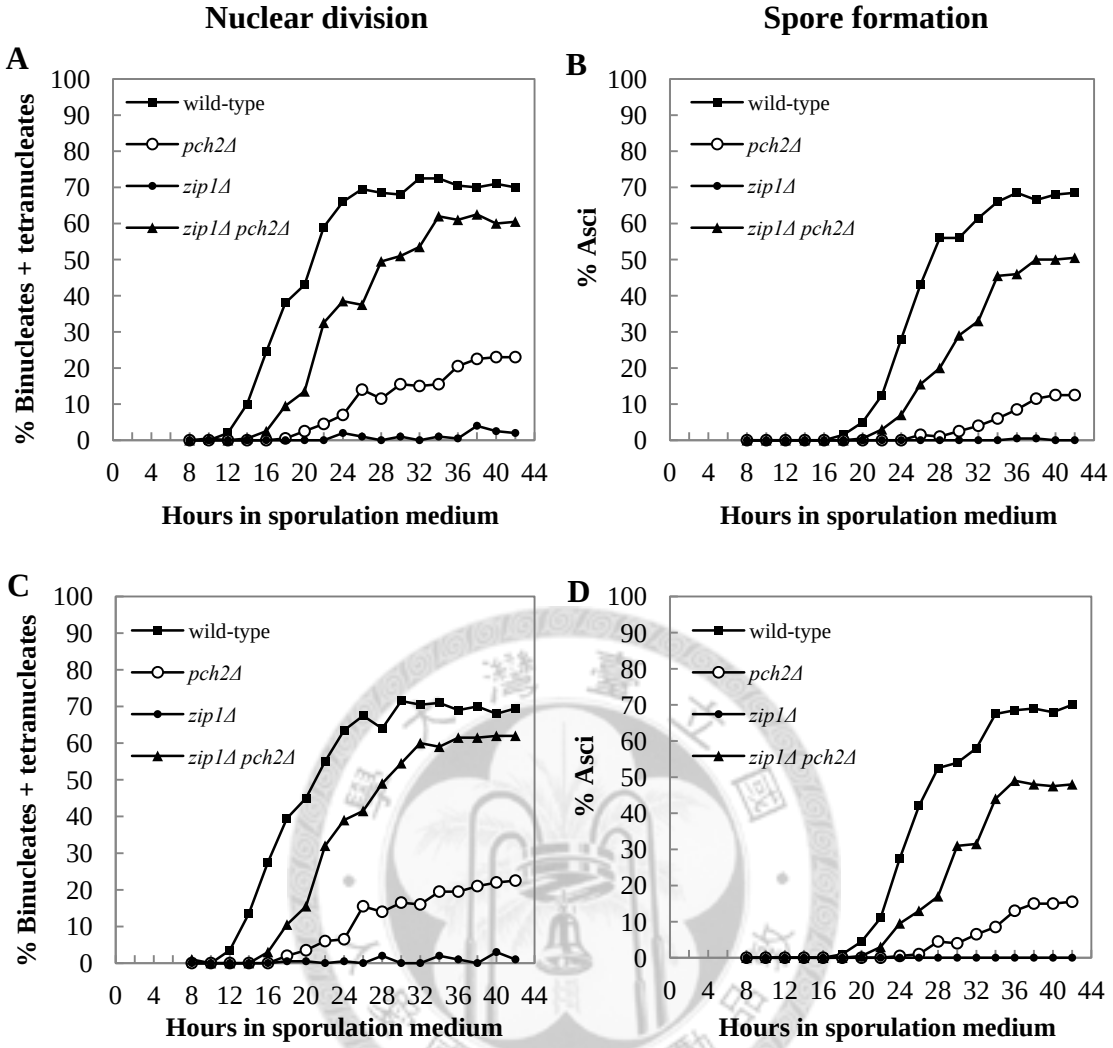

Figure 4-3. Kinetics of meiosis in wild type, *zip1*, *pch2*, *zip1 pch2* mutants at 33.5℃. Nuclear division (A, C) and spore formation (B, D) in BR2495 wild-type, *zip1* (MY63), *pch2* (K556) and *zip1 pch2* (K559) mutant cells were examined throughout meiosis. Cells were cultured in 2% KAc to induce meiosis at 33.5℃and were examined with phase contrast microscope to assess spore formation at a 2-hr interval from 8-42 hr after transfer to sporulation medium. At the same time, cells were collected, fixed, and stained with DAPI. At least 200 cells per time point were counted and these experiments were repeated two times, with qualitatively similar results.

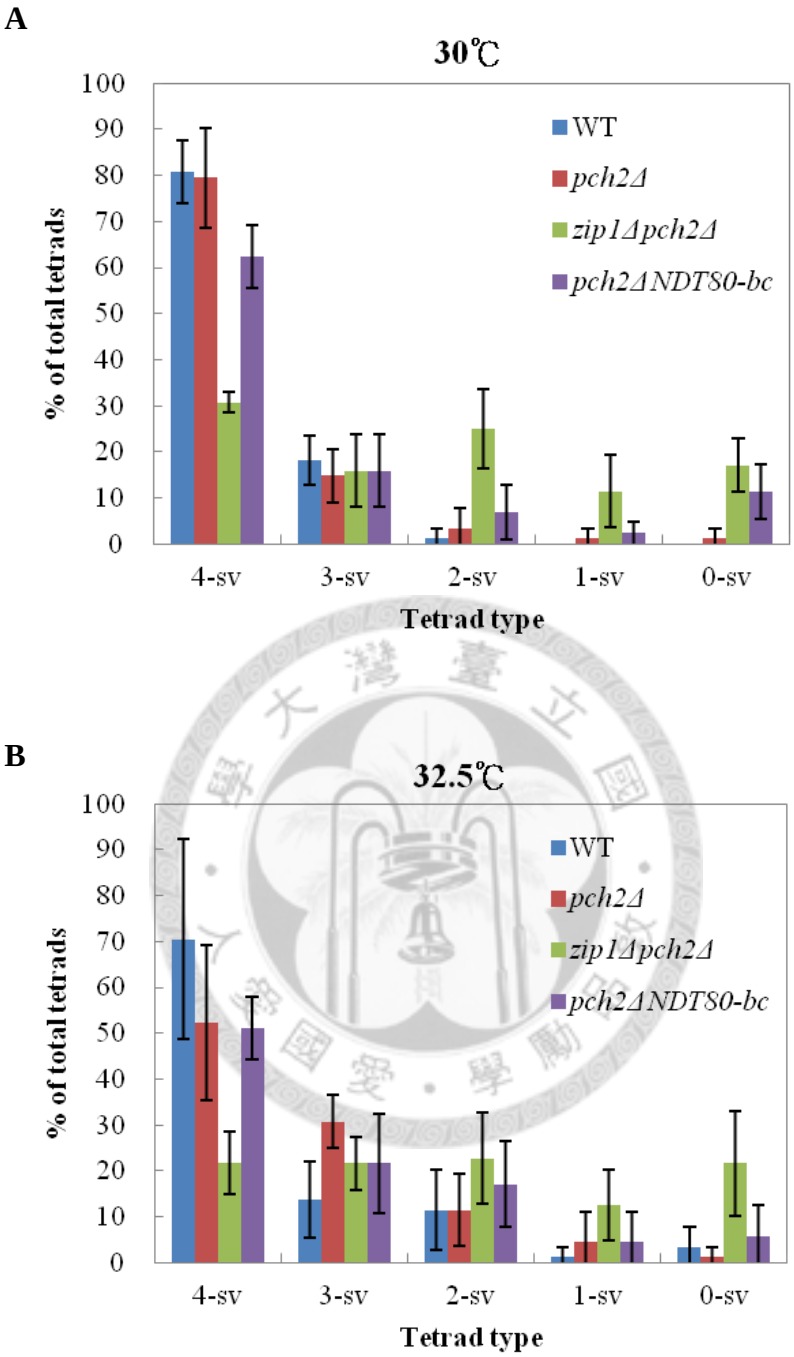

Figure 4-4. Distribution of tetrad types in wild-type, *pch2*, *zip1 pch2*, and *pch2 NDT80-bc* mutant cells at 30℃ and 32.5℃. Tetrads were dissected from BR2495 wild-type, *pch2* and *zip1 pch2* mutant cells after three days on sporulation plates at (A) 30℃ and (B) 32.5℃. 4-sv, 3-sv, 2-sv, 1-sv and 0-sv indicate the frequencies of four-spore viable, three-spore viable, two-spore viable, one-spore viable and zero-spore viable. A total of 88 tetrads were dissected from wild type (BR2495) and *zip1 pch2* (K559), and 132 tetrads were dissected from *pch2* (K556) and *pch2 NDT80-bc* (K1094).

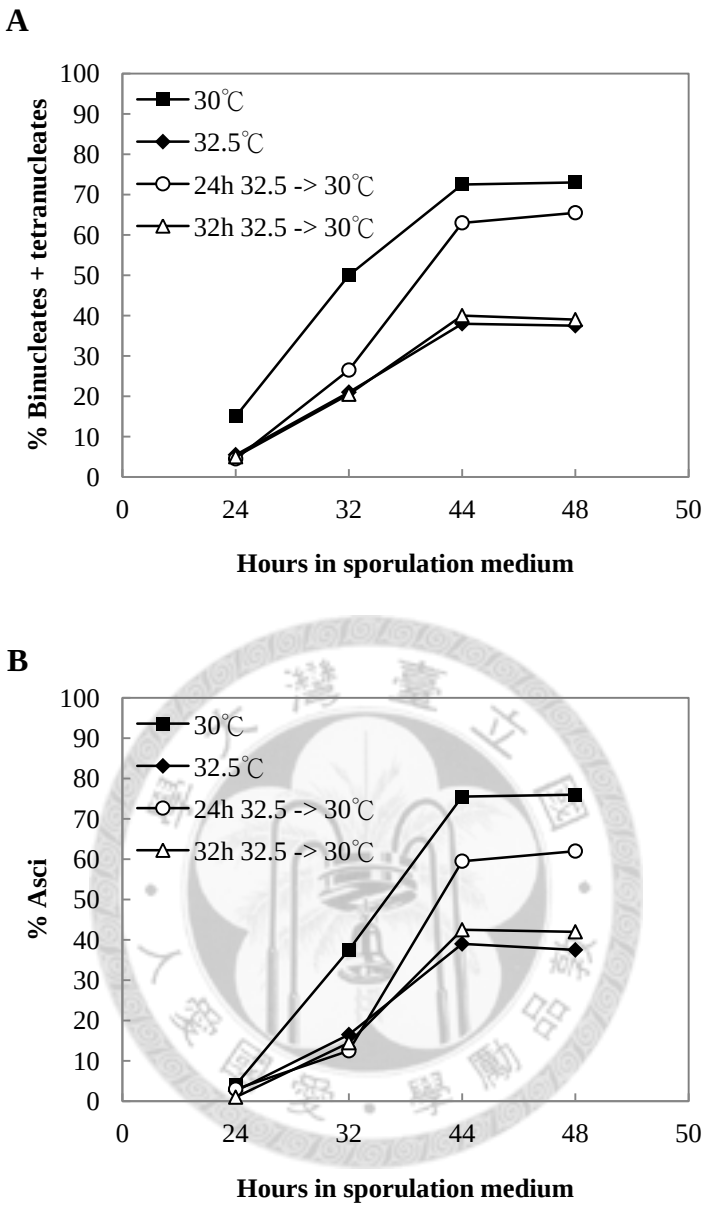

Figure 4-5. The decreased kinetics of meiosis in *pch2* mutant cells at 32.5℃ is reversible. *pch2* mutant (K556) cells were cultured in 2% KAc to induce meiosis at 32.5℃, and then downshifted to 30℃at 24 hr and 32 hr after transfer to sporulation medium. Cells were examined (A) meiotic division and (B) spore formation at 24hr, 32hr, 44hr and 48hr after transfer to sporulation medium. At least 200 cells per time point were counted.

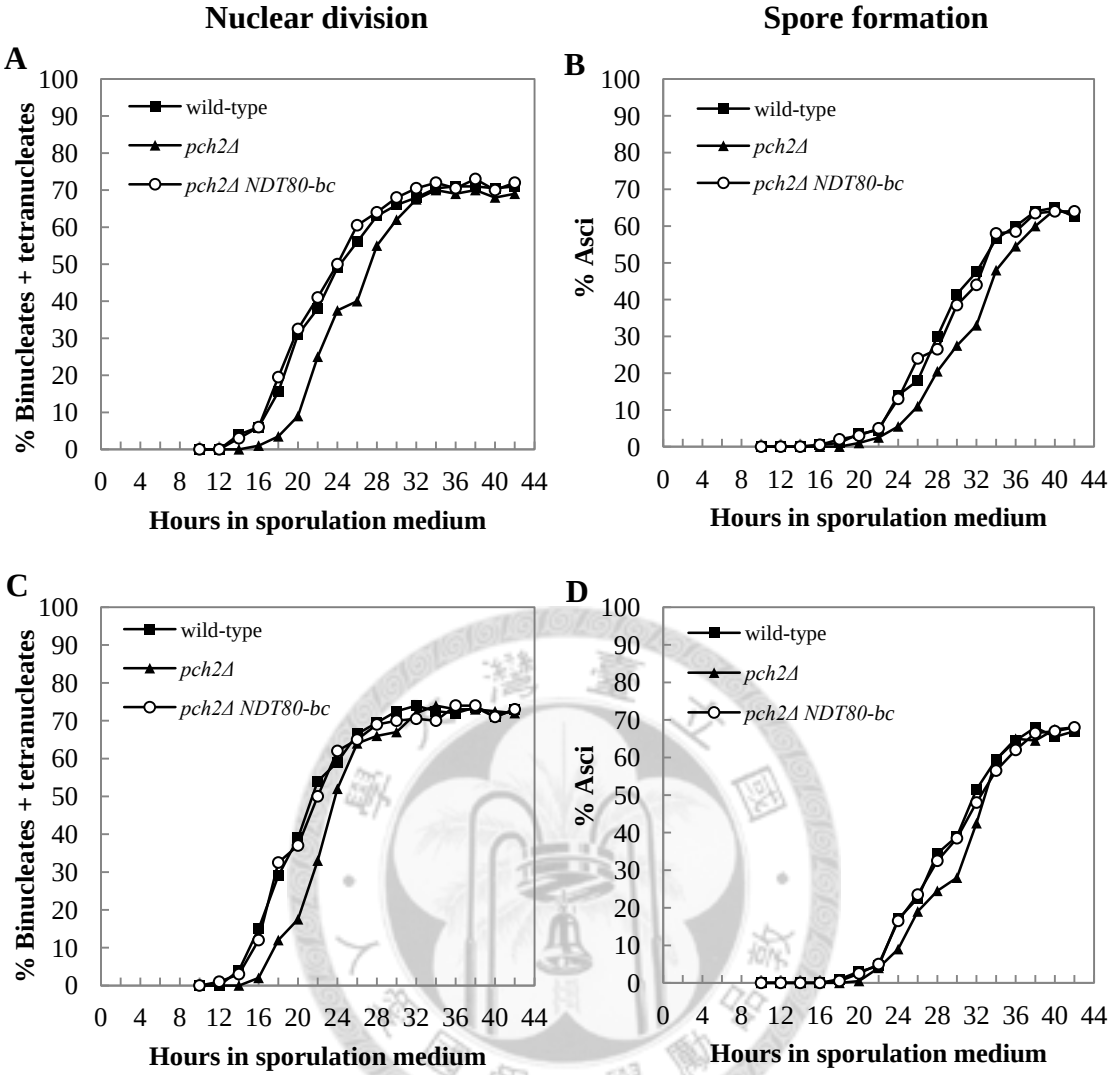

Figure 4-6. Kinetics of meiosis in wild type, *pch2*, *pch2 NDT80-bc* mutants at 30℃. Nuclear division (A, C) and spore formation (B, D) in BR2495 wild-type, *pch2* (K556) and *pch2 NDT80-bc* (K1094) mutant cells were examined throughout meiosis. Cells were cultured in 2% KAc to induce meiosis at 30℃, and were examined with phase contrast microscope to assess spore formation at a 2-hr interval from 10-42 hr after transfer to sporulation medium. At the same time, cells were collected, fixed, and stained with DAPI. At least 200 cells per time point were counted and these experiments were repeated two times, with qualitatively similar results.

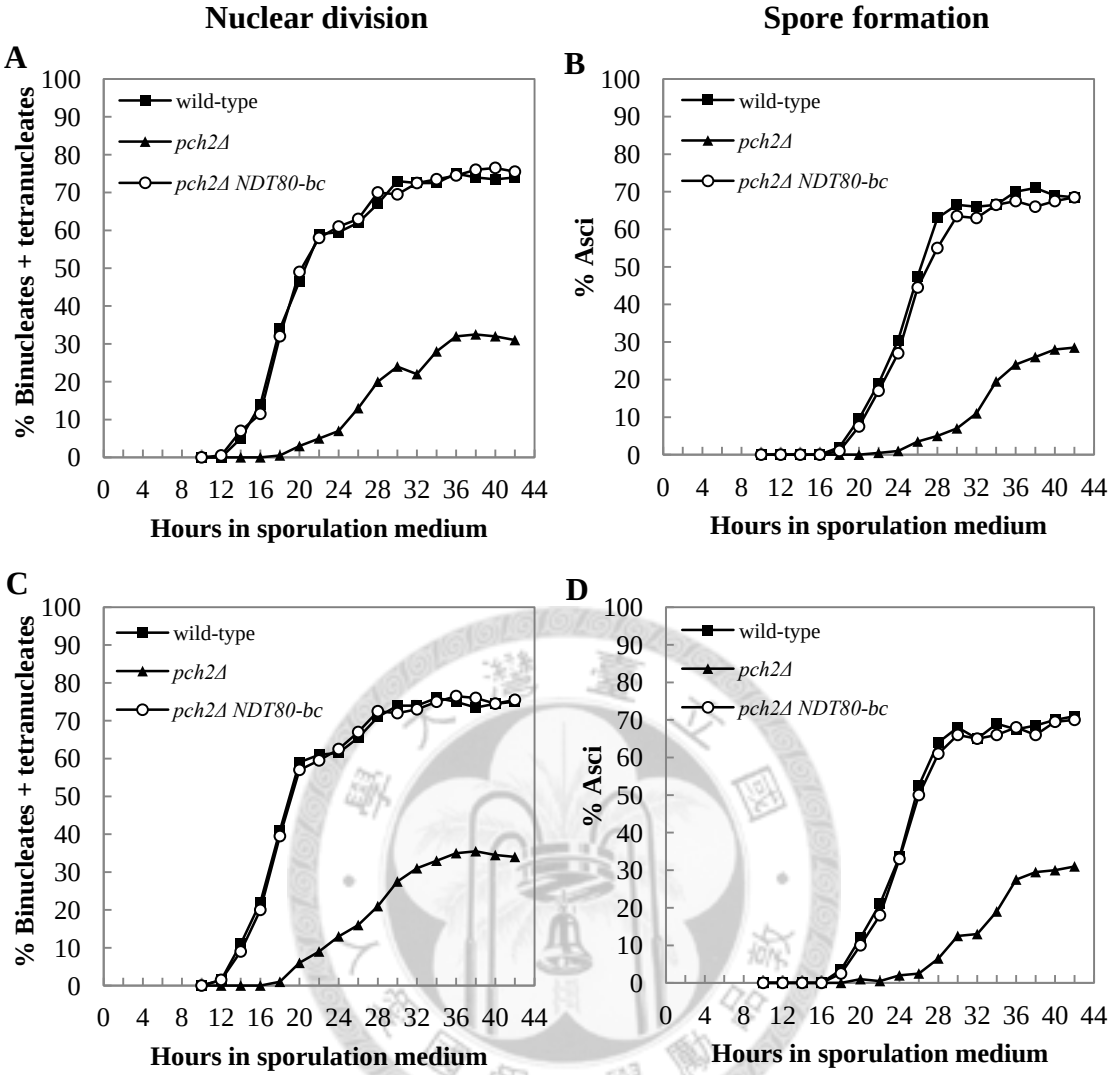

Figure 4-7. Kinetics of meiosis in wild type, *pch2*, *pch2 NDT80-bc* mutants at 32.5 ℃. Nuclear division (A, C) and spore formation (B, D) in BR2495 wild-type, *pch2* (K556) and *pch2 NDT80-bc* (K1094) mutant cells were examined throughout meiosis. Cells were cultured in 2% KAc to induce meiosis at 32.5℃, and were examined with phase contrast microscope to assess spore formation at a 2-hr interval from 10-42 hr after transfer to sporulation medium. At the same time, cells were collected, fixed, and stained with DAPI. At least 200 cells per time point were counted and these experiments were repeated two times, with qualitatively similar results.

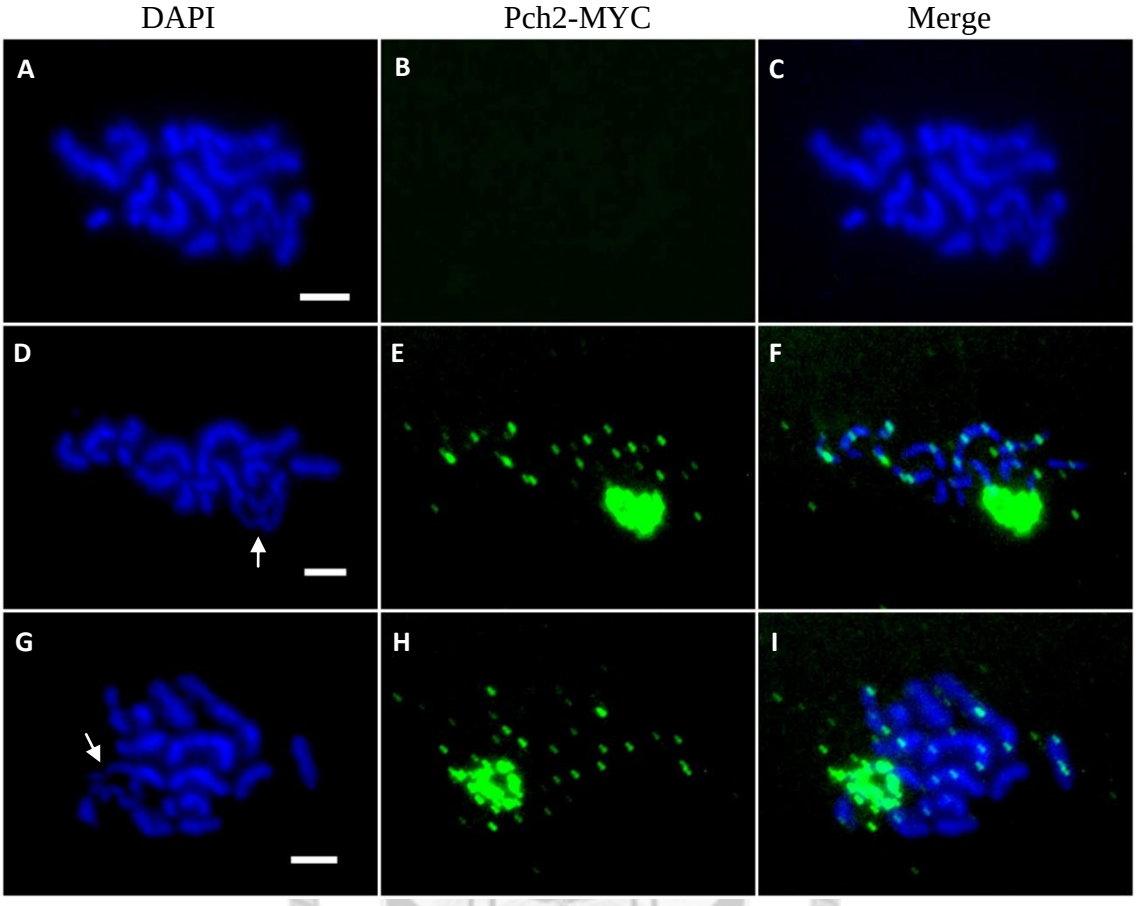

Figure 4-8. Localization of Pch2 in wild type at high temperature. Spread pachytene nuclei from wild-type BR2495 (A-C) and K1077 (D-I) were stained with DAPI (blue) and anti-MYC (green). Meiosis was induced in parallel at 32.5℃ (A-F) and 30℃ (G-I). The arrow in each panel points to the nucleolus. Bar, 2μm.

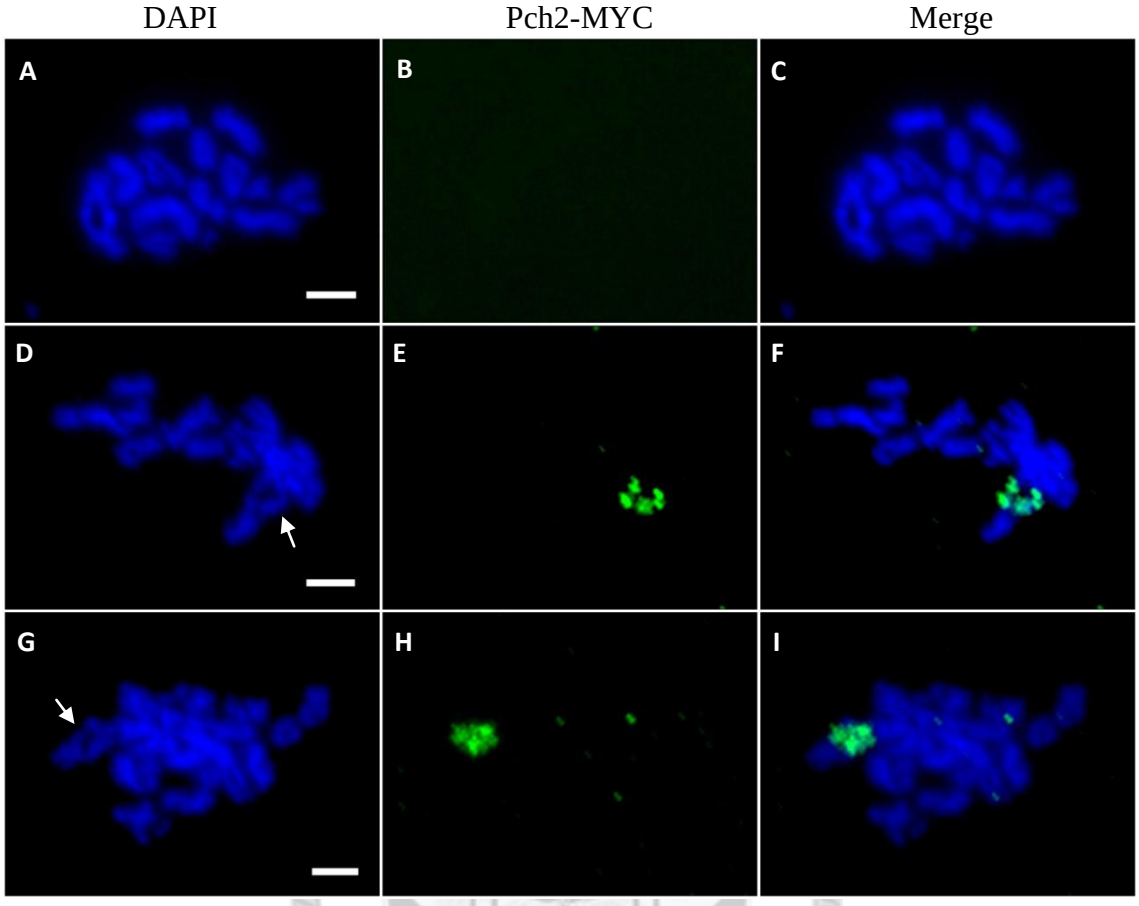

Figure 4-9. Localization of Pch2 in *zip1* mutant cells at high temperature. Spread pachytene nuclei from the *zip1* mutant MY63 (A-C) and K1071 (D-I) were stained with DAPI (blue) and anti-MYC (green). Meiosis was induced in parallel at 32.5℃ (A-F) and 30℃ (G-I). The arrow in each panel points to the nucleolus. Bar, 2μm.

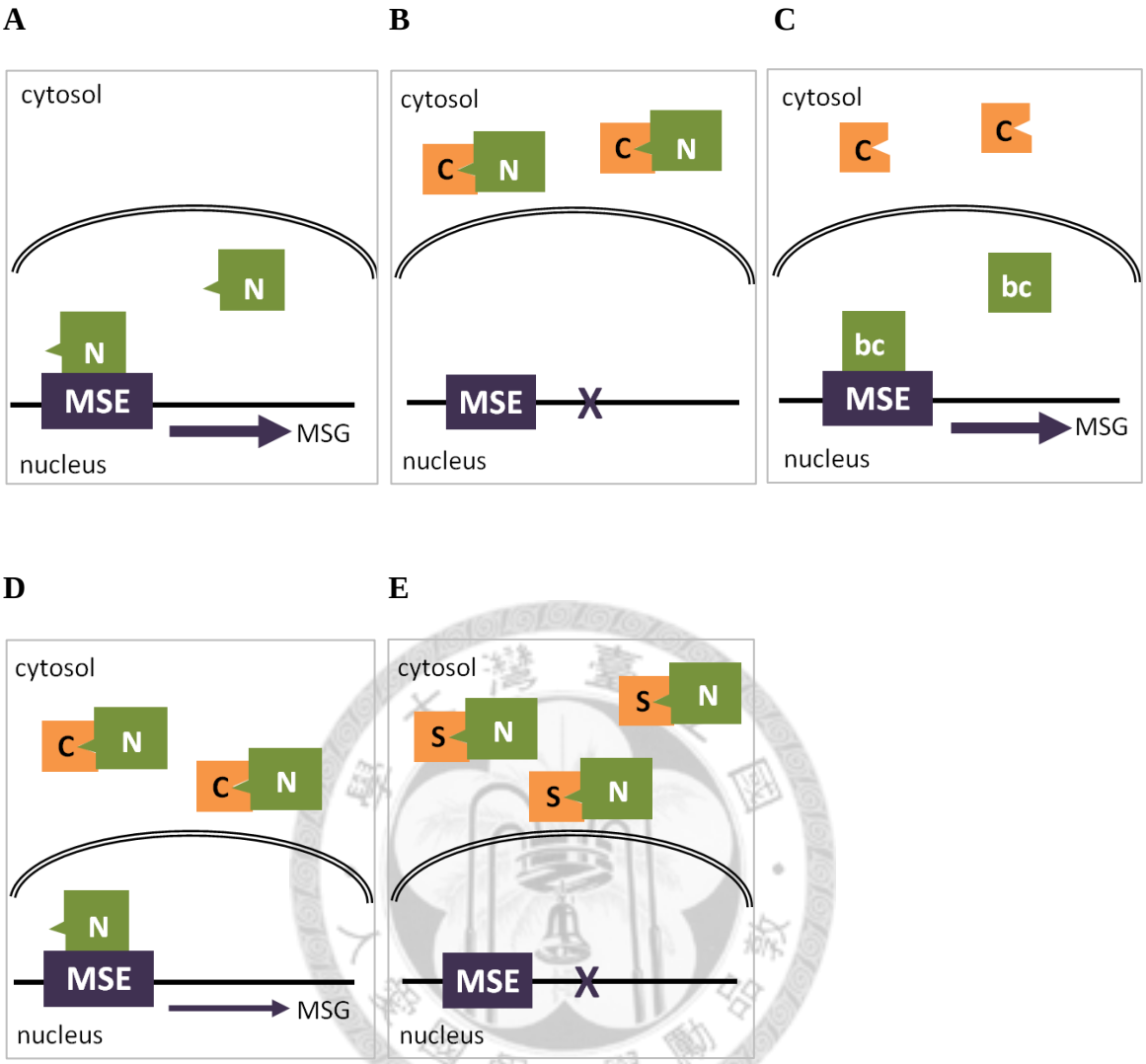

Figure 5-1. Models for the nuclear import of Ndt80 and Ndt80-bc. (A) Ndt80 protein enters nucleus and activates MSG in wild-type cells. (B) In *zip1* mutant cells. Defects in synapsis conferred by the *zip1* mutant trigger the pachytene checkpoint machinery that arrests meiotic cells at the pachytene stage through the anchor proteins fixing Ndt80 in cytosol to inhibit the nuclear import of Ndt80. (C) In *zip1 NDT80-bc* cells. (D) In *zip1 NDT80-OP* cells. (E) In *zip1 NDT80-OP SSA2-OP* cells. C, checkpoint protein; N, Ndt80; bc, Ndt80-bc; MSE, middle sporulation element; MSG, middle sporulation gene; OP, overproduction; S, Ssa2.

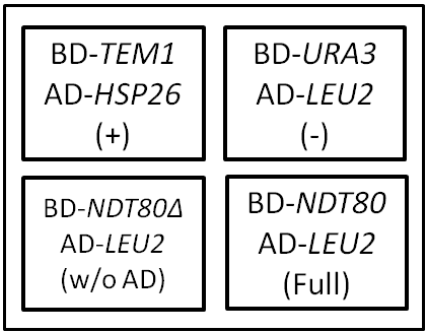

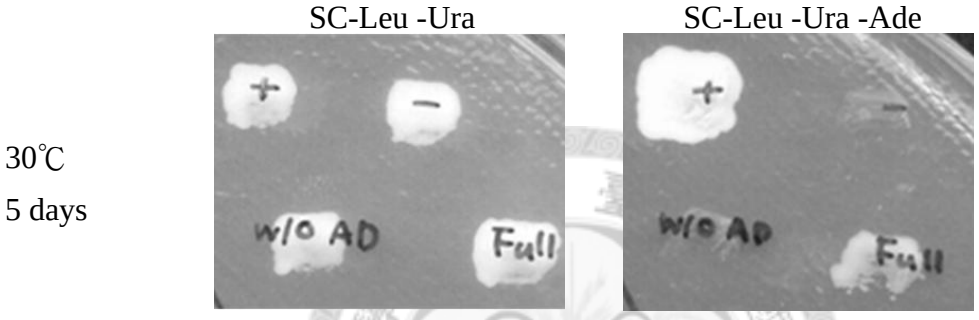

Figure 5-2. Ndt80 without the activation domain loses self-activation activity. Yeast strain PJ69-4A (K589) was co-transformed with BD-derived and AD-derived plasmids. Transformed cells were replicated onto selective media (SD-Leu -Ura -Ade) for protein-protein interaction test and incubated at 30℃ for 5 days. pGAD-C1-*HSP26* and pGBDU-C3-*TEM1* were used as a positive control (+). Vector pGAD with *LEU2* marker and pGBDU with *URA3* marker were used as a negative control (-). BD-*NDT80Δ* means deletion of Ndt80 activation domain (AD). BD-*NDT80* means Ndt80 full-length.

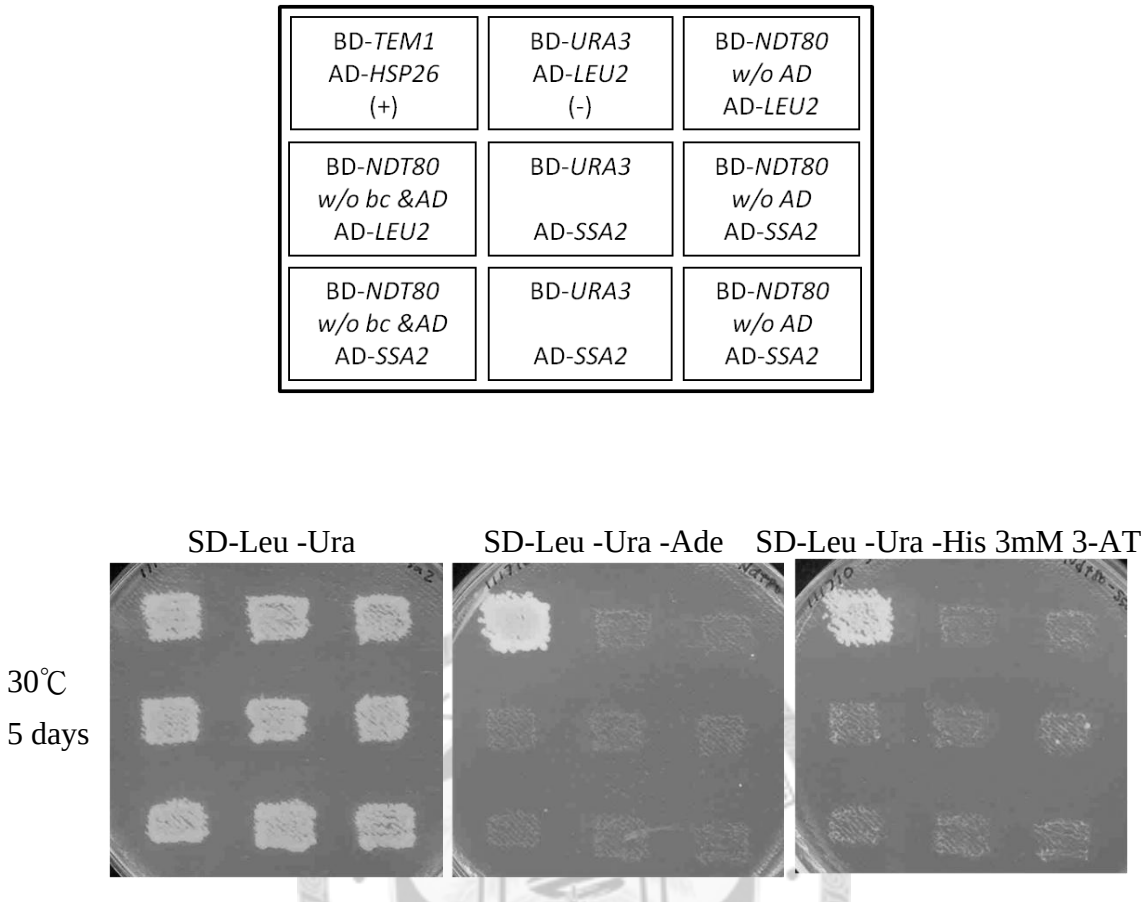

Figure 5-3. Yeast two-hybrid analysis for the Ndt80 interacts with Ssa2. Yeast strain PJ69-4A (K589) was co-transformed with BD-derived and AD-derived plasmids. Transformed cells were replicated onto selective media (SD-Leu -Ura -Ade and SD-Leu -Ura -His containing 3mM 3-AT) for protein-protein interaction test and incubated at 30 ℃ for 5 days. pGAD-C1-*HSP26* and pGBDU-C3-*TEM1* were used as a positive control (+), for the Hsp26 protein interacts with Tem1 showing on the yeast GRID database, and Ho has confirmed the interaction between Hsp26 and Tem1 by yeast two-hybrid (Ho, 2005). Vector pGAD with *LEU2* marker and pGBDU with *URA3* marker were used as a negative control (-). *NDT80 w/o AD* means deletion of activation domain (residue 404-627) of Ndt80; *NDT80 w/o bc & AD* means deletion of bc region and activation domain (residue 346-627) of Ndt80.

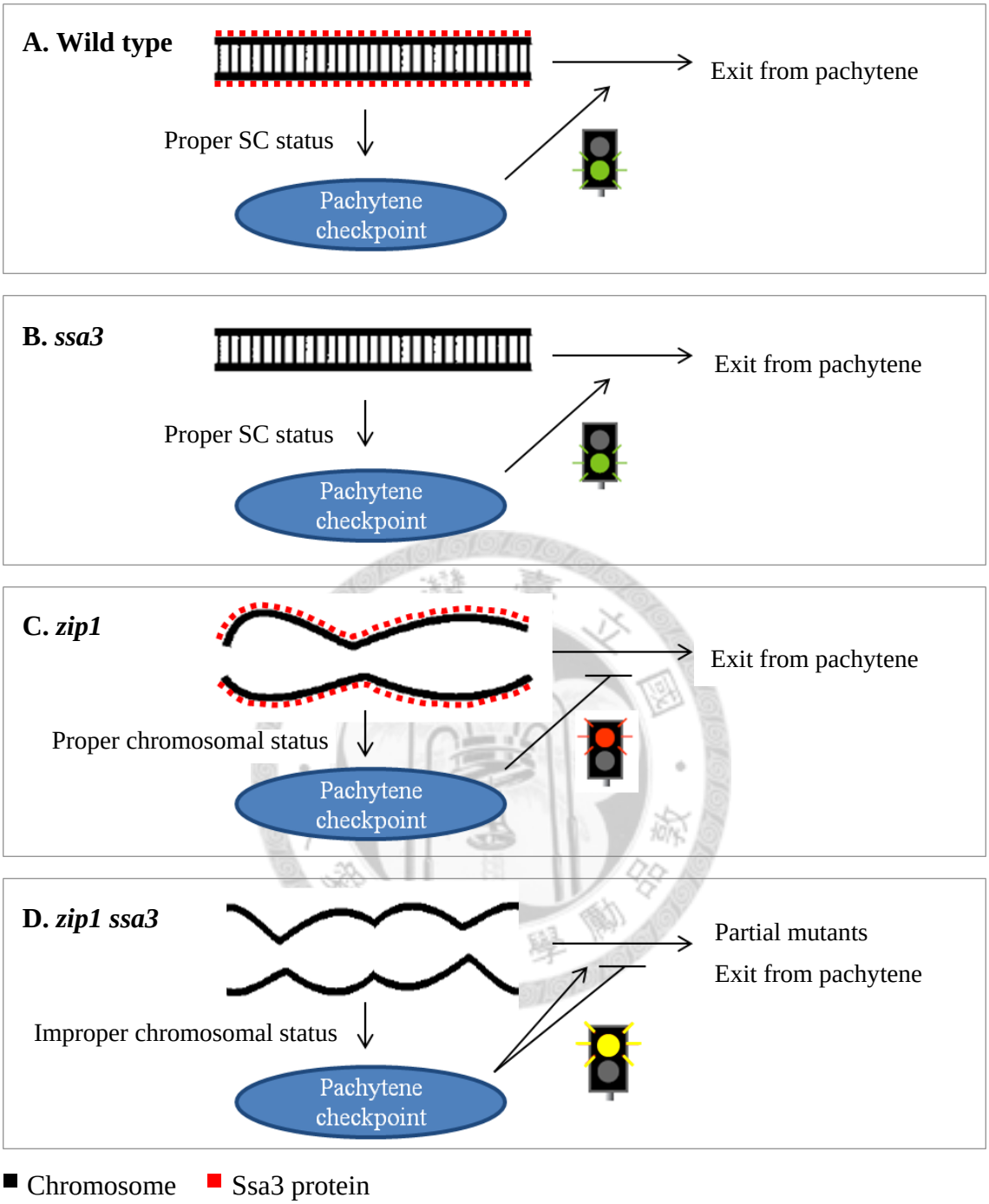

Figure 6-1. Model for the relationship between Ssa3 and the pachytene checkpoint. (A) In wild type, Ssa3 protein maintains proper SC structure for activation of the pachytene checkpoint. (B) Although absence of Ssa3, the pachytene checkpoint is still efficiently activated as SC structure is stable. (C) In *zip1*, the pachytene checkpoint is able to detect the SC defect through a proper chromosomal status conferred by Ssa3; as a result, *zip1* mutant is arrested at pachytene. (D) Absence of Ssa3 protein in *zip1*, the chromosomal status may be too unstable to efficiently activate the pachytene checkpoint, so partial *zip1 ssa3* mutant could bypass the checkpoint and complete sporulation.